

Heat Exchange Between Ocean and Atmosphere in the Eastern North Pacific for 1961-71

N. E. CLARK, L. EBER, R. M. LAURS, J. A. RENNER, and J. F. T. SAUR¹

ABSTRACT

Summaries of large-scale heat exchange between ocean and atmosphere in the eastern North Pacific Ocean are presented for the period 1961 through 1971. The summaries are based on computations made from synoptic marine radio weather reports and include 1) monthly values of total heat exchange and departures from a long-term mean; 2) long-term monthly mean values of the total heat exchange, incoming solar radiation, effective back radiation, and evaporative and sensible heat transfer; and 3) annual cycles of total heat exchange for selected areas.

Outstanding spatial and temporal features of the heat exchange values are discussed. However, little detail is given since this is a summary report, and readers can draw their own conclusions depending upon the intended use of the charts.

Comparisons are also made between the total heat exchange values and those given in two other reports. Discrepancies between values given in this report and those published in the other reports are attributed to differences in the empirical equations used to make the heat exchange computations, differences in data processing techniques, differences in the observed data used in the computations due to different methods of acquisition, and the possibility of ocean climate changes.

INTRODUCTION

The ocean's thermal structure is an important environmental variable that affects the distribution and abundance of marine fish populations (Sette, 1961; Uda, 1957, 1961). As part of a fisheries oceanography research program directed towards fisheries prediction, ocean temperature conditions and the air-sea interaction processes which are most often responsible for changes in this structure have been monitored in the eastern North Pacific since 1960. These data have been used to describe the interaction of ocean and atmosphere (Clark, 1972; Namias, 1969, 1971) in the eastern North Pacific and to identify and attempt to understand those ocean features that are important determinants of tuna distribution (Johnson, 1962; Flittner, 1970). They are also being used to evaluate the role of changing ocean conditions on other fish populations.

This report is a contribution to the MARMAP program of the National Marine Fisheries Service and presents summaries for use by fishery and other marine scientists of the derived heat exchange between ocean and atmosphere in the eastern North Pacific Ocean bounded by lat. 20° and 60°N and long. 115°W and 180° for the period 1961-71. The summaries were computed by 5° latitude-longitude quadrangles and are presented on charts of 1) the monthly values of total heat exchange and differences from the long-term mean; 2) the long-term monthly means of the total heat exchange,

incoming solar radiation, effective back radiation, and evaporative and sensible heat transfer; and 3) the annual cycles of total heat exchange in selected areas.

Since air-sea interaction processes cannot, in general, be measured directly except for solar radiation, for which there are very limited measurements over the oceans, quantitative evaluation of these processes depends upon computations based on empirically derived formulas. Because these formulas are still the subject of extensive research, the heat exchange computations should be considered only as relative indices of the magnitude of the heat flux across the air-sea interface. However, we believe that the computations represented by the charts in this report can be used to evaluate large-scale features and to show year-to-year and month-to-month variations of this heat flux.

SOURCE AND DISTRIBUTION OF THE DATA

The source of data used in preparing the charts in this report is the synoptic marine radio weather report made by ships at sea. Cooperating American and foreign-flag vessels make, record, and transmit the standard marine weather observations according to established procedures set up by the World Meteorological Organization (WMO). Observations taken at 0000, 0600, 1200, and 1800 Greenwich Mean Time daily are transmitted to designated commercial and government radio stations around the world.

Between 8,000 to 10,000 synoptic marine weather observations from the eastern North Pacific are processed by computer each month at the National Marine Fisheries Service La Jolla Laboratory, and

¹Southwest Fisheries Center, National Marine Fisheries Service, NOAA, 8604 La Jolla Shores Drive, La Jolla, CA 92037.

several summaries are compiled depending on their intended use. For a more detailed description of how the observations are received and processed, see Johnson, Flittner, and Cline (1965). Although specific program details have been changed, the present processing methods are essentially the same as those described in that publication.

Because the data are compiled from merchant and fishing vessel marine weather reports, the spatial and temporal distributions of observations over the ocean are irregular. Observations are most numerous in the major shipping lanes from San Francisco to Hawaii, from San Francisco to Japan, from Panama to San Diego, Los Angeles, and San Francisco, and from Seattle to Japan. Shipping lanes of secondary importance are from San Diego to Hawaii and Panama to Hawaii.

The average number of marine synoptic observations taken per month over the period 1961-71 by 5° quadrangles for the winter and summer seasons is shown in Figures 1a and 1b, respectively. The density of observations is shown in class intervals of 50 as indicated on the charts. Compilations made for the

spring and fall seasons show the density distribution for spring similar to that of winter and the density distribution for fall similar to that of summer.

In all seasons, most observations are taken along the shipping lane between San Francisco and Hawaii and the coastal route from Panama to U.S. west coast ports. The least number of observations are taken northwest of Hawaii and between lat. 25° and 30°N during the summer season. The main difference between the winter and summer distributions is the southward shift of greatest observation density west of long. 145°W from the great circle route to Japan during summer to between lat. 30° and 35°N during winter.

INITIAL DATA PROCESSING AND CHART PREPARATION

Marine Environmental Variable and Heat Exchange Summaries

An intermediate step between reception of the synoptic marine data and preparation of the charts presented in this report is the compilation by 5° quadrangles of monthly mean marine synoptic variables

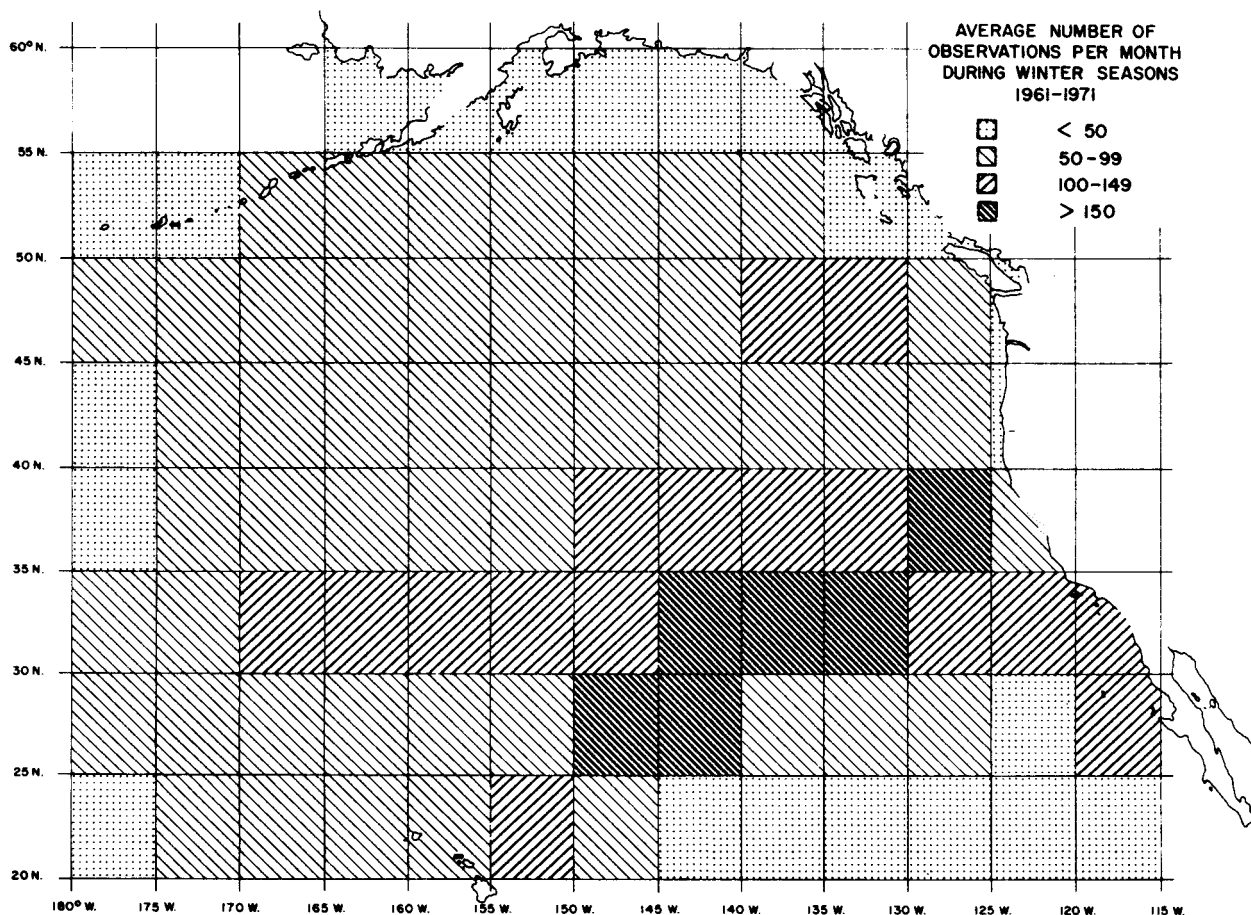


Figure 1a.—Average number of observations per month during winter seasons for 1961-71.

and heat exchange values that are computed from the variables. The initial output format consists of a deck of computer cards which are sorted and reprocessed in order to display the values in a geographic format. Each of the variables and heat exchange terms (described below) is printed in this format after three summaries have been made: 1) long-term mean monthly values computed over the years 1961-71; 2) monthly mean values computed for a given month and year; and 3) deviations of a value for a given month and year from the long-term monthly mean, i.e., anomaly values.

Heat Exchange Computations

For a given area and time period, the equation for the energy exchange at the air-sea interface is $Q_t = Q_{i0} - Q_r + Q_b + Q_e + Q_s$. Energy exchange calculations presented here do not take into account changes in heat brought about by advection.

Q_{i0} , the incoming solar radiation corrected for cloud cover (cal/cm²/day), is determined from the following equation proposed by Berliand (1960):

$$Q_{i0} = (\text{Berliand table}) (1 - aC - bC^2)$$

where C = cloudiness in tenths;
 $b = 0.38$; and
 a = a function of latitude.

Berliand's table, which lists values by month and latitude of incoming solar radiation with a clear sky, and values of "a" are given in Johnson et al. (1965).

Of the incoming radiation corrected for the screening effects of cloud cover, some is reflected at the sea surface. The amount reflected depends on the latitude and time of year and is computed from

$$Q_r = Q_{i0} \cdot r$$

where r = percentage of radiation reflected given in a table by Budyko (1956). The percentage varies from about 6% in low latitudes to more than 20% in high latitudes in winter. In preparing the charts, Q_{i0} and Q_r were combined in a single term Q_i , the incoming radiation corrected for cloud cover and reflection, defined by $Q_i = Q_{i0} - Q_r$.

Effective back radiation, Q_b (cal/cm²/day), is the difference between long-wave radiation from the sea surface and long-wave radiation from the atmosphere. The following semiempirical equation proposed by

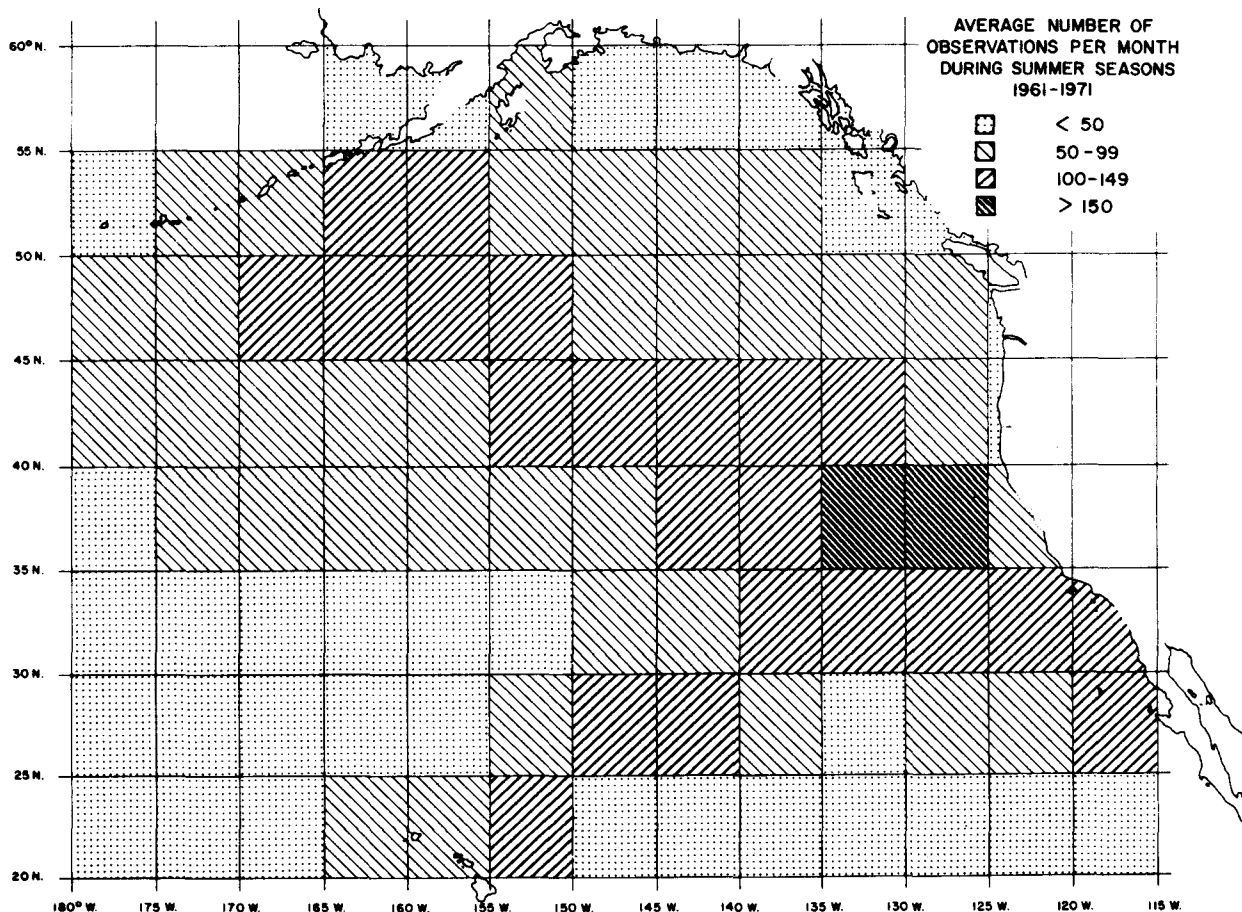


Figure 1b.—Average number of observations per month during summer seasons for 1961-71.

Berliand and Berliand (1952) has been used in this study:

$$Q_b = - \left[s\sigma(\theta_s)^4(0.39 - 0.050\sqrt{e_a})(1 - kC^2) + 4s\sigma\theta_s^3(\theta_s - \theta_a) \right]$$

where $s = 0.97$ (the ratio of the radiation of the sea surface to a black body);
 $\theta_s =$ absolute sea surface temperature ($^{\circ}\text{K}$);
 $\theta_a =$ absolute air temperature ($^{\circ}\text{K}$);
 $\sigma = 1.175 \times 10^{-7}$ (the Stefan-Boltzmann constant);
 $e_a =$ vapor pressure (mb);
 $k =$ a function of latitude (values given in Johnson et al., 1965);
 $C =$ cloudiness in tenths of celestial dome covered.

Additional energy enters or leaves the sea surface as evaporation (Q_e) and sensible heat (Q_s). Evaporation depends upon 1) the velocity of the wind and the vapor pressure difference between the sea surface and air above it, and 2) a coefficient of proportionality. The coefficient of proportionality used in our computations is given by Tabata (1958):

$$Q_e = -4.70(e_s - e_a)W$$

where $e_s =$ saturation vapor pressure at temperature of sea surface (mb);
 $e_a =$ vapor pressure of air (mb); and
 $W =$ wind speed (m/sec).

Bowen (1926) established the relation between evaporation and the heat conduction at a water surface. The equation used here for sensible heat loss by the ocean is derived from the relation found by Bowen:

$$Q_s = -3(T_s - T_a)W$$

where $T_s =$ sea temperature ($^{\circ}\text{C}$);
 $T_a =$ air temperature ($^{\circ}\text{C}$); and
 $W =$ wind speed (m/sec).

Preparation of the Heat Exchange Charts

Preparation of the charts presented in this report began by transferring the heat exchange values from computer printouts to a map of the eastern North Pacific and then contouring them by hand. In drawing the isolines, subjective smoothing was used, and, therefore, the lines do not always conform to the numbers as printed. This technique was used to eliminate the influence of values that could be an order of magnitude different from surrounding ones, a problem that is usually due to observation errors.

Caution should be exercised in interpreting the individual energy exchange values in regions having limited observational coverage (see Fig. 1a, 1b). Small errors in observation and transmission can cause large errors in some of the computations. In quadrangles having few

observations, considerable bias can be introduced by the relative positions of the reporting ships and their timing with respect to the calendar month. All computations presented assume the data centroid to be at the center of each respective quadrangle and for the middle of the month. Energy exchange calculations were not made for 5° quadrangles having fewer than five observations per month.

CHARTS PREPARED FROM THE HEAT EXCHANGE COMPUTATIONS

Monthly Average and Anomaly Charts

Monthly averages and anomalies of the total (net) heat exchange, Q_t , across the air-sea interface are shown for each month of the 11-yr period, 1961-71, in Part 1 of the chart section. A detailed description of these charts will not be given since readers can draw their own conclusions depending upon the intended use of the charts. However, some remarks will be made concerning spatial characteristics and magnitudes of the Q_t anomaly patterns.

The anomaly patterns of total heat exchange Q_t vary widely over the chart for a particular month and from month-to-month during the 11-yr period. Magnitudes of the Q_t anomalies range from less than 1% of the monthly average values to over 200%, with the largest values occurring in summer months. In addition, there appears to be very little month-to-month persistence in the Q_t anomaly patterns. This result is not surprising, since there is also very little persistence in the anomaly patterns of the four heat exchange terms that determine Q_t .

Since anomalies of Q_i and Q_b are usually small compared to those of Q_e and Q_s , spatial and temporal variations in Q_t anomalies are primarily due to fluctuations of evaporative and sensible heat flux. Anomaly patterns of Q_e and Q_s tend to be fairly large in geographical scope and coherence; at times, more than 50% of the eastern North Pacific is covered by an anomaly pattern of the same sign and magnitude. In addition, magnitudes of the anomalies can vary widely from month-to-month, ranging from less than 1% to over 100% of the monthly average.

Long-Term Mean or Normal Charts

In order to facilitate description of the heat exchange normals, the first two harmonics (first harmonic has a period equal to 1 yr or 12 mo) of the Fourier Series for each heat exchange term were computed for each of the 93 5° quadrangles on the chart. In addition to the two Fourier coefficients, the percentage of series variance accounted for by each of the harmonics was also computed. This type of analysis was useful in interpreting seasonal cycles of the data, since the two harmonics usually accounted for over 95% of the variance in each quadrangle; in fact, over most areas of the chart the first harmonic or yearly cycle accounted for over 90% of the variance. By de-

termining the phase of the harmonics, it was also possible to compare relative times of maximum and minimum values of each series.

Part 2 of the chart section shows the long-term mean monthly values (normals) of the total heat flux across the air-sea interface, \overline{Q}_t . Negative values of \overline{Q}_t , implying heat loss from the ocean surface, occur from September through March, while positive values, implying heat gain by the surface layer, occur from March through September. A regular yearly cycle is found in the \overline{Q}_t series with maximum values occurring in June and minimum values in December.

Part 3 of the chart section shows the normal values of net incoming solar radiation, \overline{Q}_i . As expected, a regular yearly cycle is found in the \overline{Q}_i series with maximum values in each quadrangle occurring in June and minimum values in December due to the motion of the

earth around the sun and the tilt of the earth's axis of rotation with respect to the plane of revolution.

Part 4 of the chart section shows the effective back radiation, \overline{Q}_b . A regular yearly cycle is also found in the \overline{Q}_b series. Maximum values occur in December and January due to the relatively low values of air vapor pressure and large values of sea-air temperature differences during these months, while minimum values occur in June and July.

Part 5 of the chart section shows the normal values of evaporative heat transfer between ocean and atmosphere, \overline{Q}_e . A pronounced yearly cycle is found in the \overline{Q}_e series with maximum values occurring in December and minimum values in June. Negative values of \overline{Q}_e occur in all months, reflecting the fact that on the average sea-air vapor pressure differences are positive throughout the year.

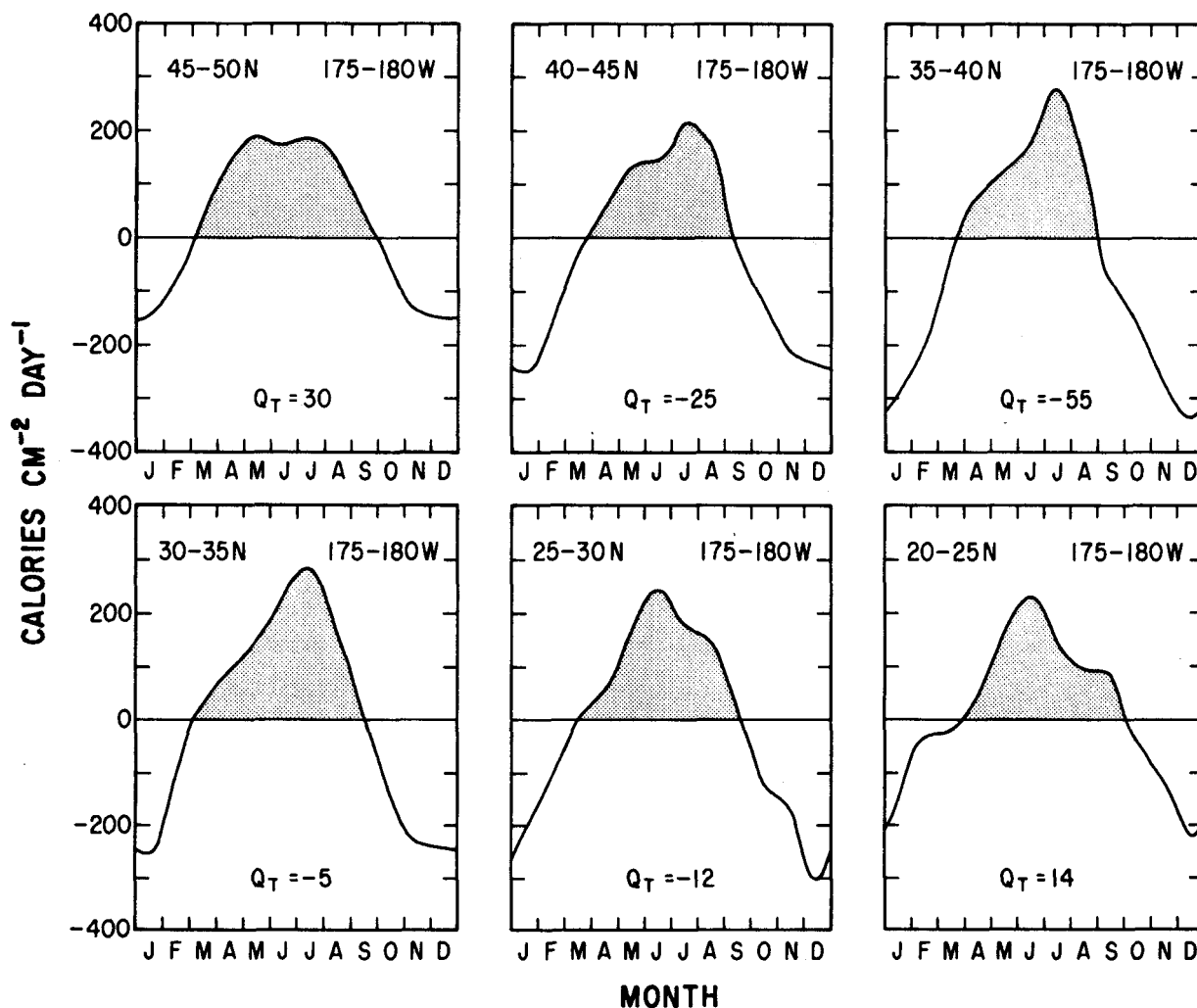


Plate 1.—Seasonal variation of average monthly total heat exchange, \overline{Q}_t , by 5° quadrangles from lat. 20° to 50°N in the meridional strip long. 175°W to the 180° meridian. Q_T is the average annual total heat exchange.

Part 6 of the chart section shows the normal values of sensible heat transfer between ocean and atmosphere, \overline{Q}_s . A regular yearly cycle is also found in the \overline{Q}_s series with maximum values occurring in November and December and minimum values in May and June. Positive values of \overline{Q}_s (heat gained by sea surface) occur in high latitudes from April through September, reflecting the fact that air temperatures in this region of the eastern North Pacific are warmer than sea temperatures during these months.

The yearly cycles in \overline{Q}_e and \overline{Q}_s reflect the fact that sea-air temperature and vapor pressure differences and observed wind speeds also have regular yearly cycles with maxima and minima that occur at the same times as those of the heat flux terms.

Seasonal Variation of the Normal Total Heat Exchange

The seasonal variation of the 1961-71 normal

monthly total heat exchange, \overline{Q}_T , was plotted for each 5° quadrangle and the annual average computed from

$$Q_T = \frac{1}{12} \sum_{i=1}^{12} \overline{Q}_{Ti}$$

where i represents the month. Except in the near coastal region of North America, the character of the normal seasonal variation changes less with latitude than with longitude. Therefore, for the oceanic region lat. 20° to 50°N and long. 130°W to 180°, the seasonal curves and the average annual values are shown here for only three selected meridional strips. Plate 1 shows the seasonal variation for each 5° quadrangle in the longitudinal strip between long. 175°W and 180° at the western boundary of the area. Similarly, Plate 2 represents the area between long. 150° and 155°W northward from Hawaii toward Kodiak, and Plate 3 represents the area between long. 130° and

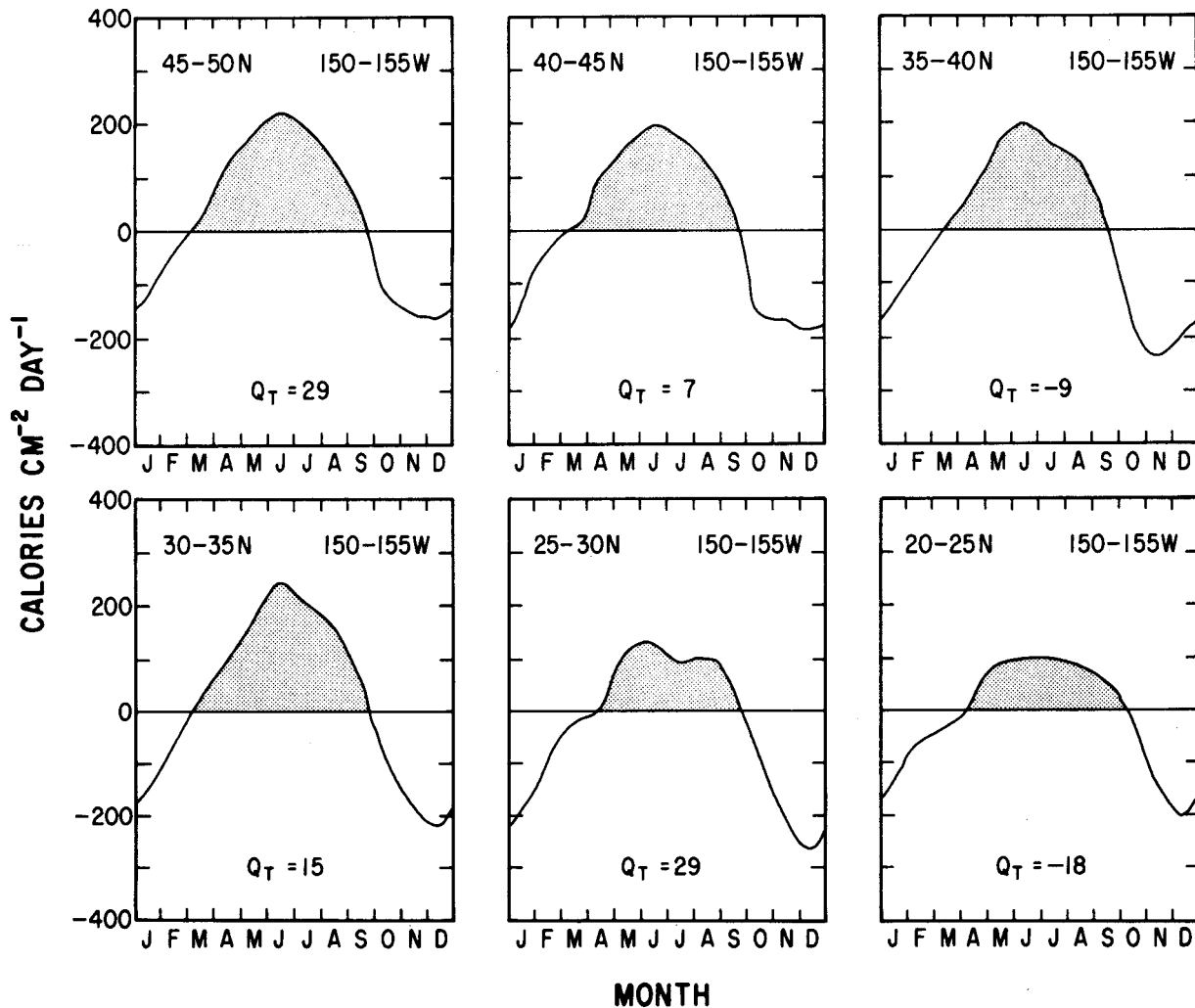


Plate 2.—Seasonal variation of average monthly total heat exchange, \overline{Q}_T , by 5° quadrangles from lat. 20° to 50°N in the meridional strip long. 150° to 155°W. Q_T is the average annual total heat exchange.

135°W just westward of the strong influence of the continental boundary. Plates 4 and 5 show the seasonal variation in 5° quadrangles in coastal regions from the northern Gulf of Alaska to Washington and from Oregon to Baja California, respectively.

The general character of the seasonal variations can be described in terms of the average annual net heat exchange, the range of the variations and the months in which the maximum and minimum values occur. In the open ocean, lat. 20° to 50°N and long. 130°W to 180°, the distribution of average annual net heat exchange, Q_T , is highly zonal with the largest (positive) values occurring in the lat. 45° to 50°N band. To the west of long. 155°W a secondary maximum appears in the lat. 30° to 35°N band. The maximum seasonal range, nearly 600 cal/cm²/day, occurs in the lat. 35° to 40°N, long. 175°W to 180° quadrangle. The lowest seasonal ranges (205 to 230 cal/cm²/day) occur in the lat.

20° to 25°N band between long. 125° and 145°W. The maximum monthly heat exchange (greatest rate of heat gain by the ocean) occurs in June in all but a few quadrangles where peak gains are in May or July and with the exception of the area from Baja California west to long. 140°W in which August maximums dominate. Minimum values (greatest rate of heat loss from the ocean) generally occur in December except for a few quadrangles with November or January minimums.

In the coastal regions the ranges of the average seasonal variation are consistently large, from about 430 to 525 cal/cm²/day from the Gulf of Alaska to the central California coast. In the northern portion of the section the annual average Q_T is negative. In the absence of declining average annual sea temperatures, a negative annual Q_T implies that heat is transported into the region by currents. Similarly, in the southern region, in the absence of increasing average annual sea

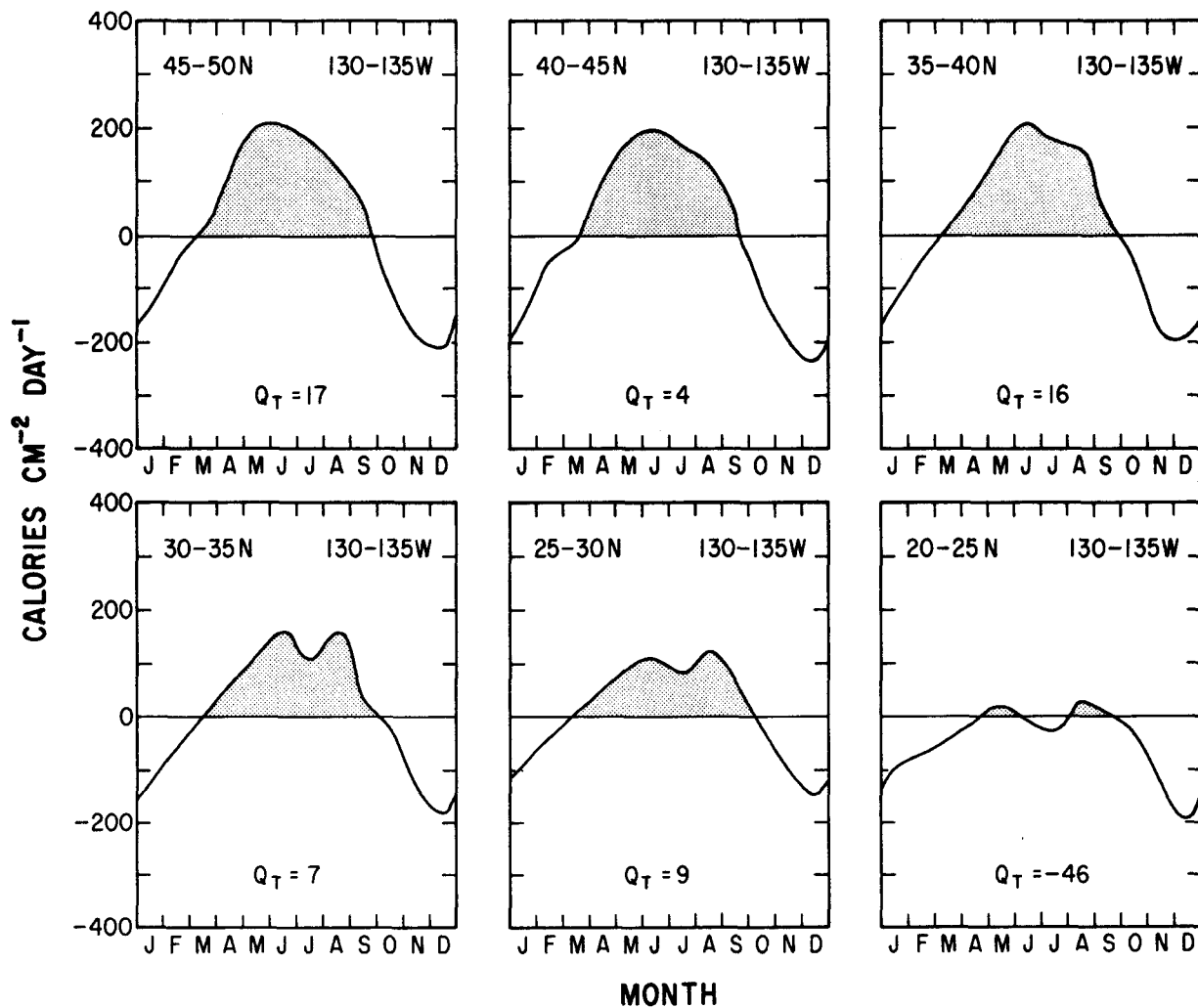


Plate 3.—Seasonal variation of average monthly total heat exchange, \bar{Q}_T , by 5° quadrangles from lat. 20° to 50°N in the meridional strip long. 130° to 135°W. Q_T is the average annual total heat exchange.

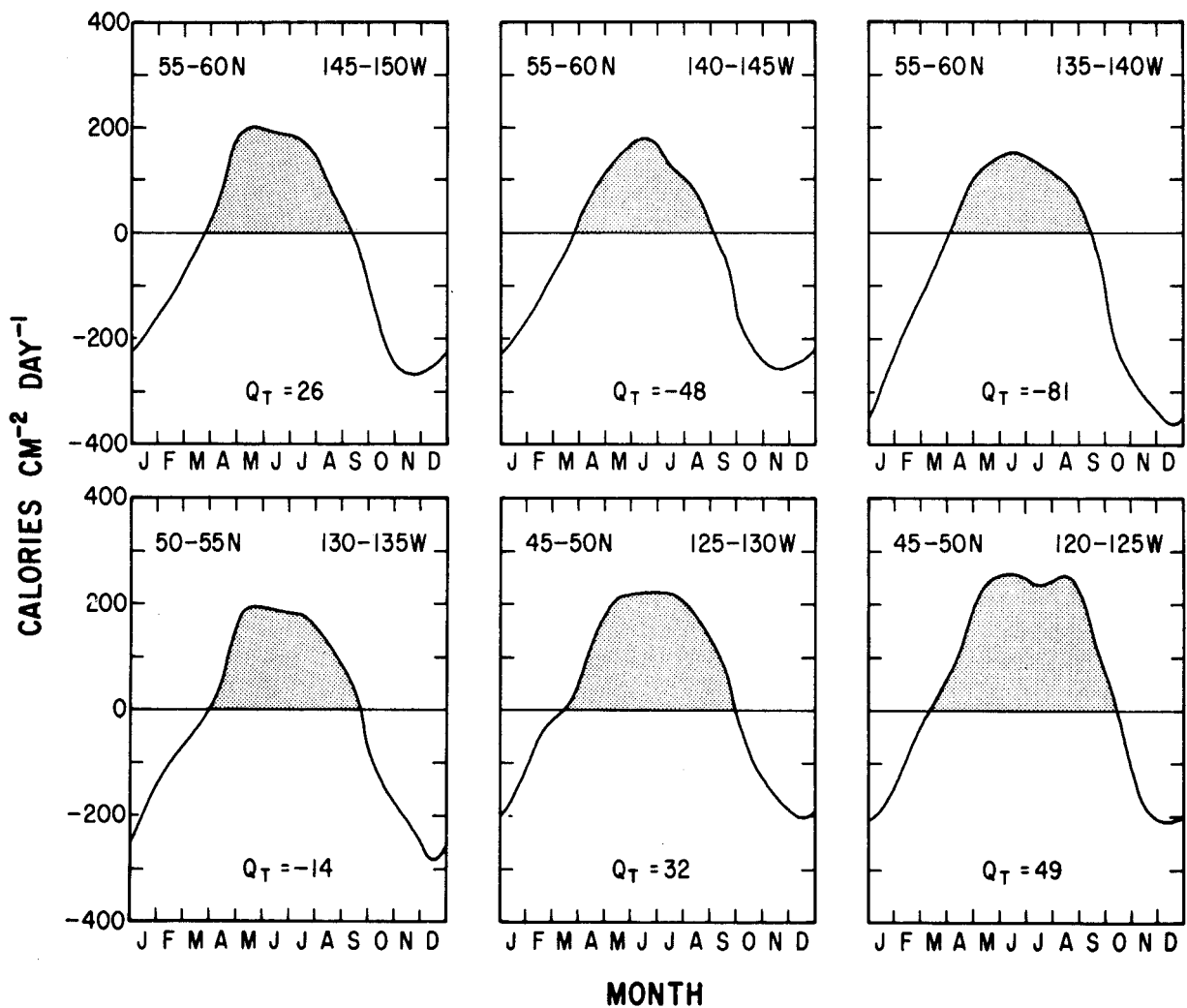


Plate 4.—Seasonal variation of average monthly total heat exchange, \bar{Q}_T , in coastal regions from northern Gulf of Alaska to Washington. Q_T is the average annual total heat exchange.

temperatures, a positive annual Q_T implies that heat is extracted from the region by currents.

EVALUATION OF THE CHARTS

The validity of these charts as quantitative representations of heat flux across the sea surface is subject to the quality and geographical coverage of the source data, the accuracy of the empirically derived formulas used for computation and the method of processing. Seckel (1970) has made a thorough analysis of each of these factors in producing a 2-yr series of monthly heat exchange tabulations by 5° quadrangles for the North Pacific trade wind zone. Seckel's tabulations provide an excellent set of heat flux values for comparison with those presented in this report.

Both were based on marine synoptic weather obser-

vations as the principal data source. However, for our report we utilized observations radioed ashore, while Seckel's data were derived from written logs archived by the National Weather Records Center.² Sets of data acquired by these two methods for particular areas and time periods will be similar but not identical due to card-punching and transmission errors and to the fact that not all data entered in weather logs are transmitted by radio, and not all observations reported by radio reach the archives.

Seckel's method of averaging the observations for each 5° quadrangle and month gave equal weight by 1° quadrangle and by day. These weighted averages of the variables needed for heat exchange computations were plotted on charts at the mean locations of the observa-

²Now the National Climatic Center, National Oceanic and Atmospheric Administration.

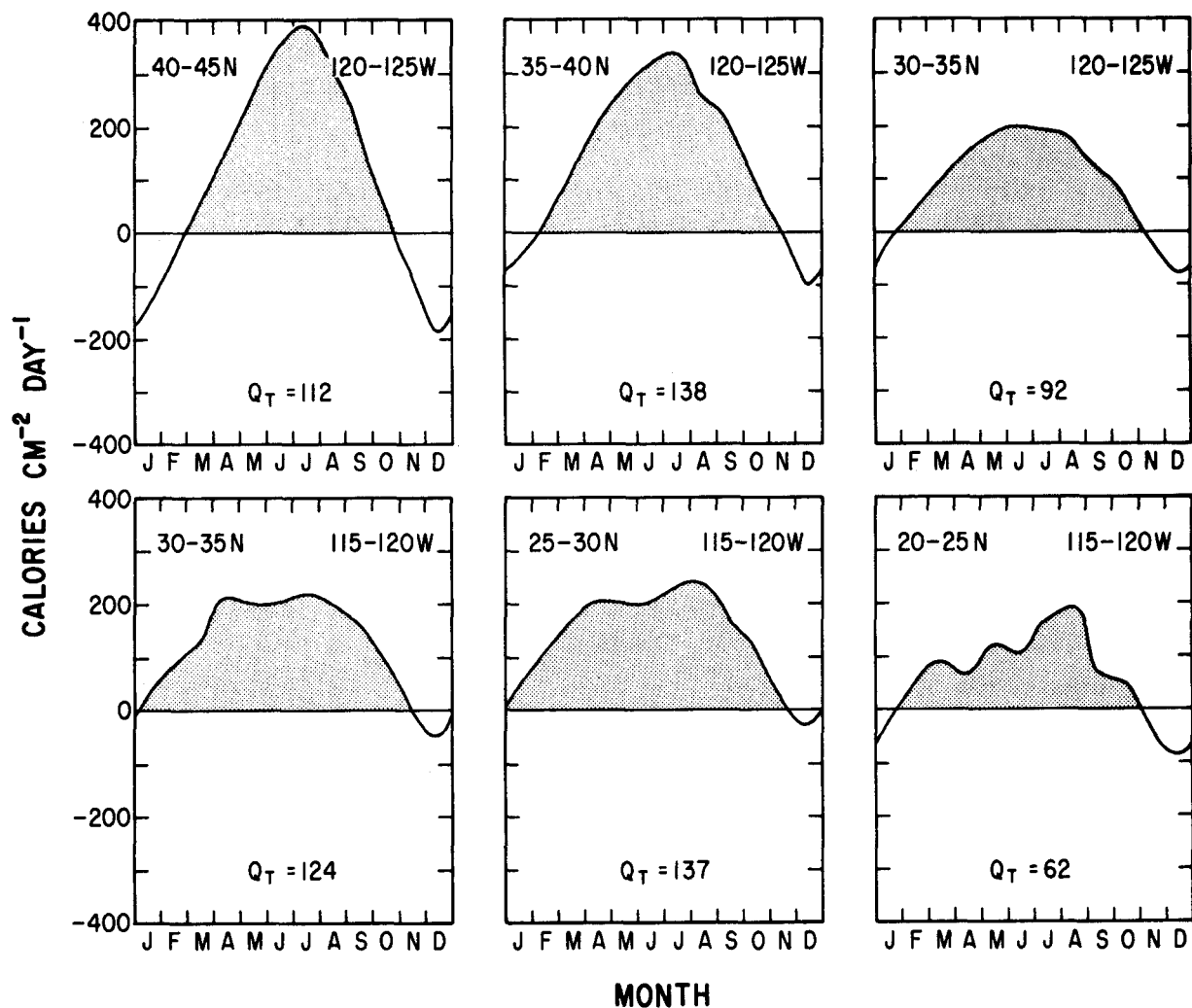


Plate 5.—Seasonal variation of average monthly total heat exchange, $\overline{Q_T}$, in coastal regions from Oregon to Baja California. Q_T is the average annual total heat exchange.

tions. The charts were then contoured and used to obtain values of each variable at the centers of the 5° quadrangles by interpolation.

In the method of Johnson et al. (1965), which was used in the preparation of this report, unweighted averages of the meteorological variables for each 5° quadrangle and month were used to compute the heat exchange components. The refinements employed in Seckel's method improve the accuracy of his results because of the fact that observations are concentrated along shipping routes and generally are not distributed evenly in either time or space.

The empirical equations used by Seckel to compute the components of heat exchange differ in some respects from those used to obtain the results presented in this report. The greatest difference occurs in the equations for heat loss through evaporation. Seckel used a variable drag coefficient which is formulated as

a function of wind speed. His equation would give approximately the same values of evaporation as that of Johnson et al. (1965) at a wind speed of about 7 m/sec.

The equation for incoming radiation employing Berliand's table, used by Johnson et al. (1965), gives higher values of heat flux than the corresponding equation used by Seckel for equivalent conditions. Computed values of sensible heat conduction, on the other hand, would be 25% greater in magnitude using Seckel's equation due to a difference in constants. The equations used for effective back radiation are the same.

In consequence, discrepancies between values of total heat exchange given in this report and those published by Seckel may arise from differences in the empirical equations, from differences in processing techniques and from differences in the observational data

actually used for computation due to different methods of acquisition.

No attempt will be made to make a critical evaluation of these factors, however, a simple comparison of independently computed net heat flux values may be helpful in the utilization of the charts in this report.

The region studied by Seckel overlapped that represented by our charts from long. 130° to 170°W, between lat. 20° and 35°N. This comprises 24 5° quadrangles; consequently, 24 pairs of computed net heat flux values were available for comparison for each of the 24 mo of Seckel's series, which ran from July 1963 through June 1965.

The mean difference and the root mean square (RMS) difference of net heat flux for each 5° quadrangle are given in Table 1.

Positive differences are predominant and indicate that Seckel's values of net heat flux are larger. The RMS differences range from 40 to 106 cal/cm²/day and are generally smallest in areas having the most observations. The RMS difference for the entire sample is 72 cal/cm²/day.

Correlation coefficients were also computed for each 5° quadrangle from paired values of monthly heat flux over the 2-yr period. The results ranged from 0.93 to 0.98 for areas lat. 30° to 35°N, 0.88 to 0.95 for areas lat. 25° to 30°N, and 0.62 to 0.91 for areas lat. 20° to 25°N. Only three quadrangles had a correlation coefficient smaller than 0.86 which reflects the fact that the seasonal cycle of net heat flux, as represented by both sets of computations, is several times larger

than the RMS differences. Furthermore, the apparent improvement of correlation with latitude reflects an increase in the seasonal range of heat flux northward from lat. 20° to 35°N. The areas for which the correlations were lowest were also the areas with the least observations.

Averaging over larger areas reduces the effect of random variations which adversely affect the correlation by 5° quadrangles between the two sets of values. Figure 2 shows Seckel's monthly total heat flux averaged for the entire region from long. 130° to 170°W and from lat. 20° to 35°N plotted against corresponding averages from our data. The correlation coefficient for the 24 pairs of monthly averages is 0.99 indicating that the effect of random differences has been essentially eliminated.

Systematic differences, however, are revealed by the regression line which crosses the horizontal axis at 12 cal/cm²/day, indicating that Seckel's formulas and processing technique give higher values of the total heat flux. Also, the slope of the regression line differs from 1.0, indicating another systematic discrepancy that stems, at least in part, from Seckel's use of a drag coefficient which varies with wind speed in the equations for evaporation and sensible heat transfer. His formulation gives higher evaporative heat loss with winds stronger than about 7 m/sec (other factors being equal) than those presented in this report, and lower evaporative heat loss with winds weaker than 7 m/sec.

Wind speed frequencies tallied from tables in Seckel's report indicate that in the region and period

Table 1.--Mean difference (upper value) and RMS difference (in parenthesis) of Q_t in cal/cm²/day for 5° quadrangles

Long. Lat.	167° W	162° W	157° W	152° W	147° W	142° W	137° W	132° W
32° N	-34 (101)	-30 (96)	-16 (63)	-14 (38)	-1 (51)	9 (54)	36 (48)	30 (40)
27° N	2 (106)	-3 (55)	21 (79)	39 (80)	26 (52)	39 (69)	26 (59)	9 (51)
22° N	66 (91)	16 (73)	29 (64)	-5 (55)	-9 (63)	20 (96)	8 (89)	23 (93)

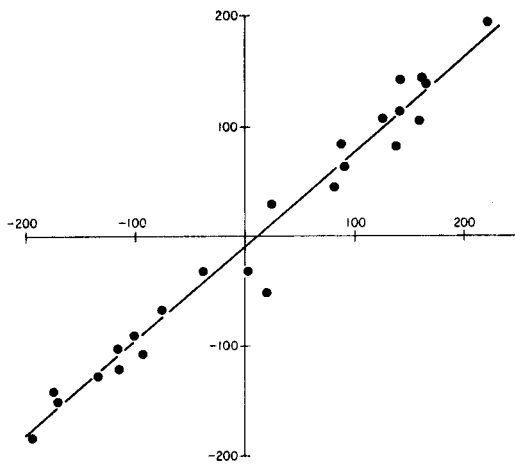


Figure 2.—Comparison of total heat transfer values (cal/cm²/day) taken from Seckel (horizontal axis) and this report (vertical axis). Each of the 24 monthly values for the period July 1963 to June 1965 was averaged over the region lat. 20° to 35°N and long. 130° to 170°W.

for which the comparison was made, wind speeds were less than 7 m/sec in about two-thirds of the cases for June through September and greater than 7 m/sec in about two-thirds of the cases for November through February. These factors combine to make Seckel's computed values of heat loss by evaporation lower than ours in the warming season and greater in the cooling season, which is reflected by his higher maximum and lower minimum values of net heat flux shown in Figure 2.

Computations of heat exchange at the sea surface have also been carried out by Wyrтки (1966) who prepared charts of heat loss by evaporation and of total heat exchange for the Pacific Ocean north of lat. 20°S. Wyrтки's charts are based on marine synoptic weather observations taken during the period 1947-60. The equations used for computation of the various components are equivalent to those described in this report, except for differences in certain empirical constants which give Wyrтки larger values of heat loss by evaporation and conduction under otherwise similar conditions. Wyrтки's method of data processing also differed from that of Johnson et al. (1965). Considering all circumstances, however, results obtained with the equations and procedures of Johnson et al. (1965) for a given set of data would probably agree as well or better with corresponding results from Wyrтки's method than with Seckel's.

Since Wyrтки's charts represent a time period antecedent to the 11 yr covered by our charts, they afford an opportunity to verify climatological patterns of net heat flux and, with caution, to infer changes in such patterns. We will make no attempt at interpretive comparison in this respect, other than to point out a few of the main characteristics in the mean cycle of heat exchange.

The beginning of the cooling season is first evident

in September in the northernmost part of the Gulf of Alaska and in an area west of long. 155°W between lat. 35° and 45°N. However, large positive heat flux values still occur at this time of year along the North American coast south of lat. 45°N. By October, the mean net flux is generally negative north of lat. 25°N, except in coastal areas out to about long. 125°W. From October through January, negative heat flux is most intense in the Gulf of Alaska and west of long. 150°W, between lat. 25° and 45°N. Heat loss is minimal between lat. 45° and 50°N west of long. 165°W, and our charts show an area of positive heat flux off southern California and Baja California in every month except December. Wyrтки's charts include all of these features and, in addition, show small areas of positive heat flux even in December. In February, positive values of heat flux appear in coastal areas south of lat. 40°N, out to long. 125°W. The largest negative flux of heat at this time occurs south of lat. 30°N, from long. 165° to 170°W according to Wyrтки's charts and somewhat north and west of that area on our charts.

March is a transition month with marked intensification of positive heat flux south of lat. 40°N from the coast out to long. 125°W, while the flux elsewhere is both positive and negative and generally weak. The principal features in the heat exchange pattern which characterize spring and summer are the areas of maximum positive heat flux along central and northern California and to the west of long. 150°W at lat. 30° to 35°N. Wyrтки also found a relative maximum along the southern stretch of Baja California which does not appear on our charts because of the cutoff east of long. 115°W. A relative minimum in the pattern occurs in the vicinity of long. 130°W at about lat. 20° to 25°N. Our charts show a negative flux in this area in every month except August and September. Wyrтки found negative values in the same area in every month except July and September.

The values of net heat flux computed by Wyrтки differ from those presented in this report by 50 cal/cm²/day or more in many areas. Such differences may reflect dissimilarities in data distribution, methods of processing or real climatological trends. The main features in the mean seasonal patterns of net heat exchange depicted by our charts appear, however, to be well substantiated by comparison with those of Wyrтки.

ACKNOWLEDGMENTS

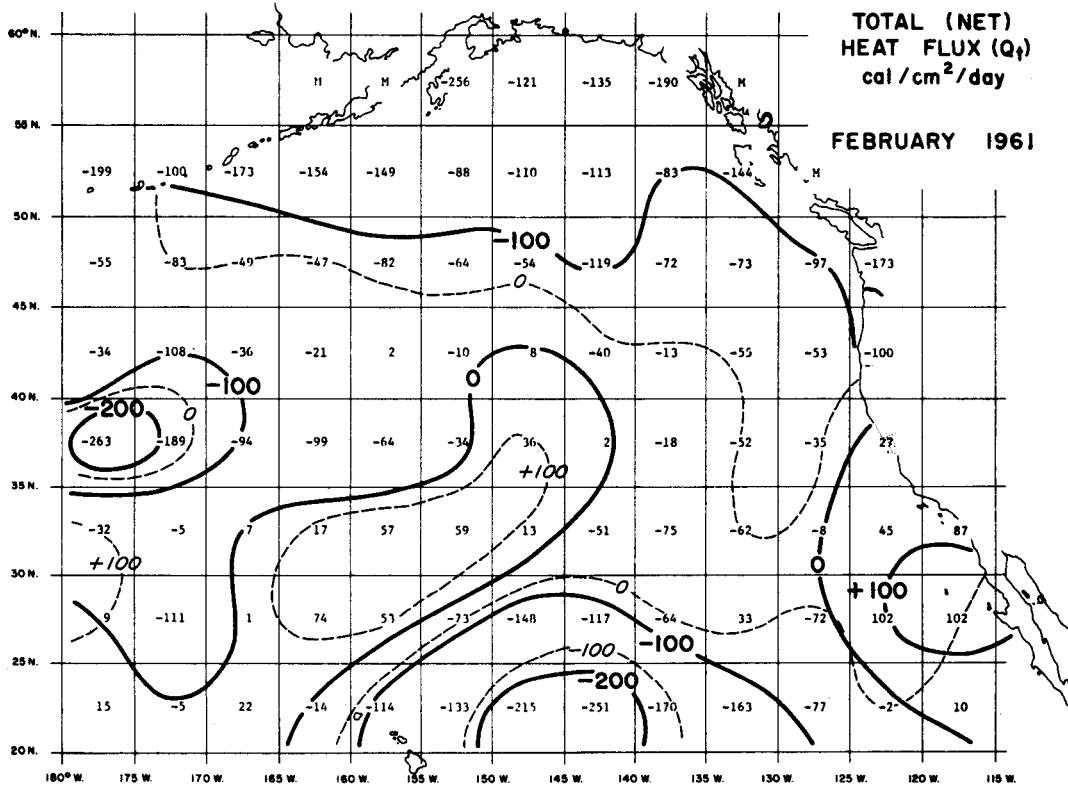
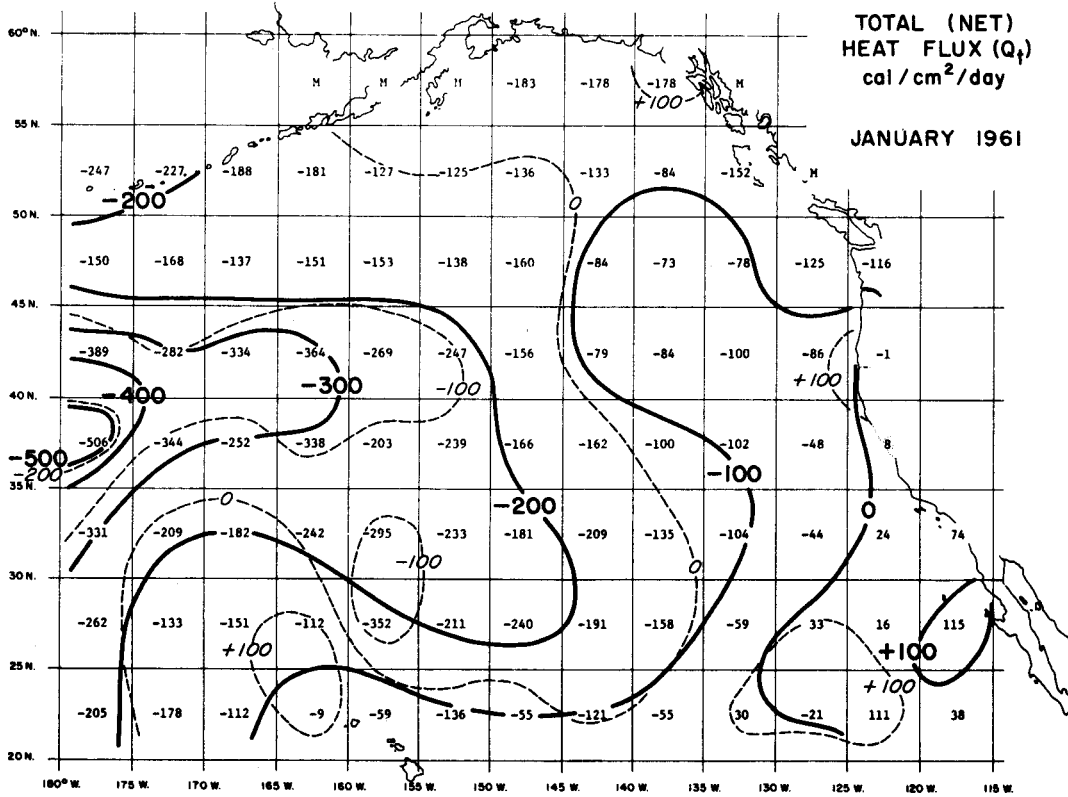
The authors express their thanks to Albert J. Good and Dorothy D. Roll for special programming and technical assistance and to Gunter R. Seckel for his thorough review of the original manuscript.

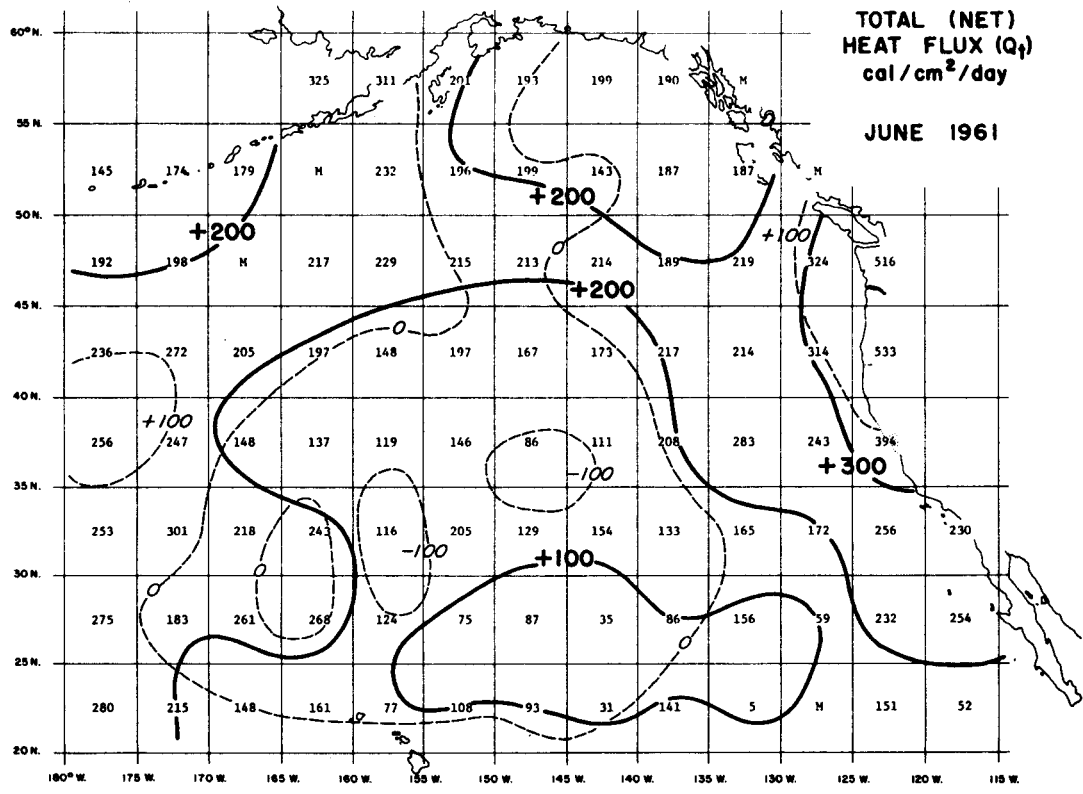
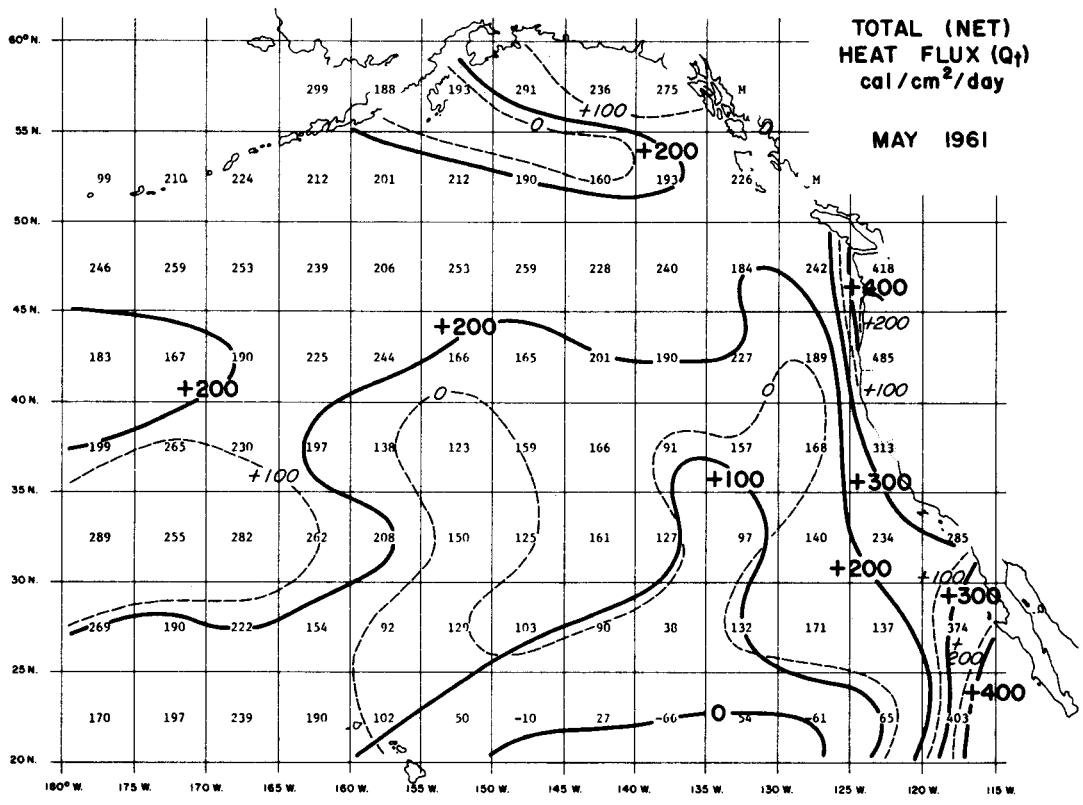
LITERATURE CITED

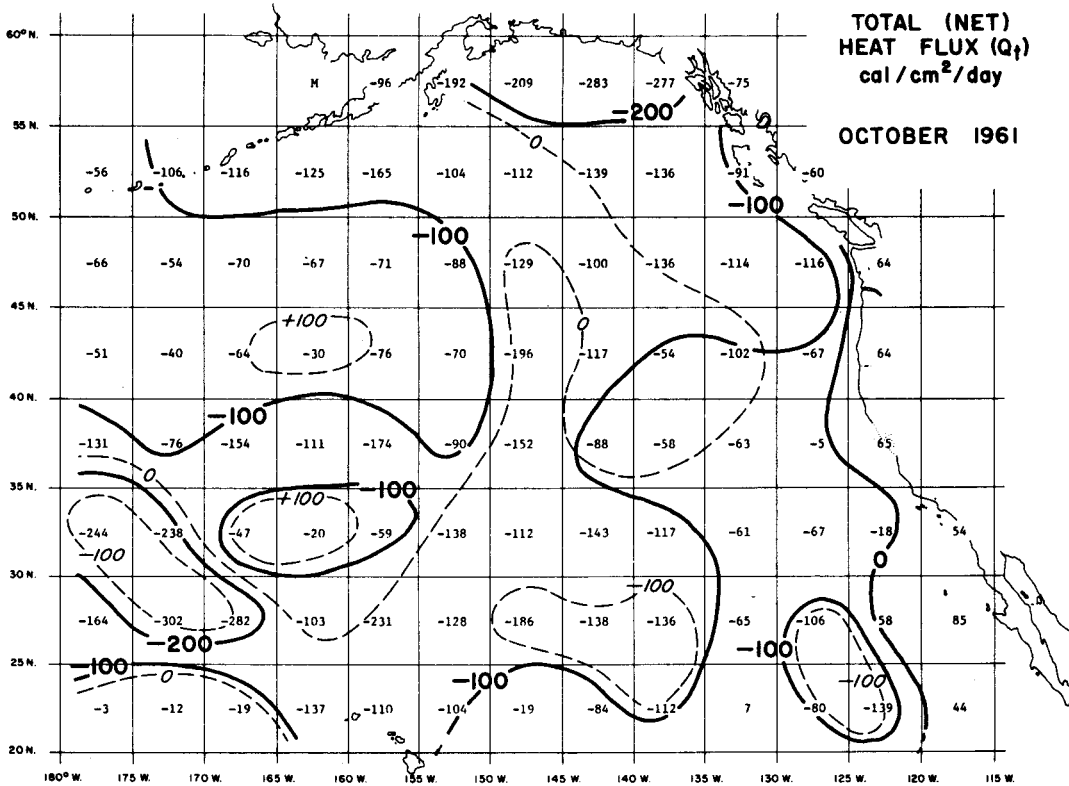
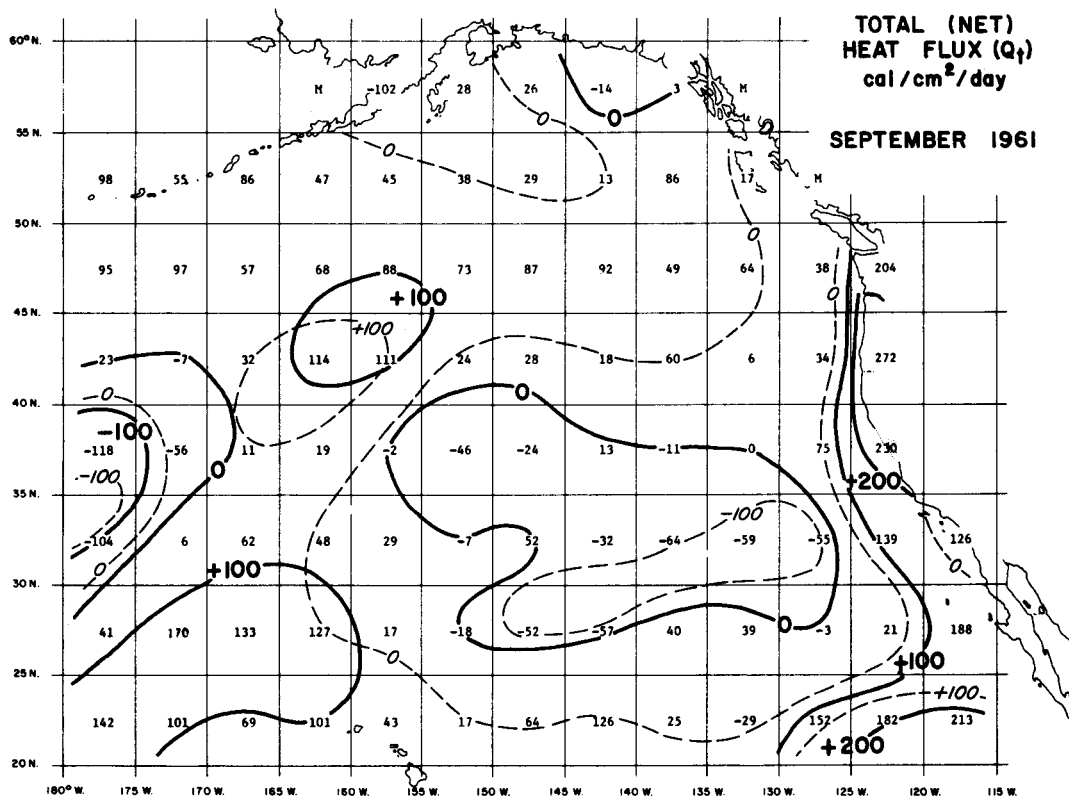
- BERLIAND, M. E., and T. G. BERLIAND.
1952. Opređenje effektivno izlučenja zemli s uchetom vli-janja oblachnosti (Determination of effective radiation of the

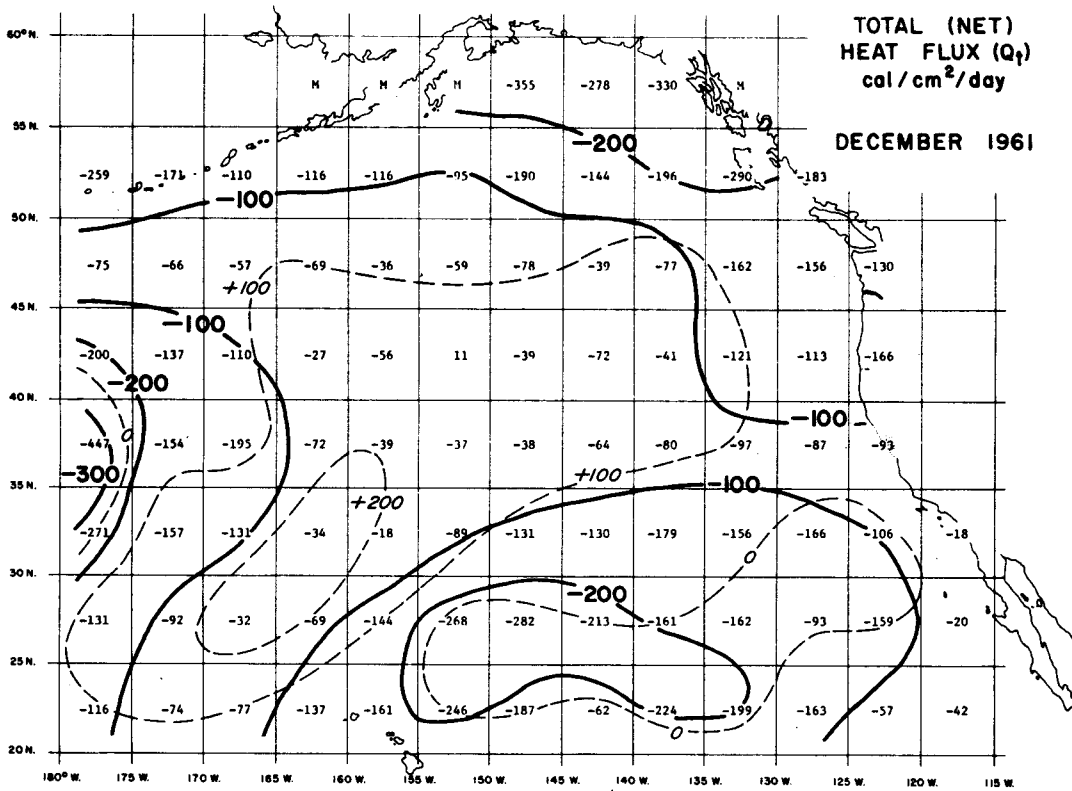
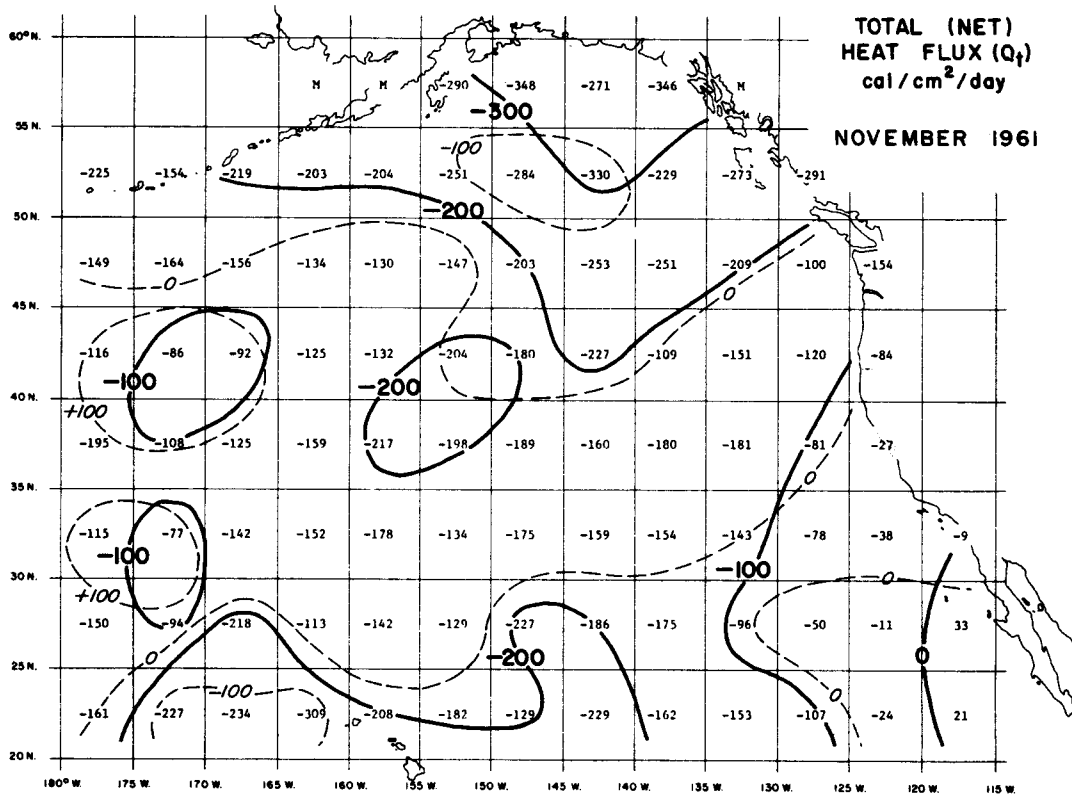
- earth as influenced by cloud cover). *Izvestiia Akad. Nauk USSR, Ser. Geofizicheskaiia*. No. 1. [Original not seen].
- BERLIAND, T. G.**
1960. Metodika klimatologicheskikh raschetov summarnoi radiatsii (Climatological method of total radiation calculations). *Meteorol. Gidrol.* 6:9-12.
- BOWEN, I. S.**
1926. The ratio of heat losses by conduction and by evaporation from any water surface. *Phys. Rev., Ser. 2*, 27:779-787.
- BUDYKO, M. I.**
1956. Teplovoy balans zemnoy poverkhnosti (The heat balance of the earth's surface). [In Russ.] *Gidrometeorol. Izd.* 255 p. [Translated by N. A. Stepanova, 1958, 259 p.; available U.S. Dep. Commer., Off. Tech. Serv., Wash., D.C.]
- CLARK, N. E.**
1972. Specification of sea surface temperature anomaly patterns in the eastern North Pacific. *J. Phys. Oceanogr.* 2:391-404.
- FLITTNER, G. A.**
1970. Forecasting availability of albacore tuna in the eastern Pacific Ocean. *In* T. Laevastu and I. Hela (editors), *Fisheries oceanography*, p. 116-158. Fishing News (Books) Ltd., Lond.
- JOHNSON, J. H.**
1962. Sea temperatures and the availability of albacore off the coasts of Oregon and Washington. *Trans. Am. Fish. Soc.* 91:269-274.
- JOHNSON, J. H., G. A. FLITTNER, and M. W. CLINE.**
1965. Automatic data processing program for marine synoptic radio weather reports. U.S. Fish Wildl. Serv., Spec. Sci. Rep. Fish. 503, iv + 74 p.
- NAMIAS, J.**
1969. Seasonal interactions between the North Pacific Ocean and the atmosphere during the 1960's. *Mon. Weather Rev.* 97:173-192.
1971. The 1968-69 winter as an outgrowth of sea and air coupling during antecedent seasons. *J. Phys. Oceanogr.* 1:65-81.
- SECKEL, G. R.**
1970. The trade wind zone oceanography pilot study. Part VIII: Sea-level meteorological properties and heat exchange processes, July 1963 to June 1965. U.S. Fish Wildl. Serv., Spec. Sci. Rep. Fish. 612, iv + 129 p.
- SETTE, O. E.**
1961. Problems in fish population fluctuations. *Calif. Coop. Oceanic Fish. Invest. Rep.* 8:21-24.
- TABATA, S.**
1958. Heat budget of the water in the vicinity of Triple Island, British Columbia. *J. Fish. Res. Board Can.* 15:429-451.
- UDA, M.**
1957. A consideration on the long years trend of the fisheries fluctuations in relation to sea conditions. *Bull. Jap. Soc. Sci. Fish.* 23:368-372.
1961. Fisheries oceanography in Japan, especially on the principles of fish distribution, concentration, dispersal and fluctuation. *Calif. Coop. Oceanic Fish. Invest. Rep.* 8:25-31.
- WYRTKI, K.**
1966. Seasonal variation of heat exchange and surface temperature in the North Pacific Ocean. Report for NSF Grant No. GP-5534, Hawaii Inst. Geophysics, Univ. Hawaii, 80 p.

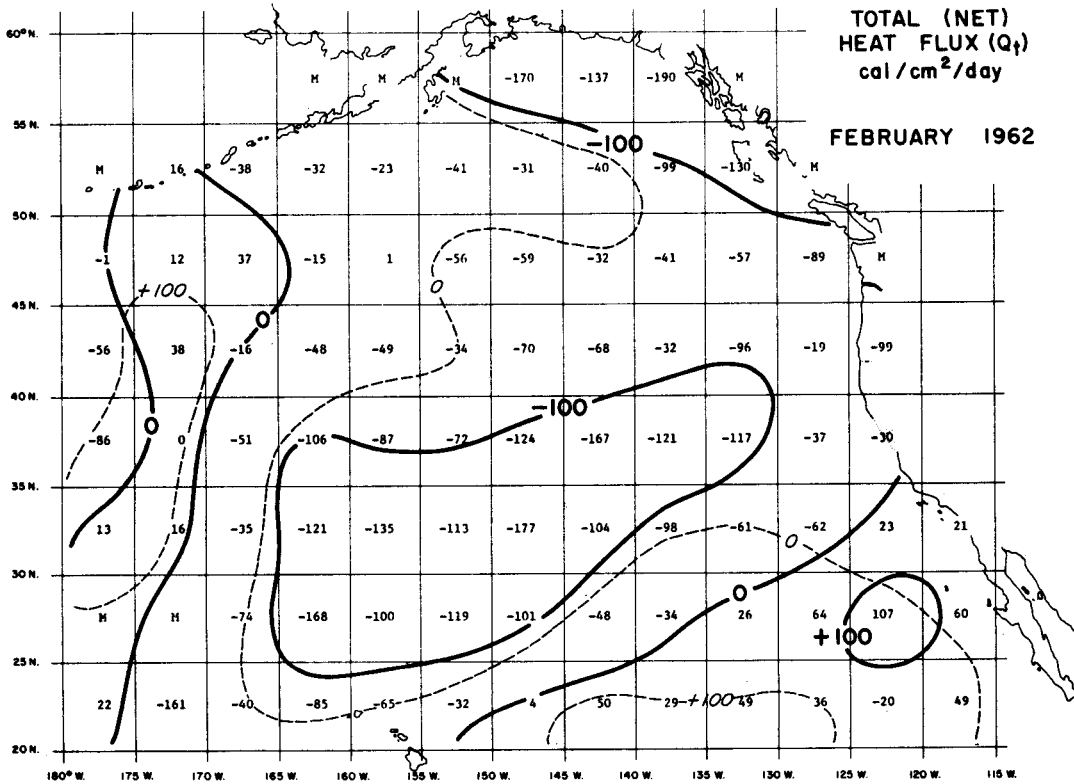
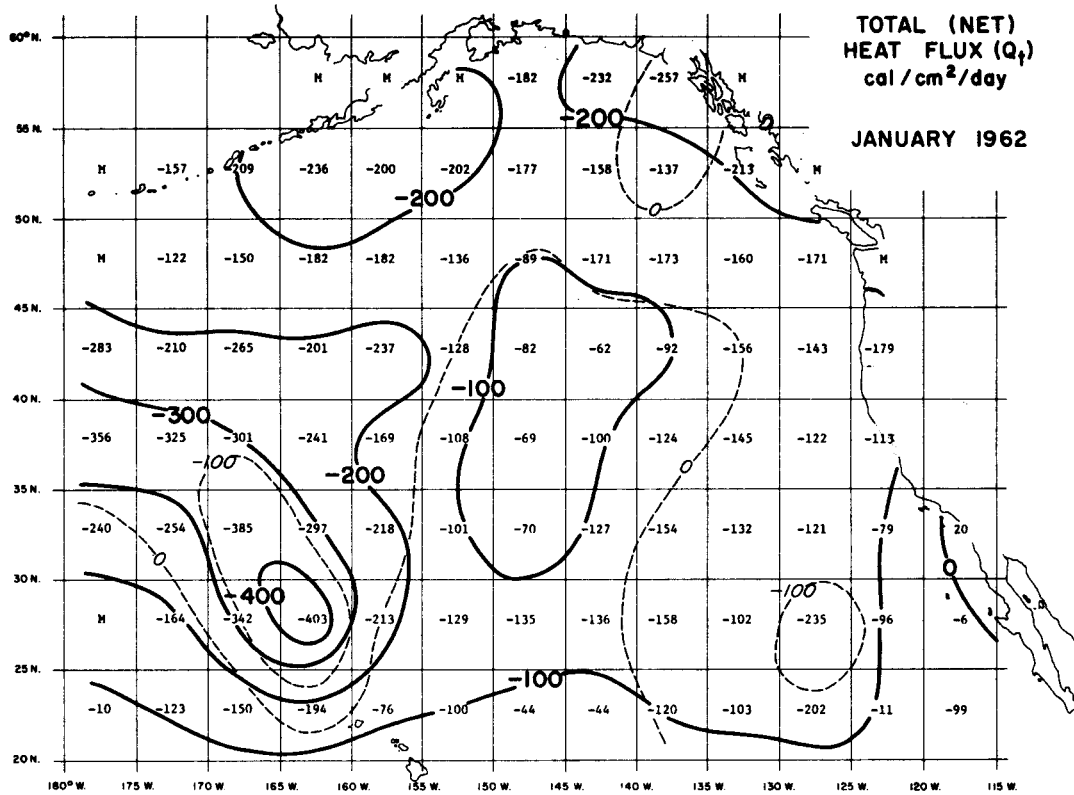
**PART 1. TOTAL (NET) HEAT FLUX MONTHLY AVERAGES AND ANOMALIES, JANUARY
1961 TO DECEMBER 1971.**

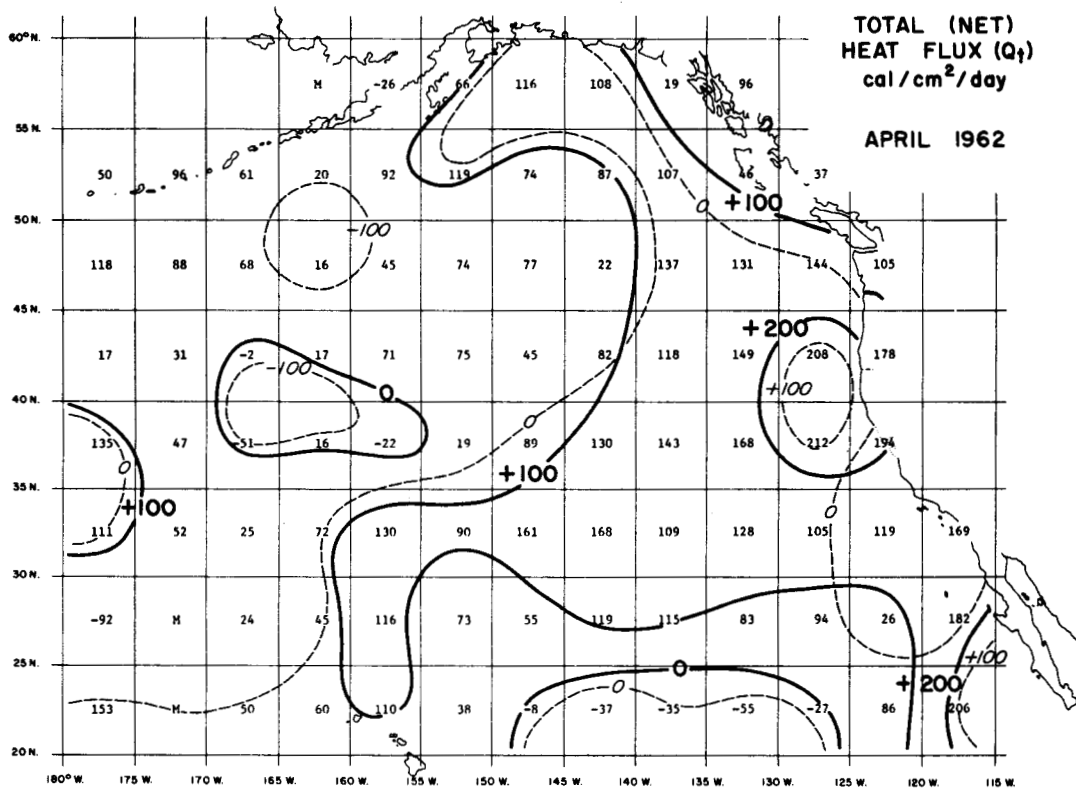
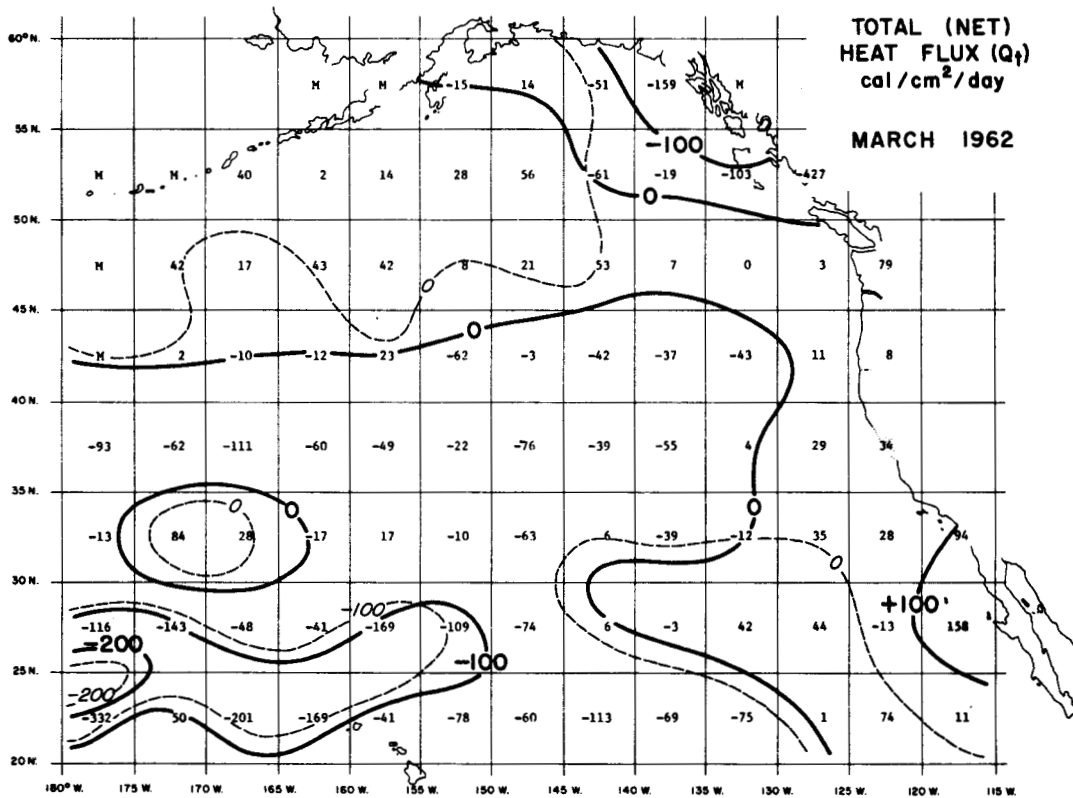


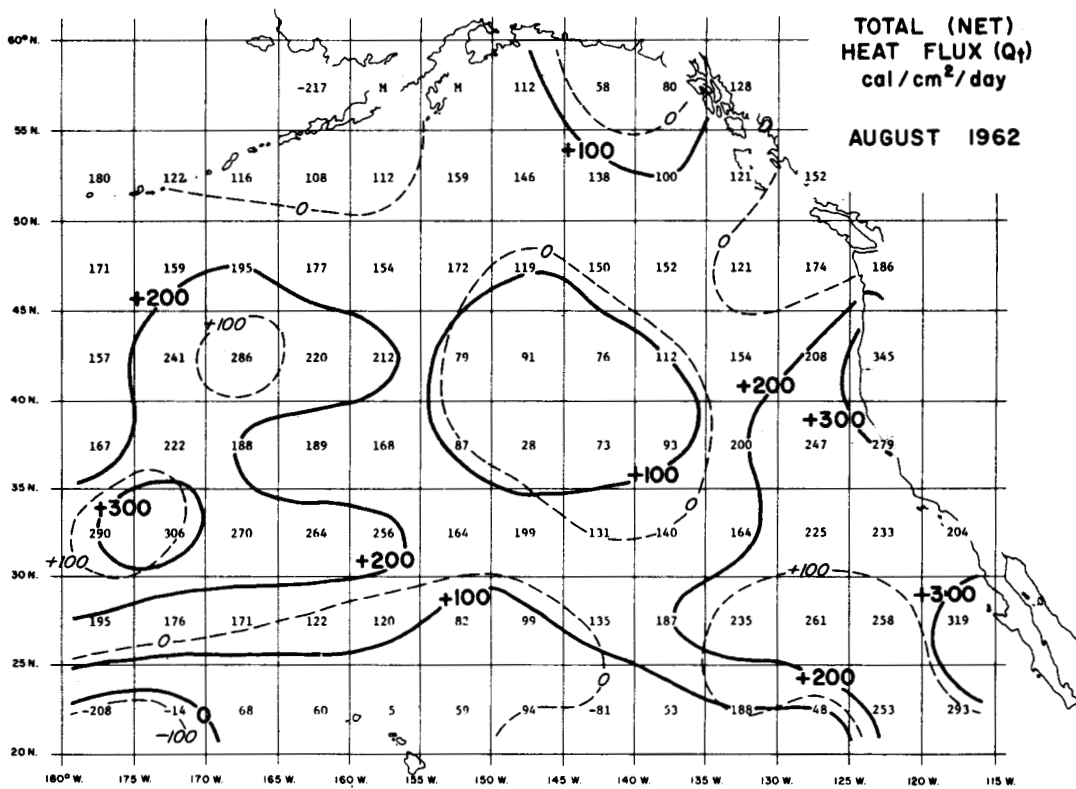
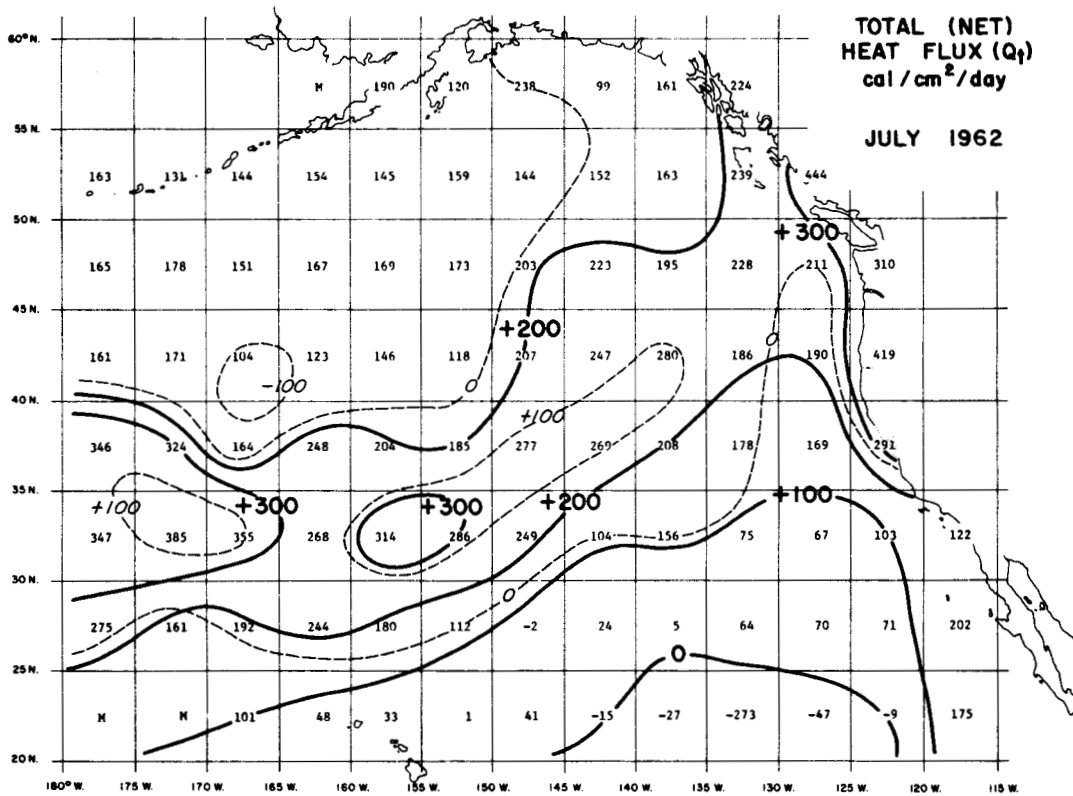


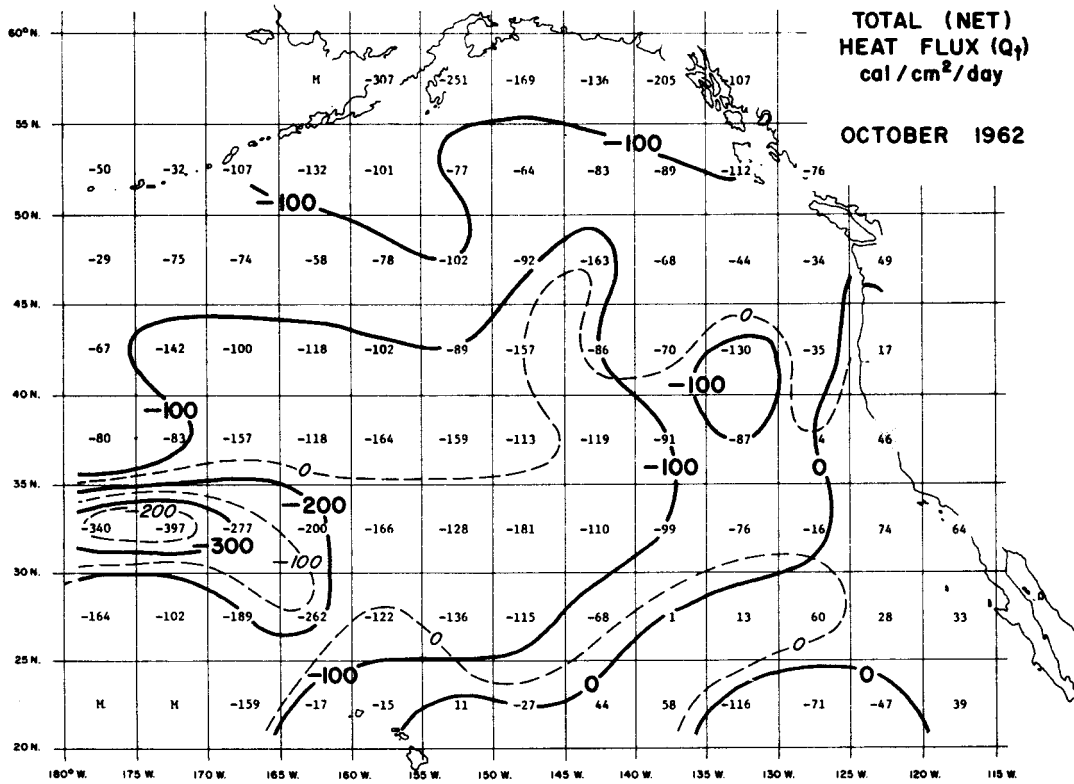
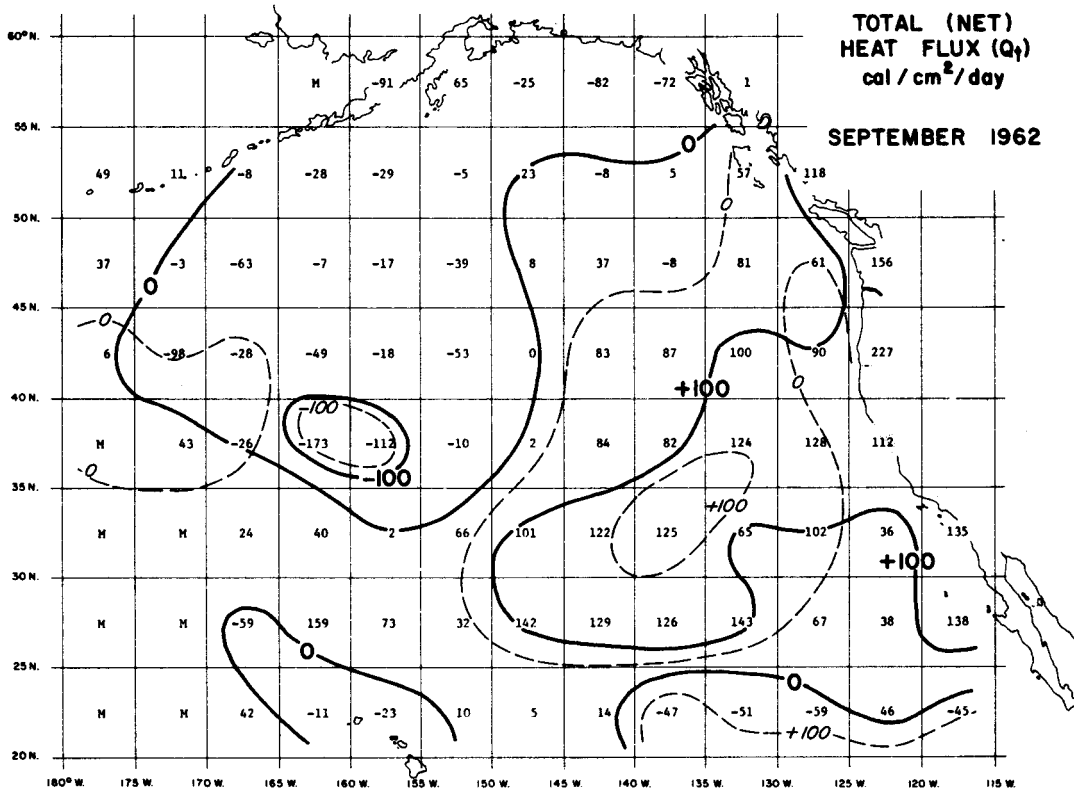


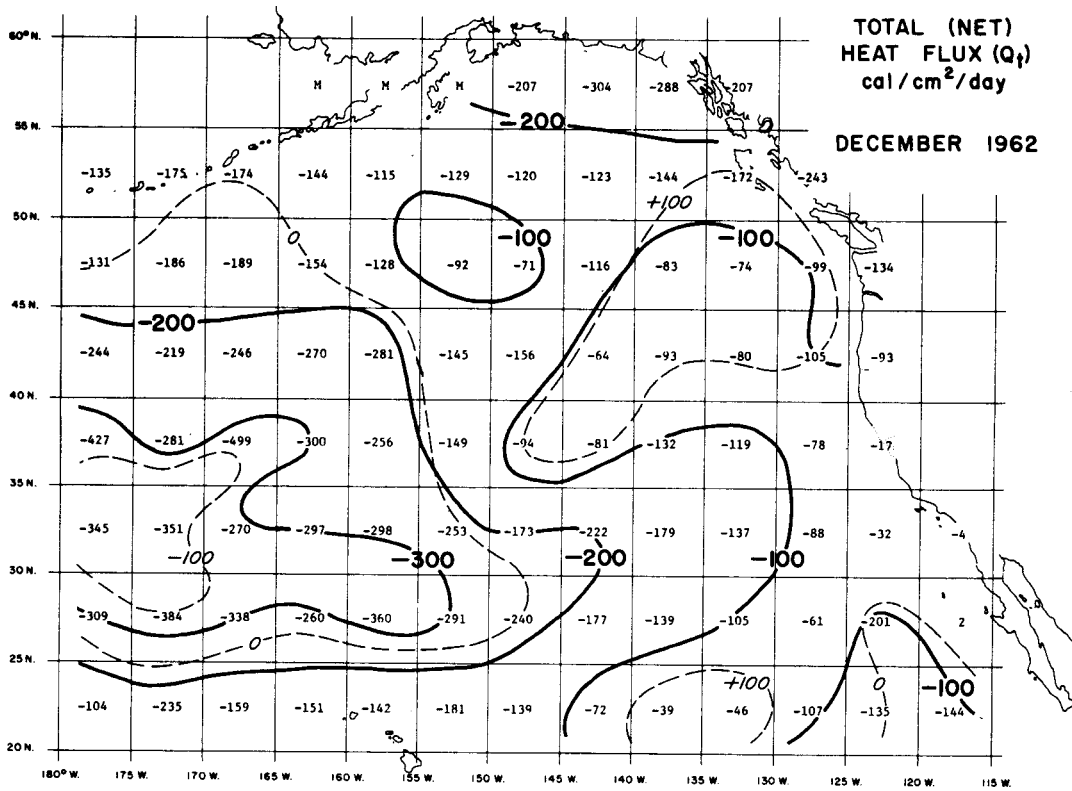
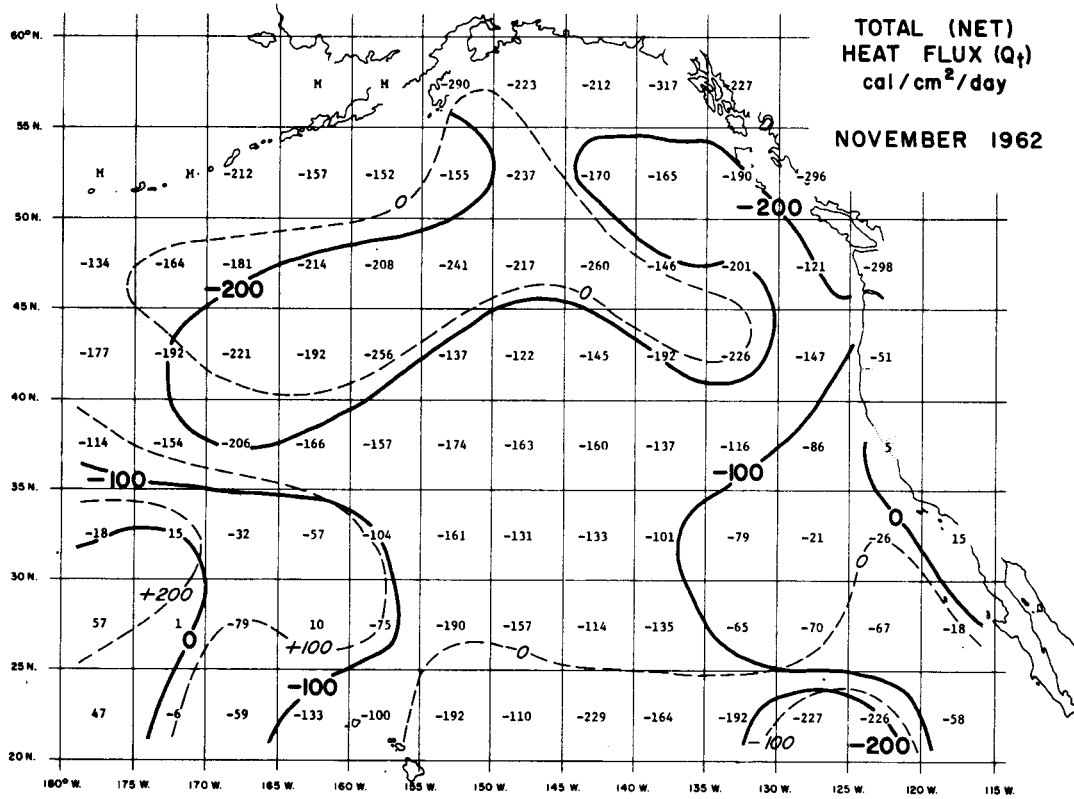


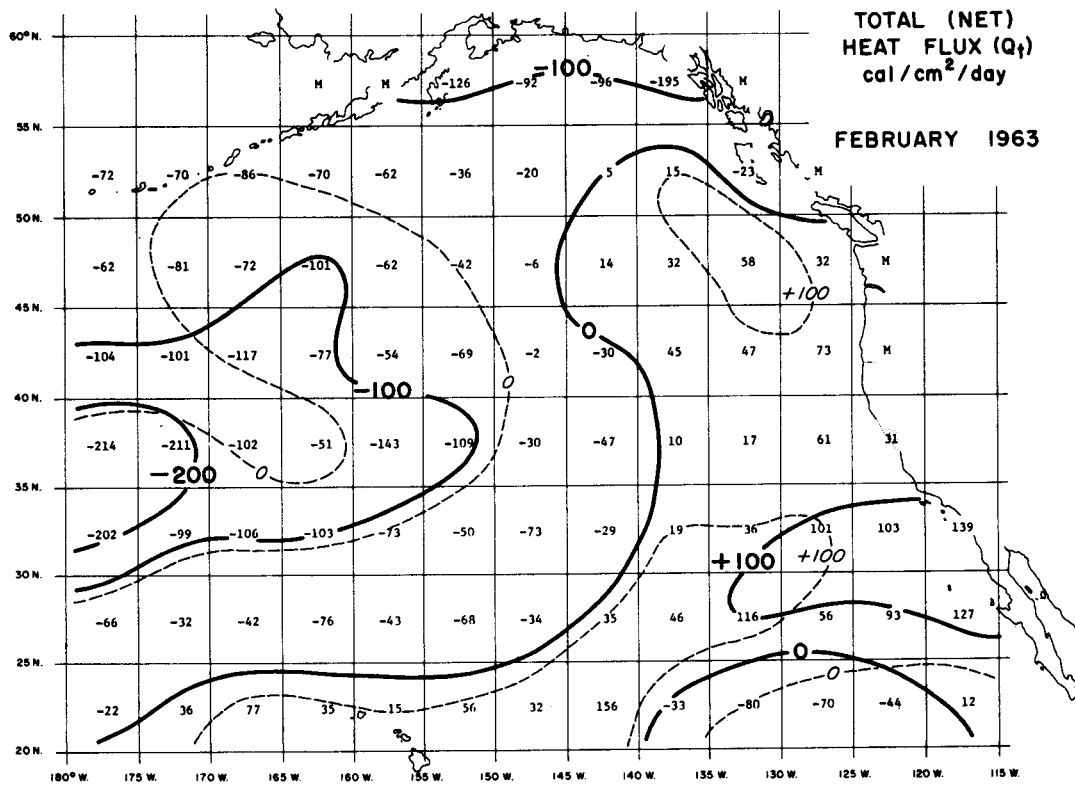
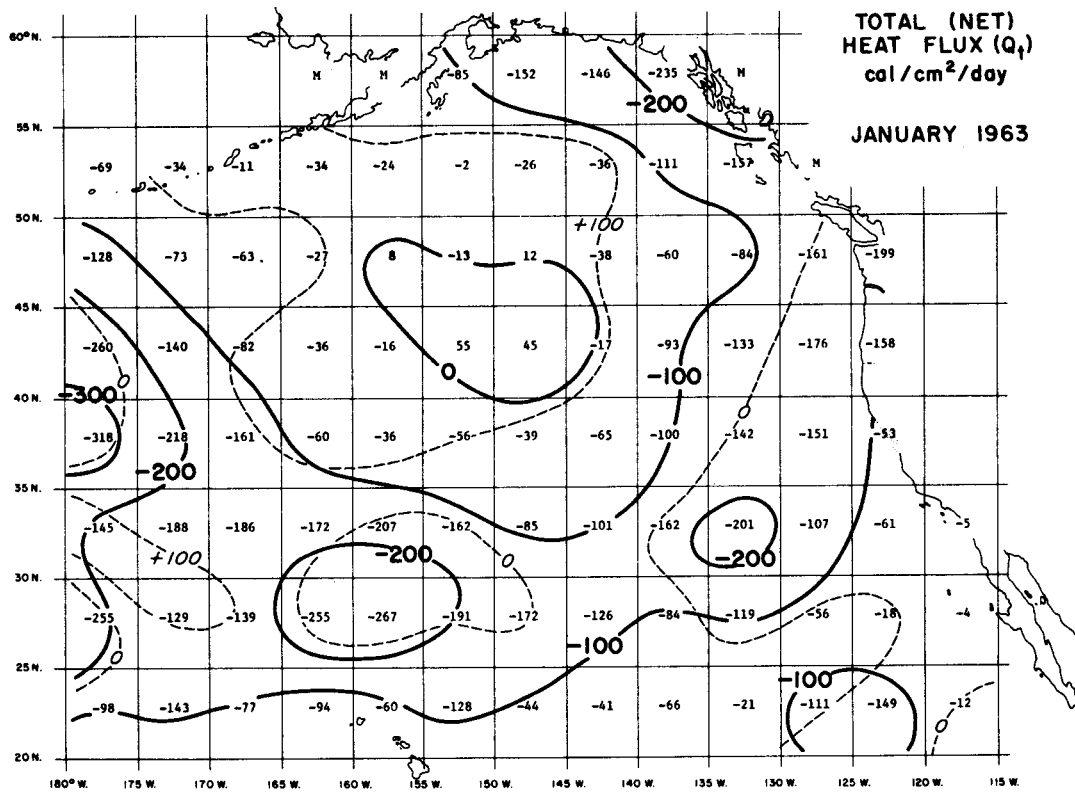


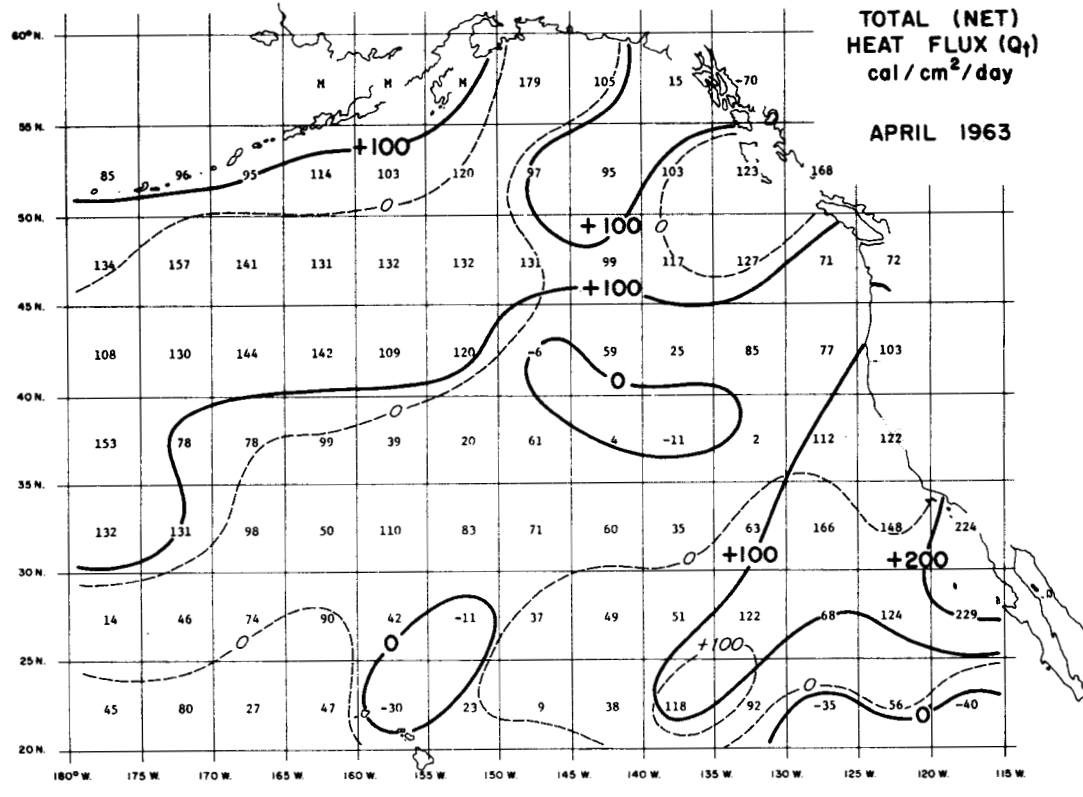
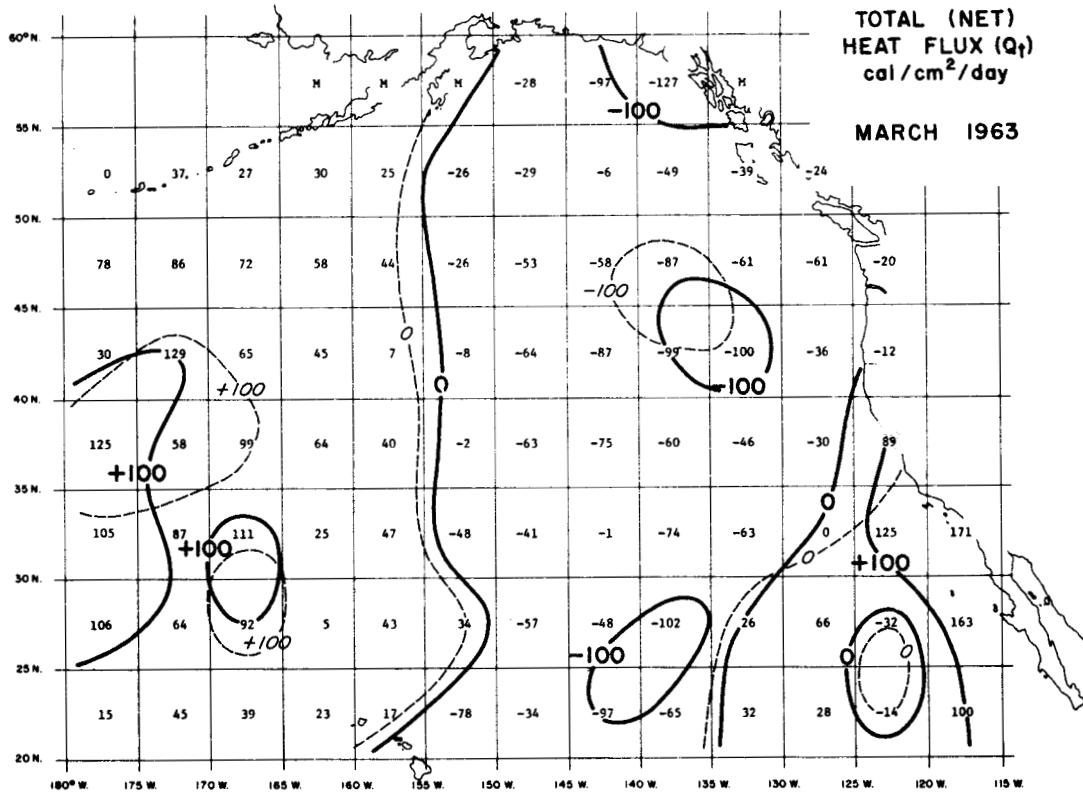


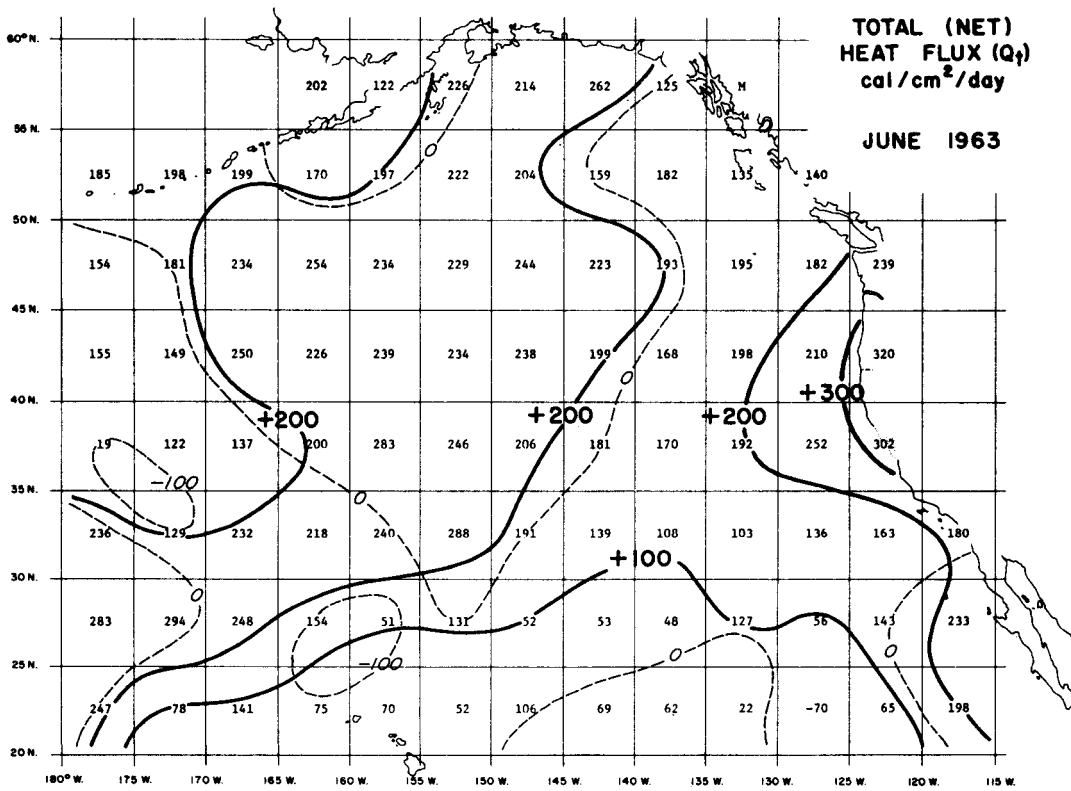
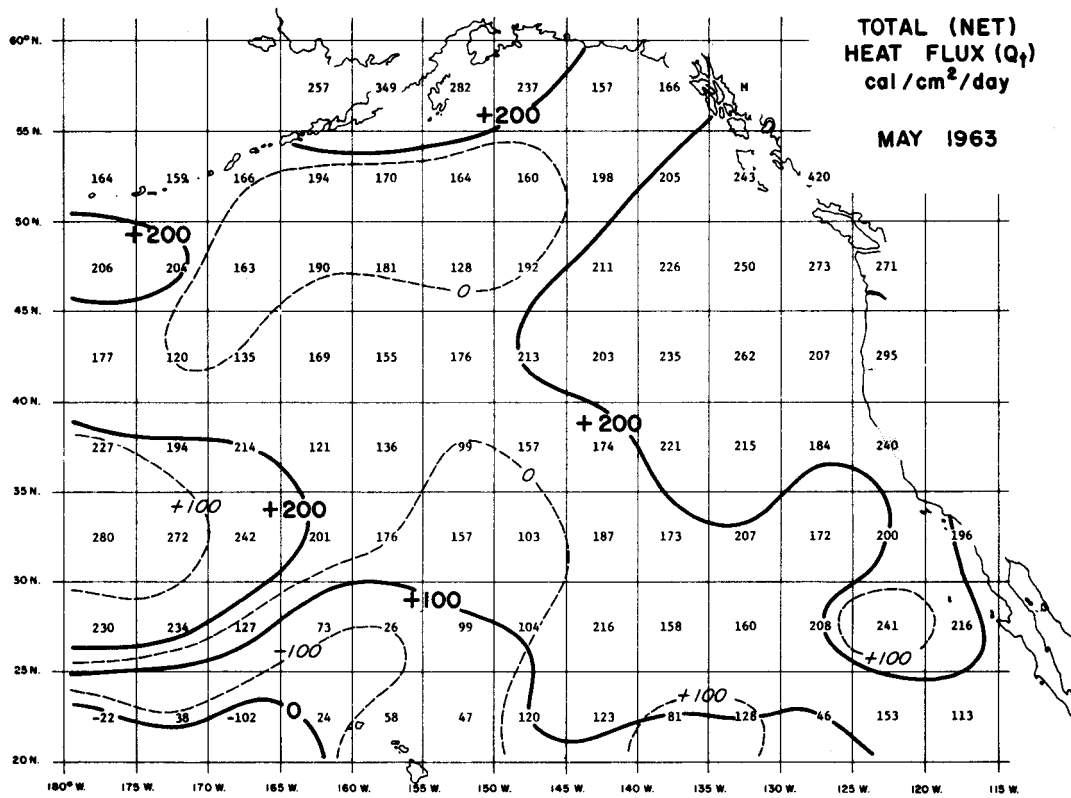


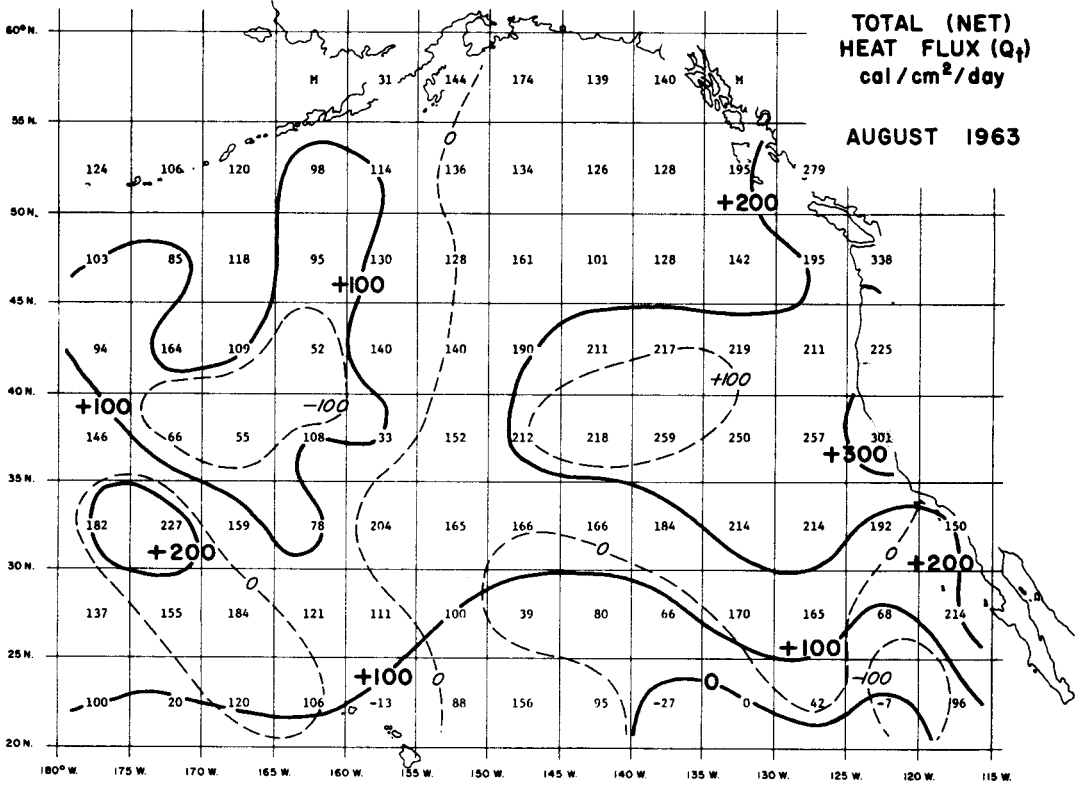
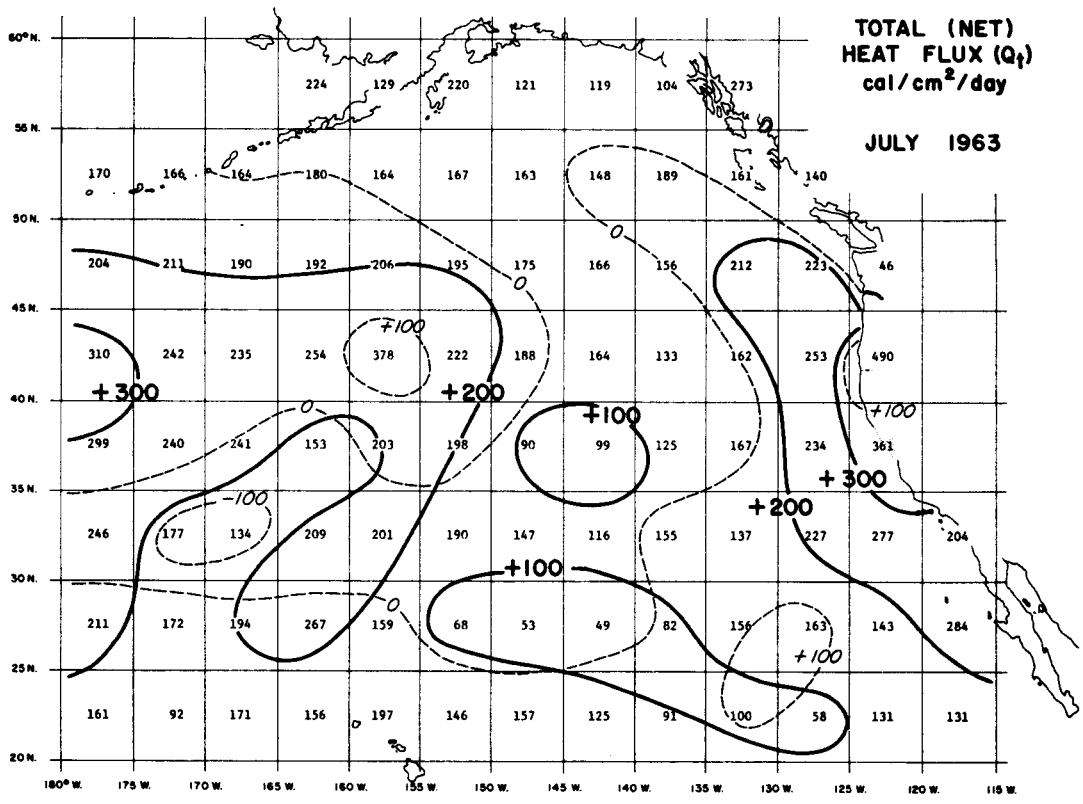


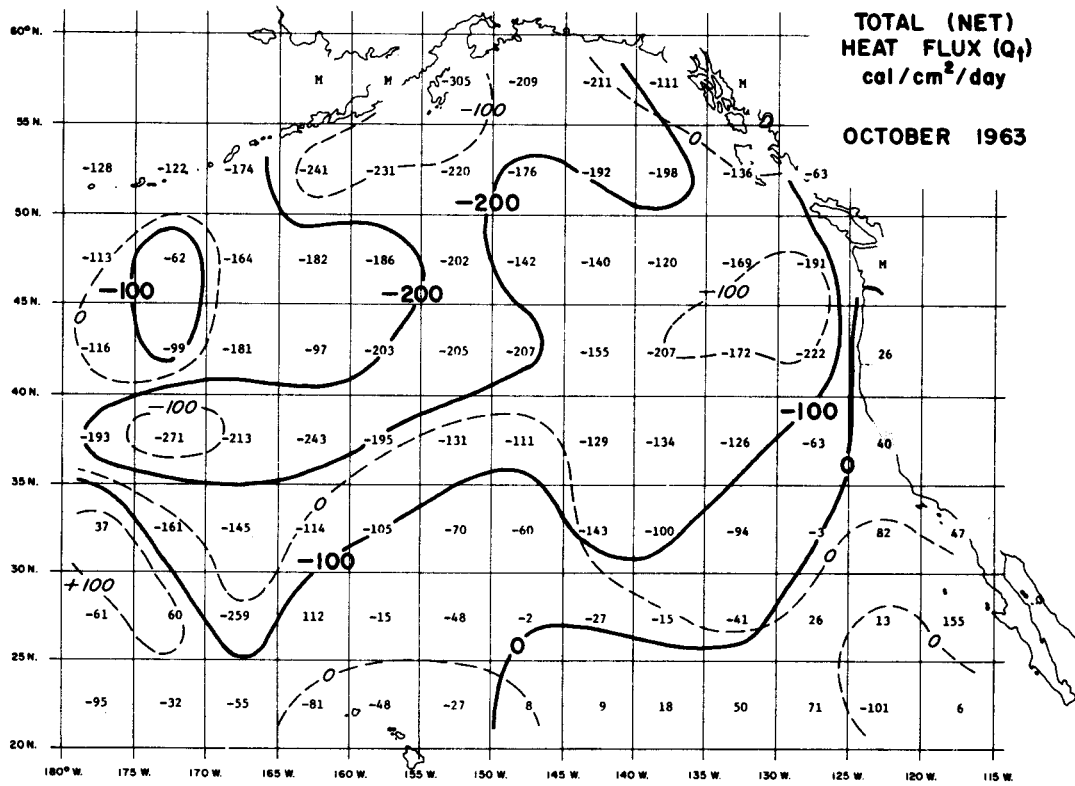
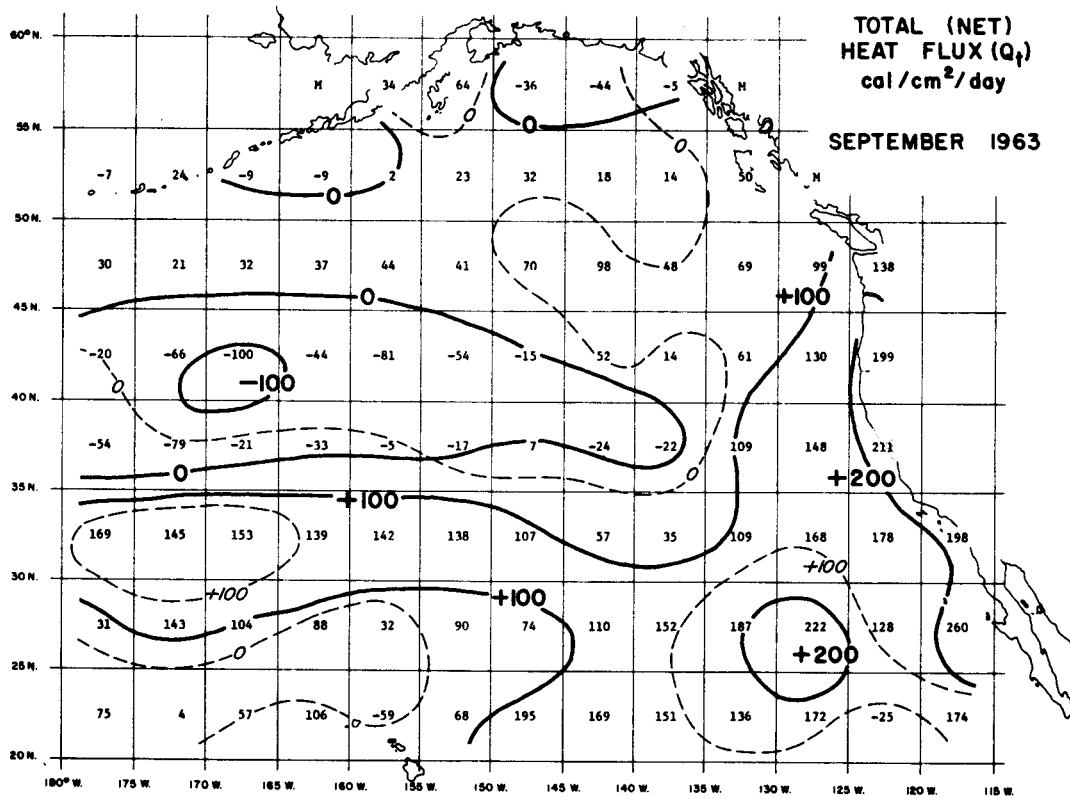


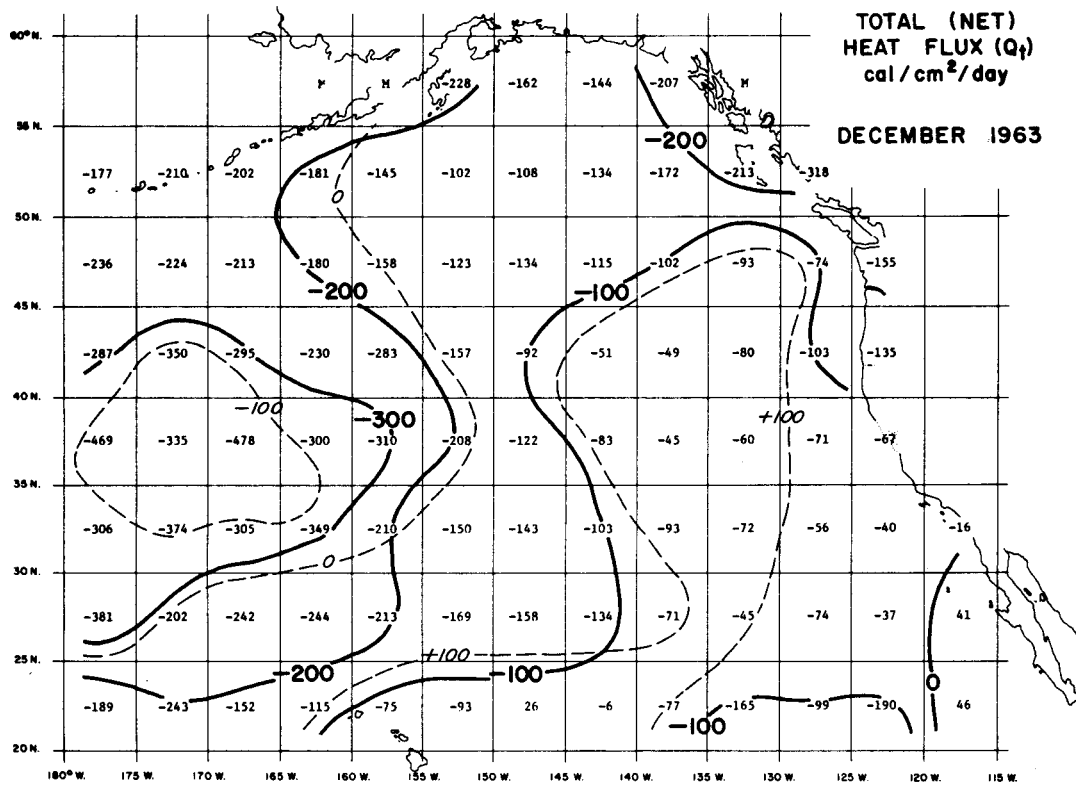
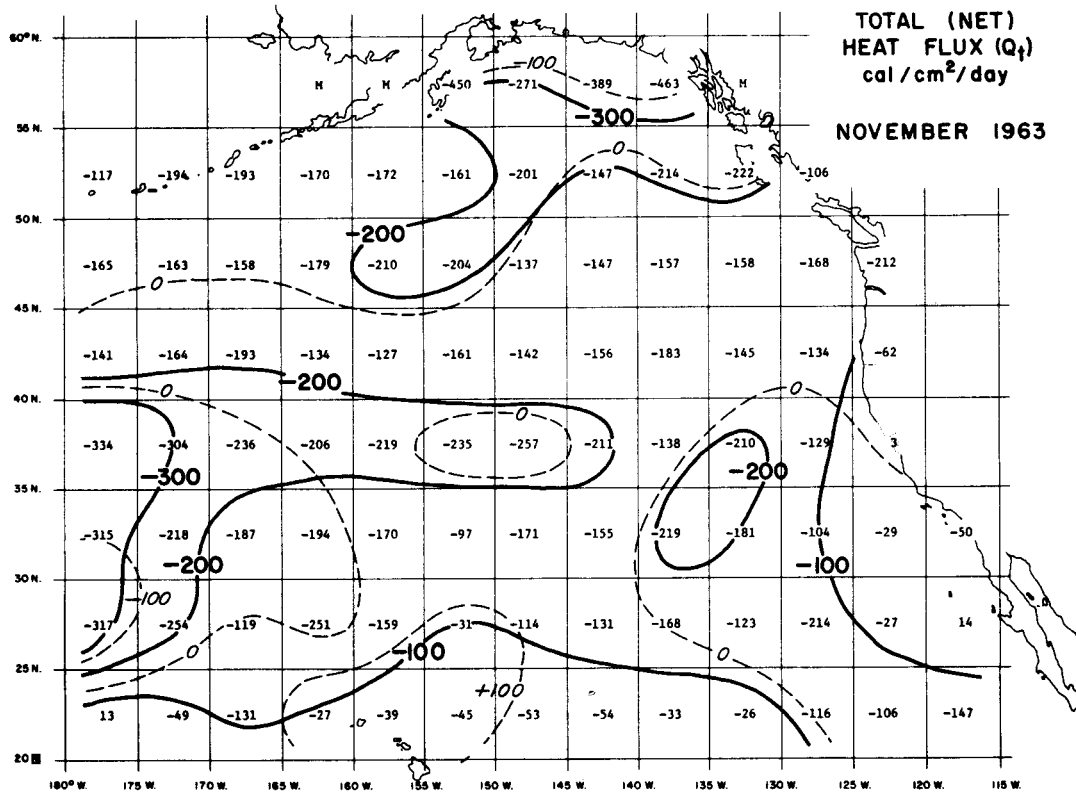


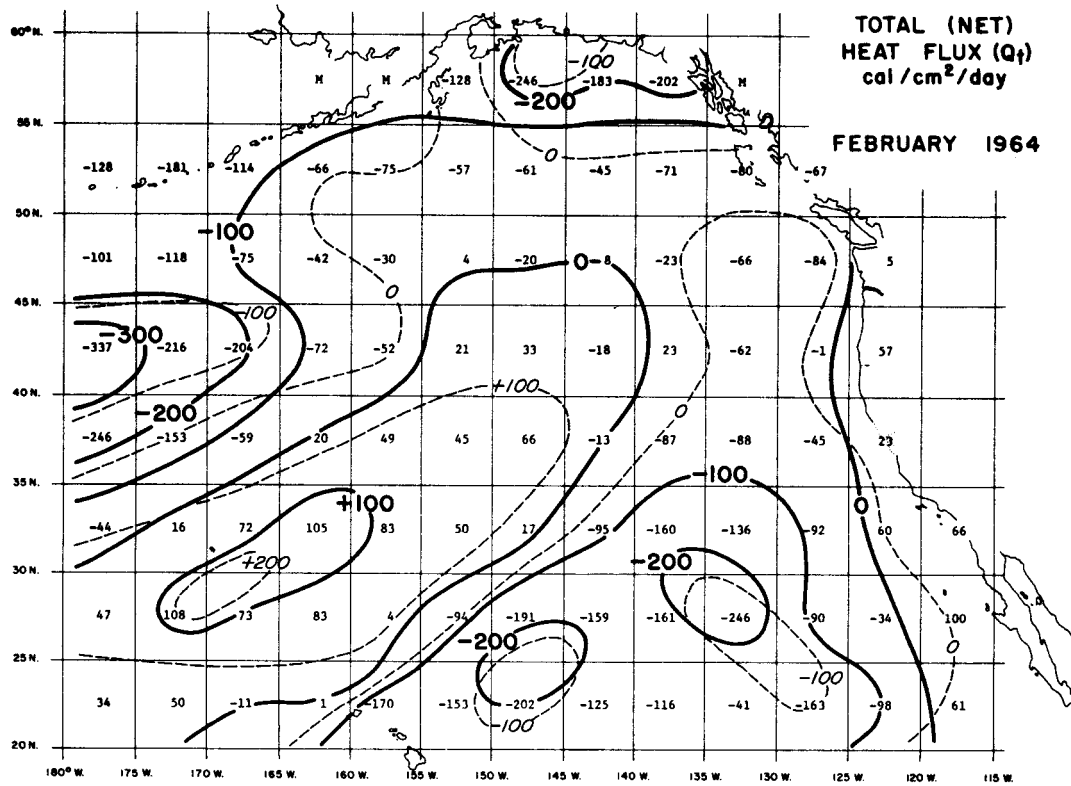
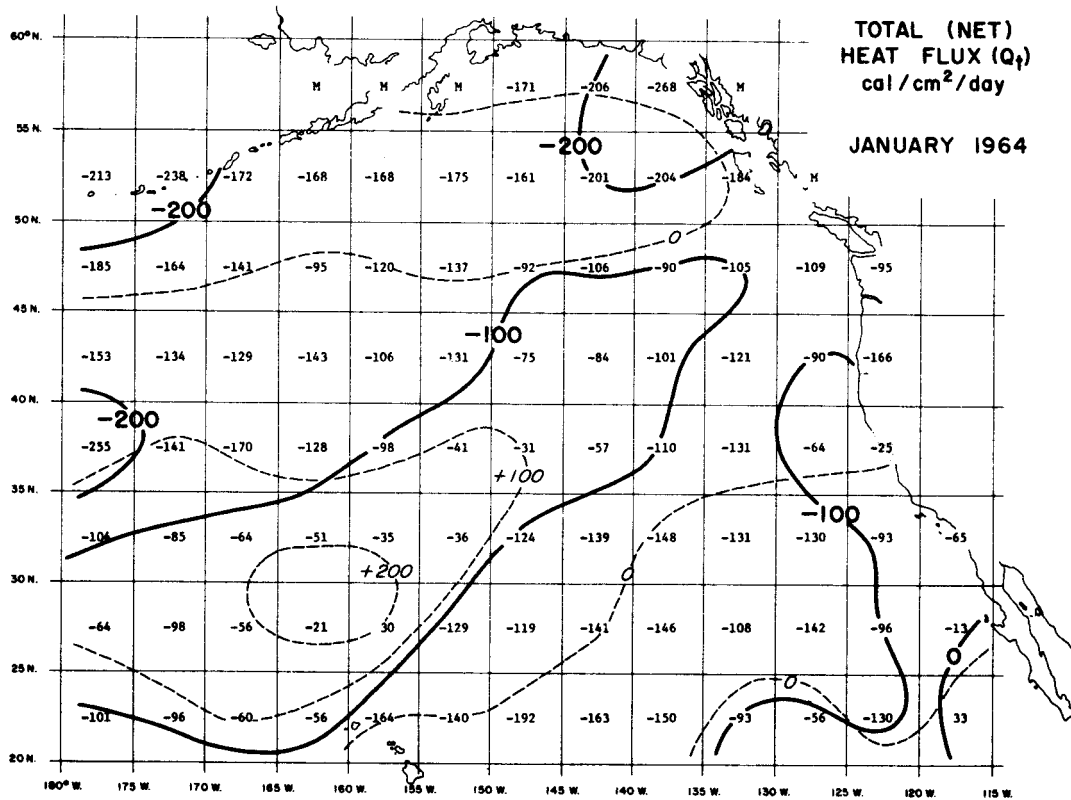


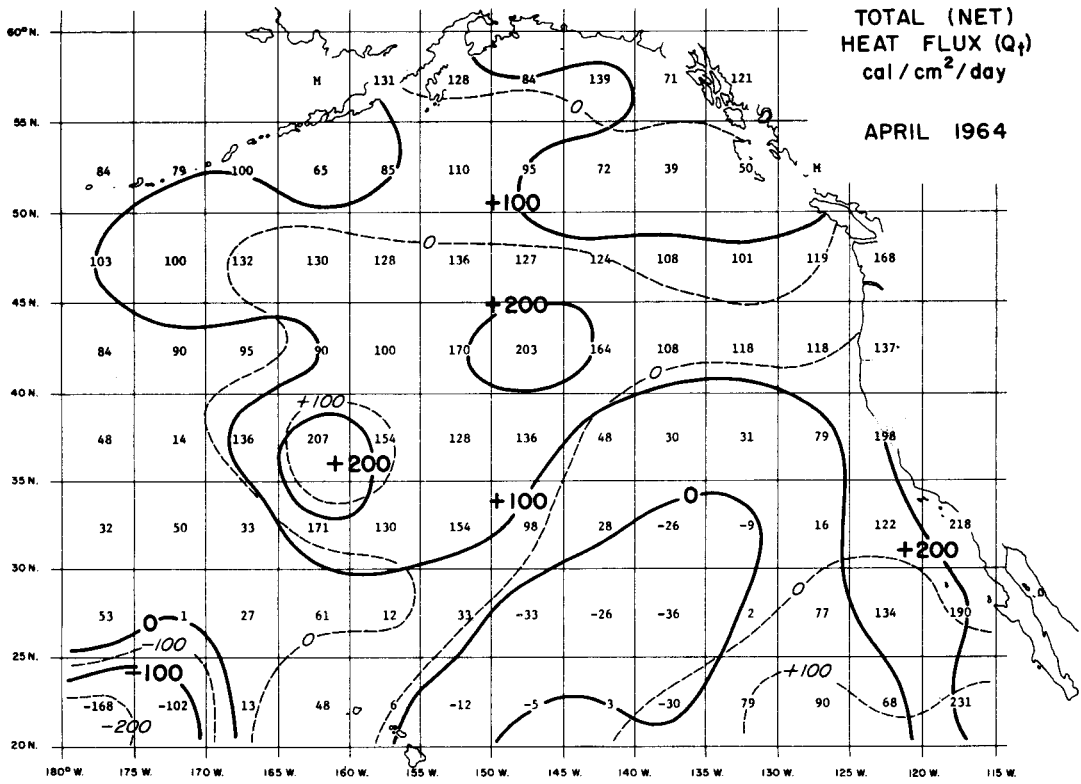
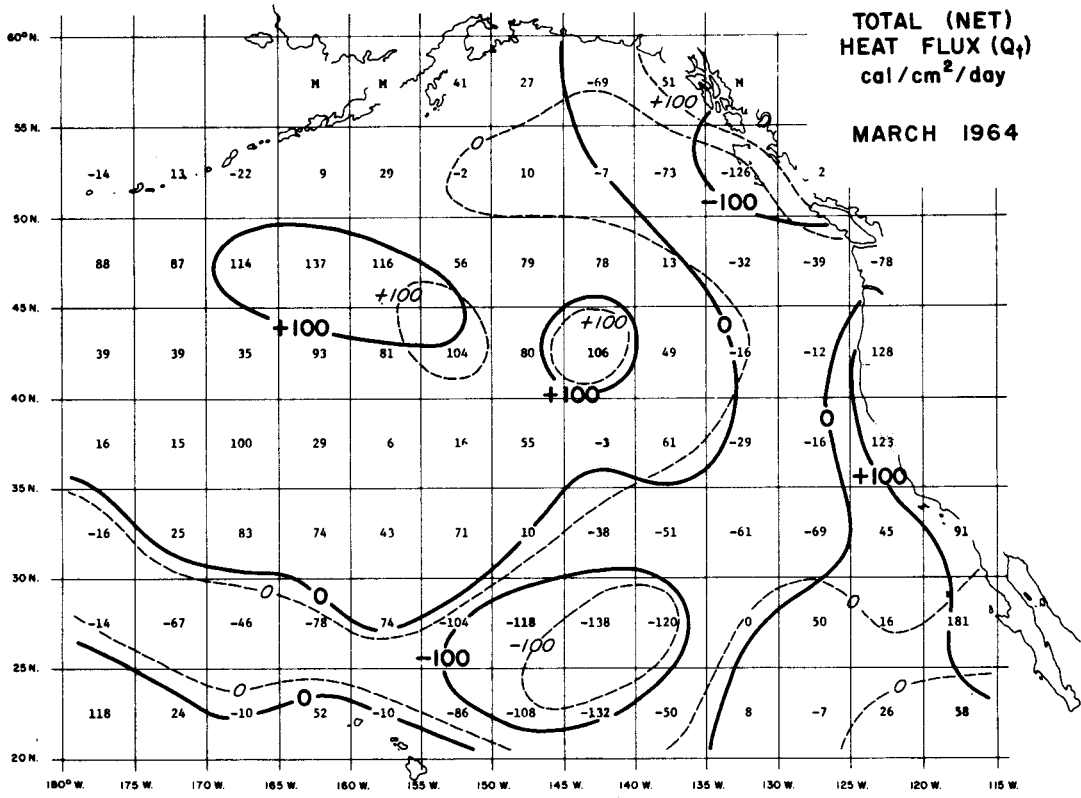


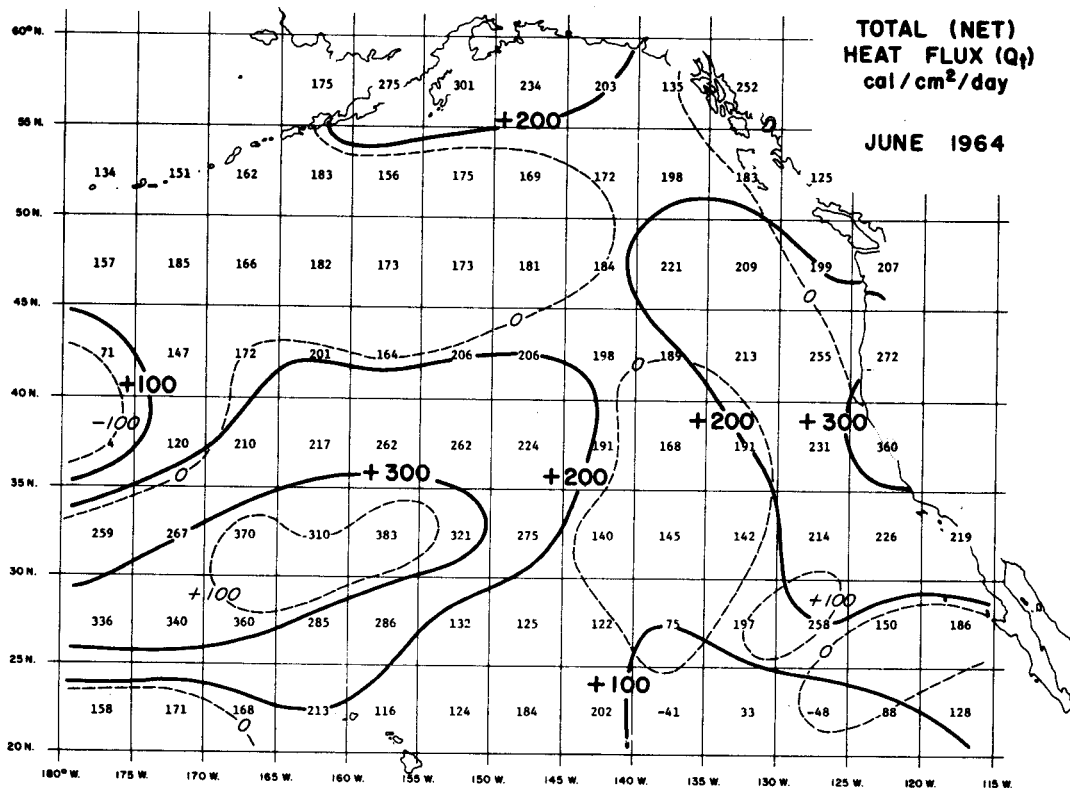
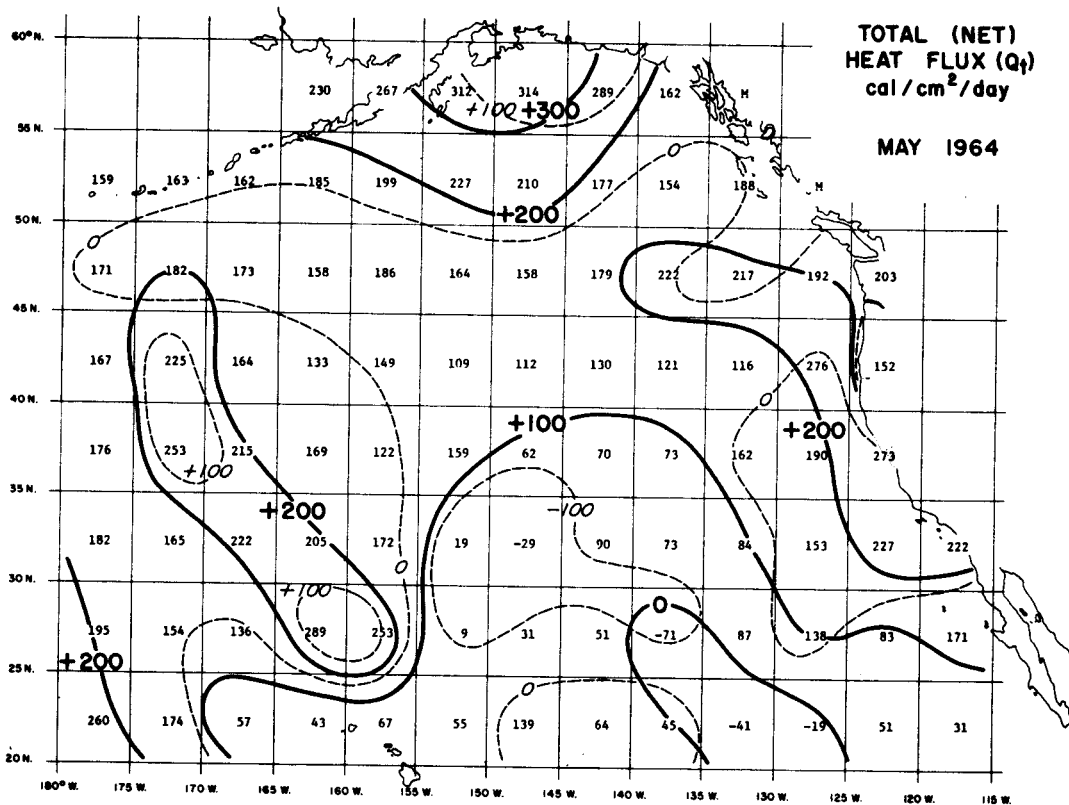


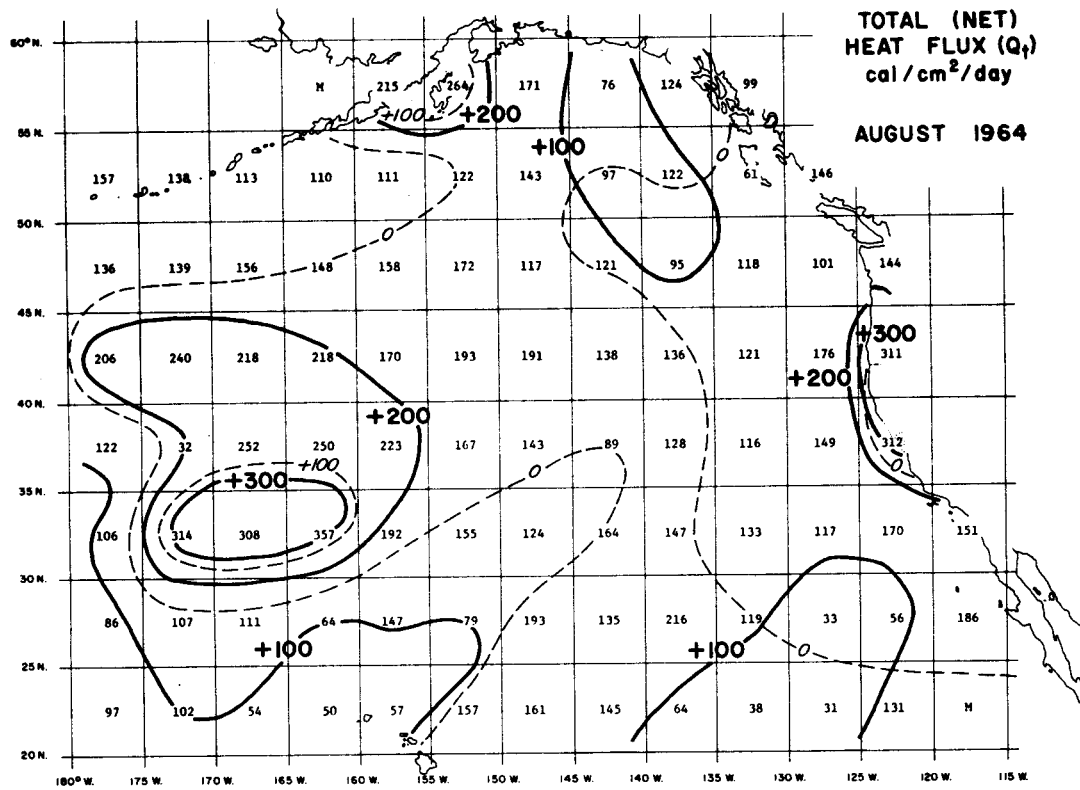
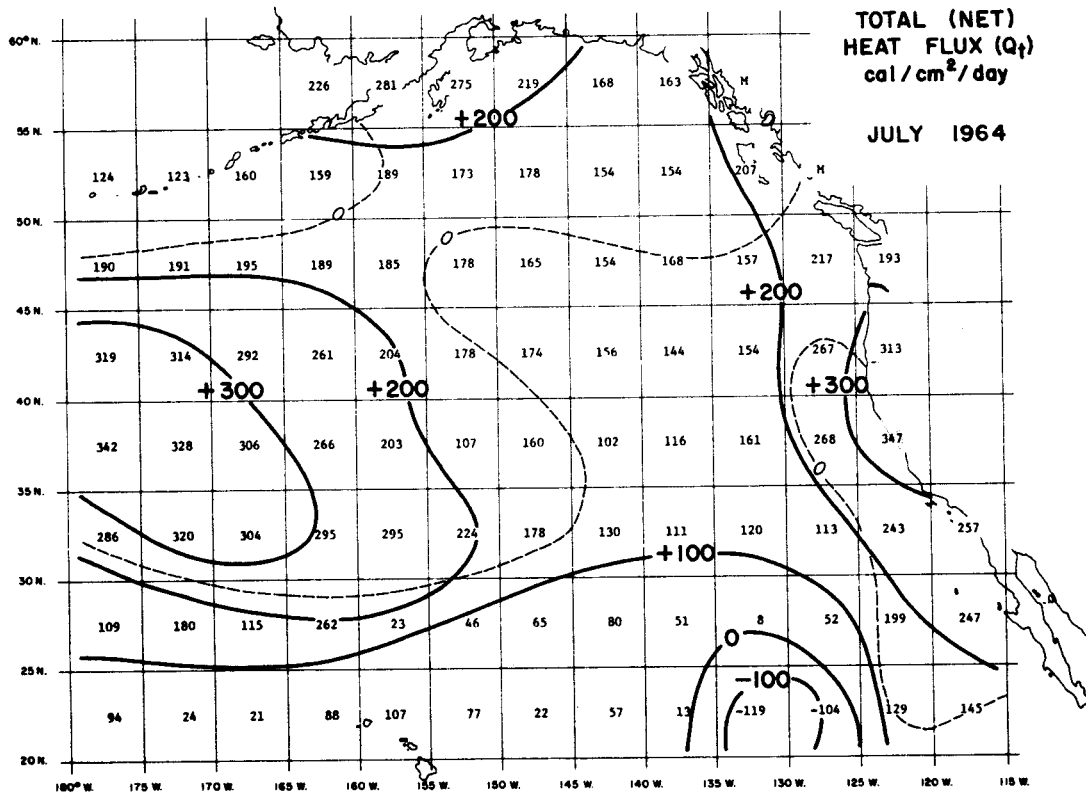


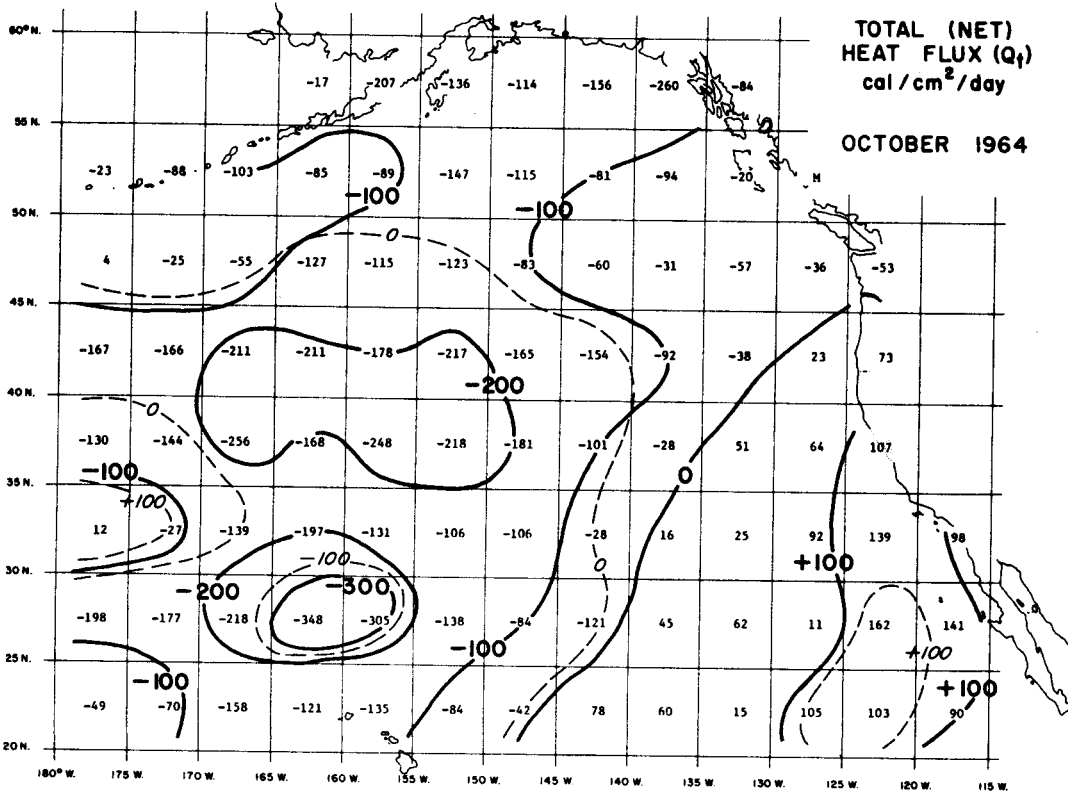
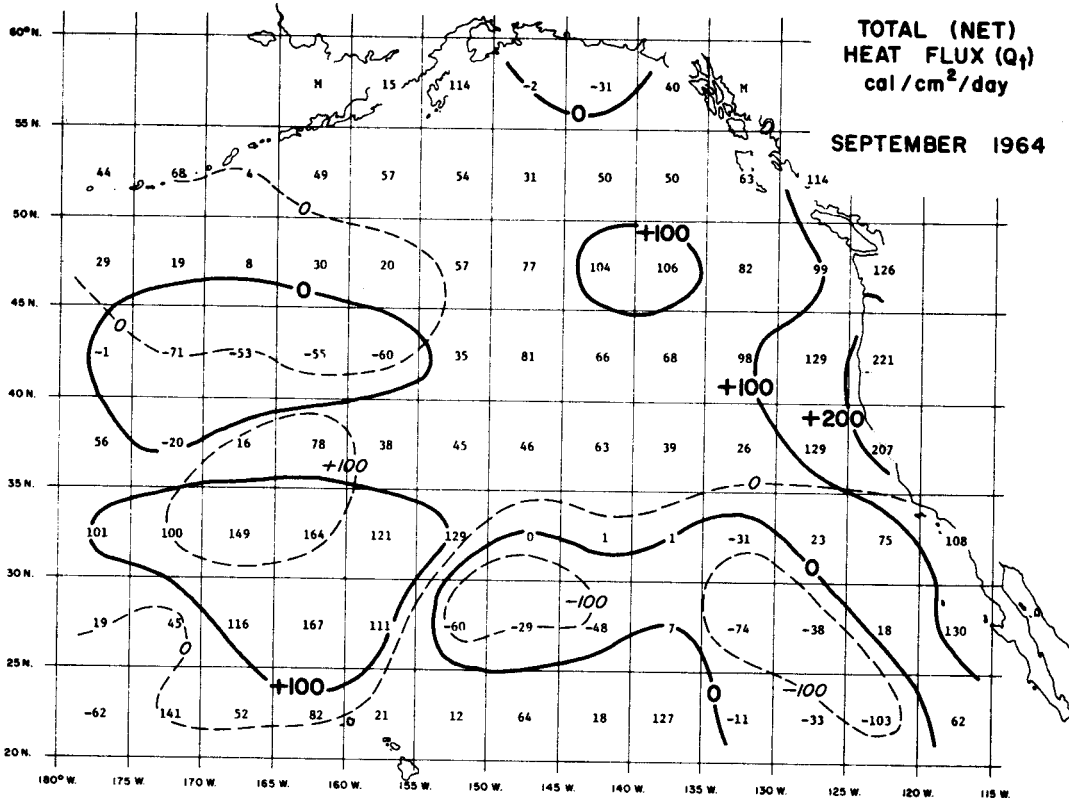


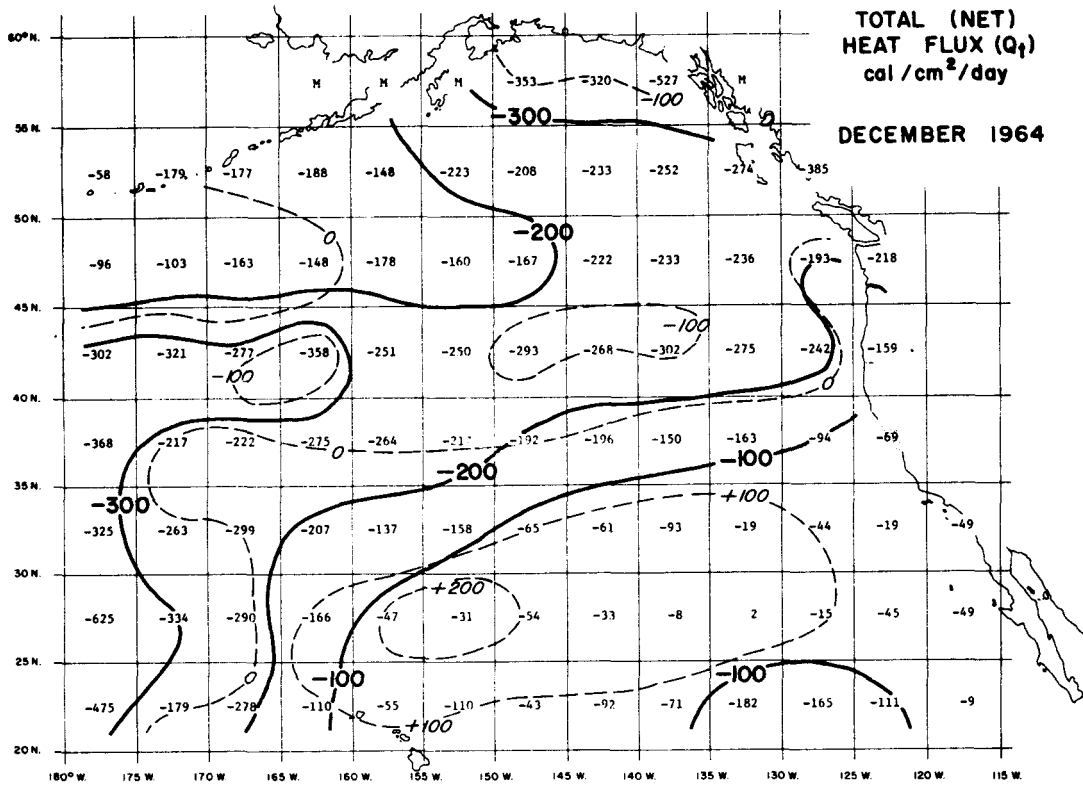
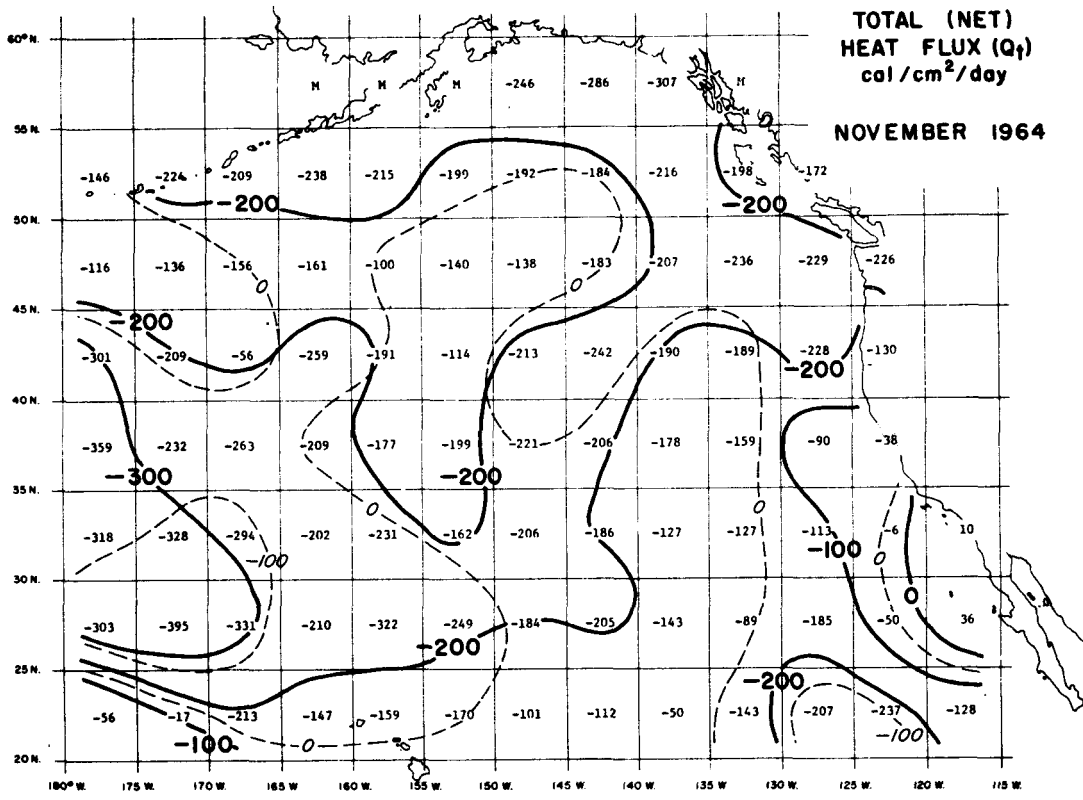


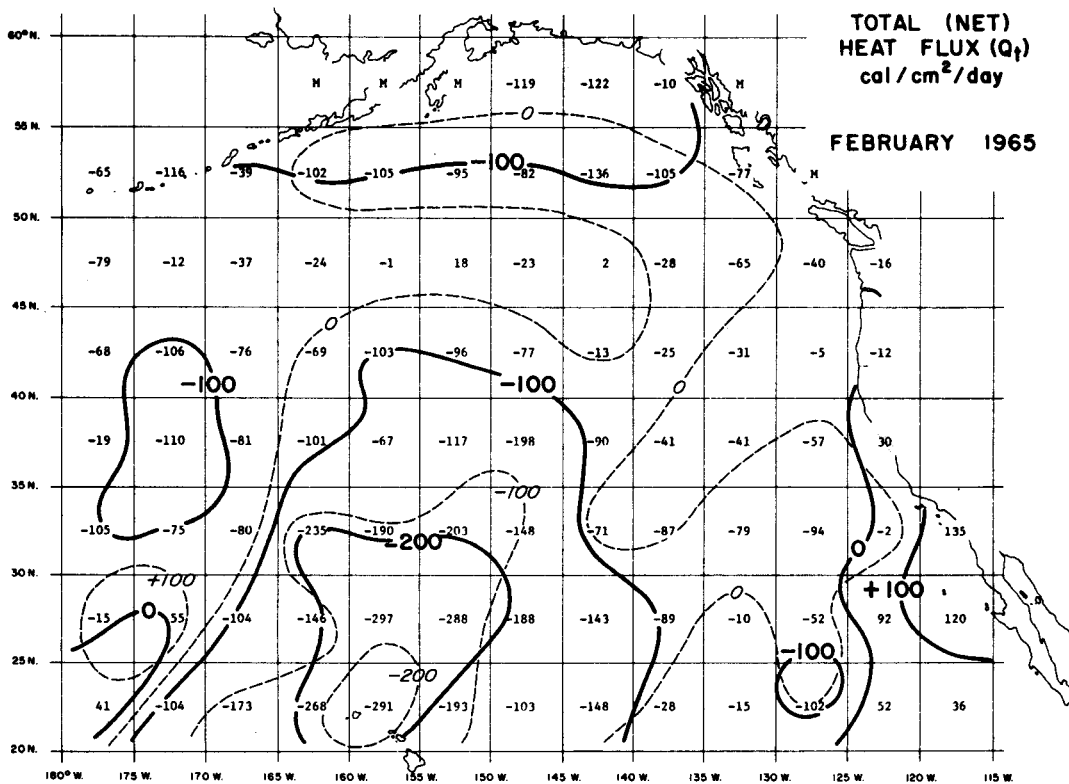
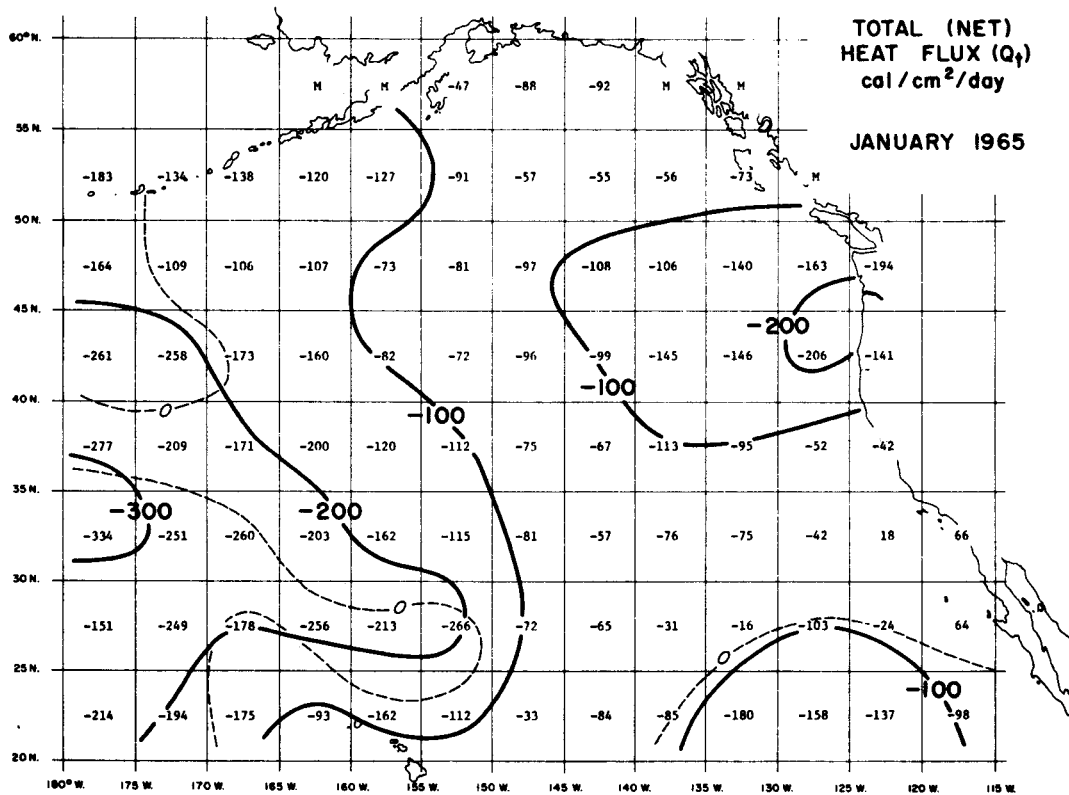


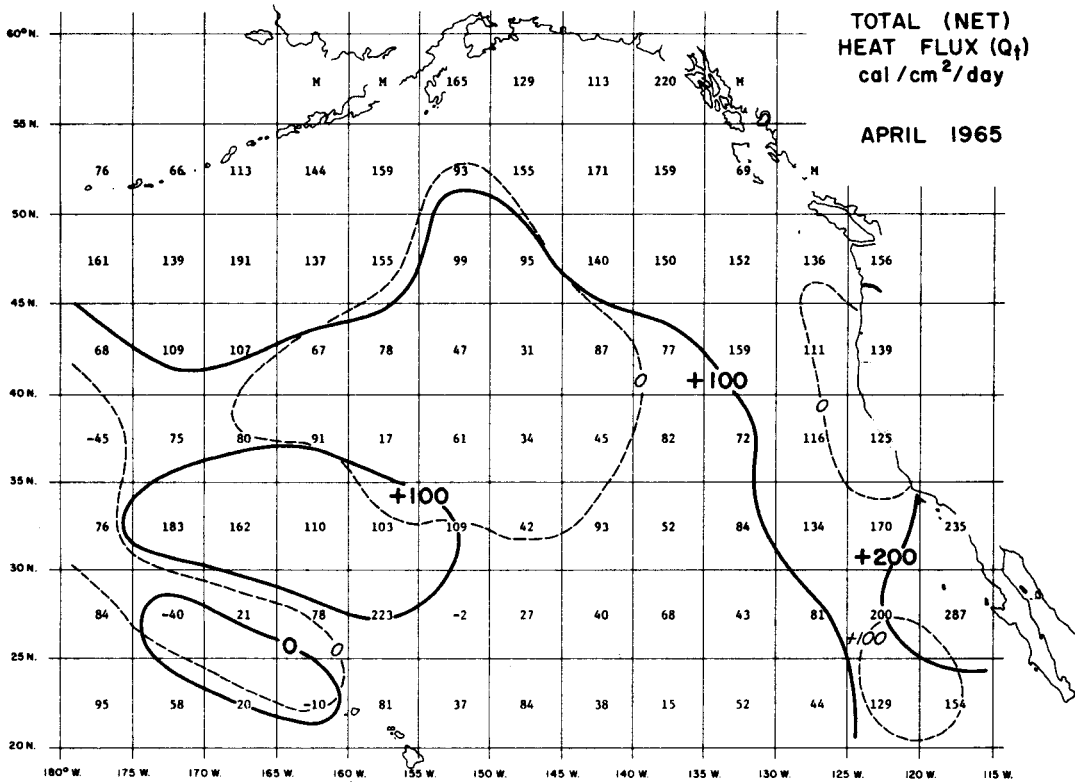
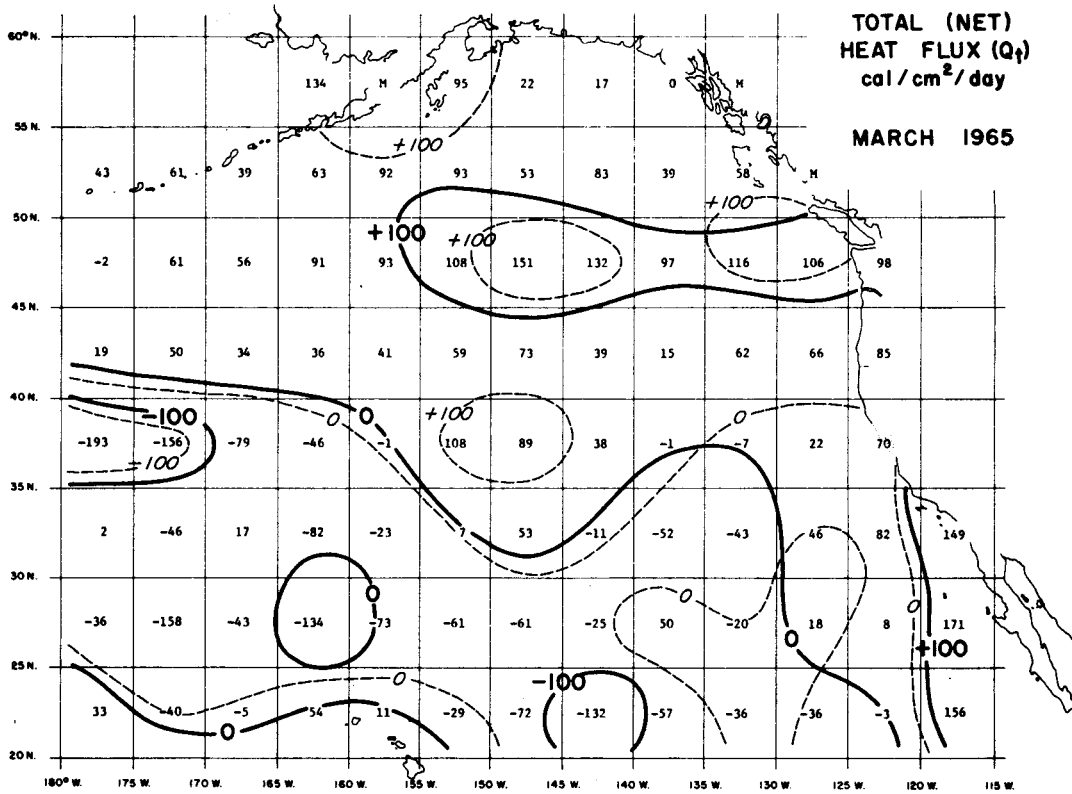


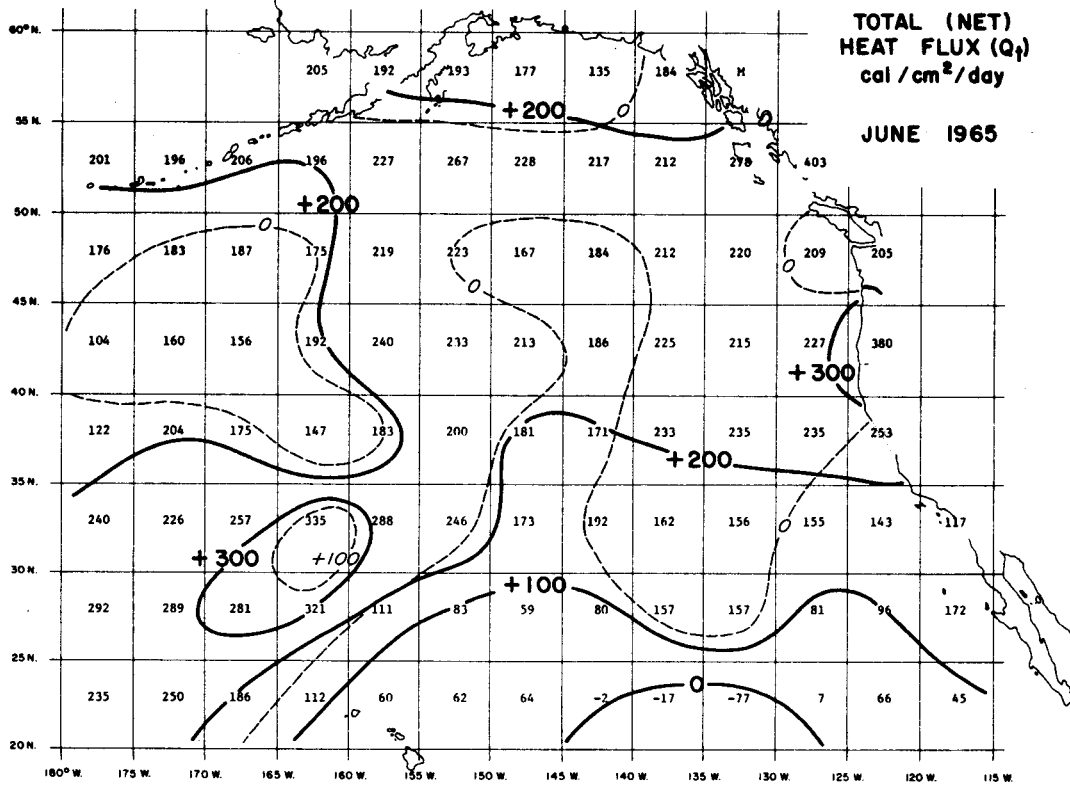
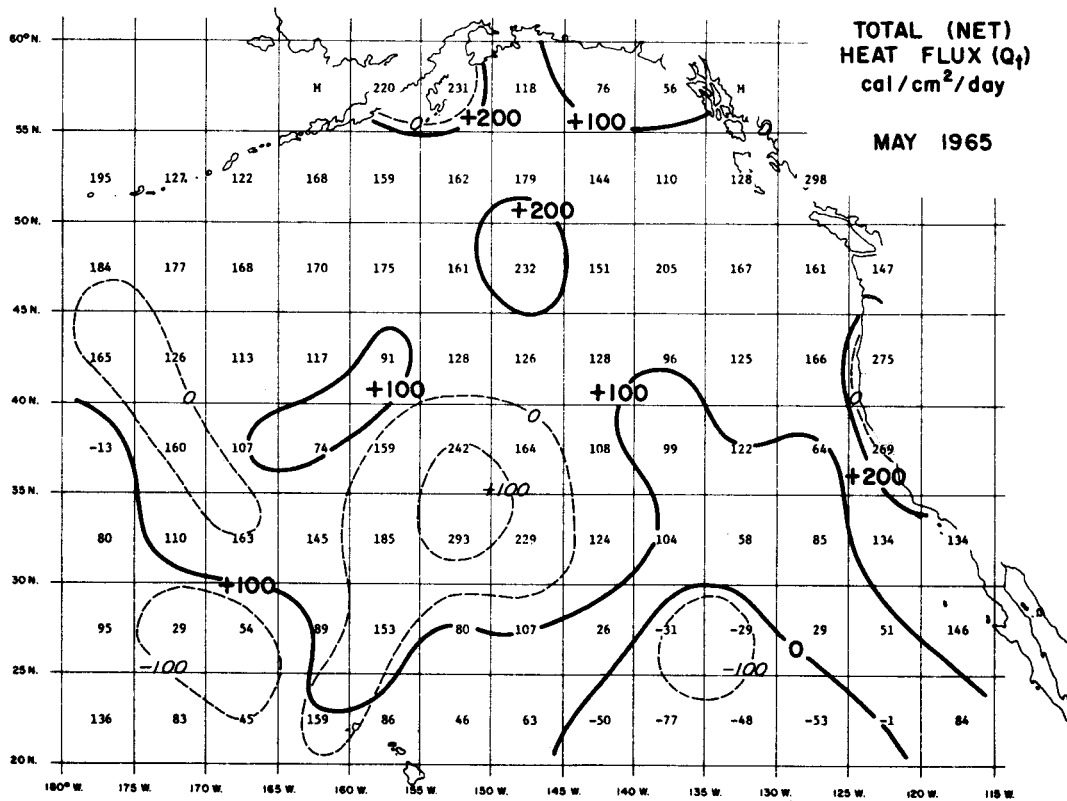


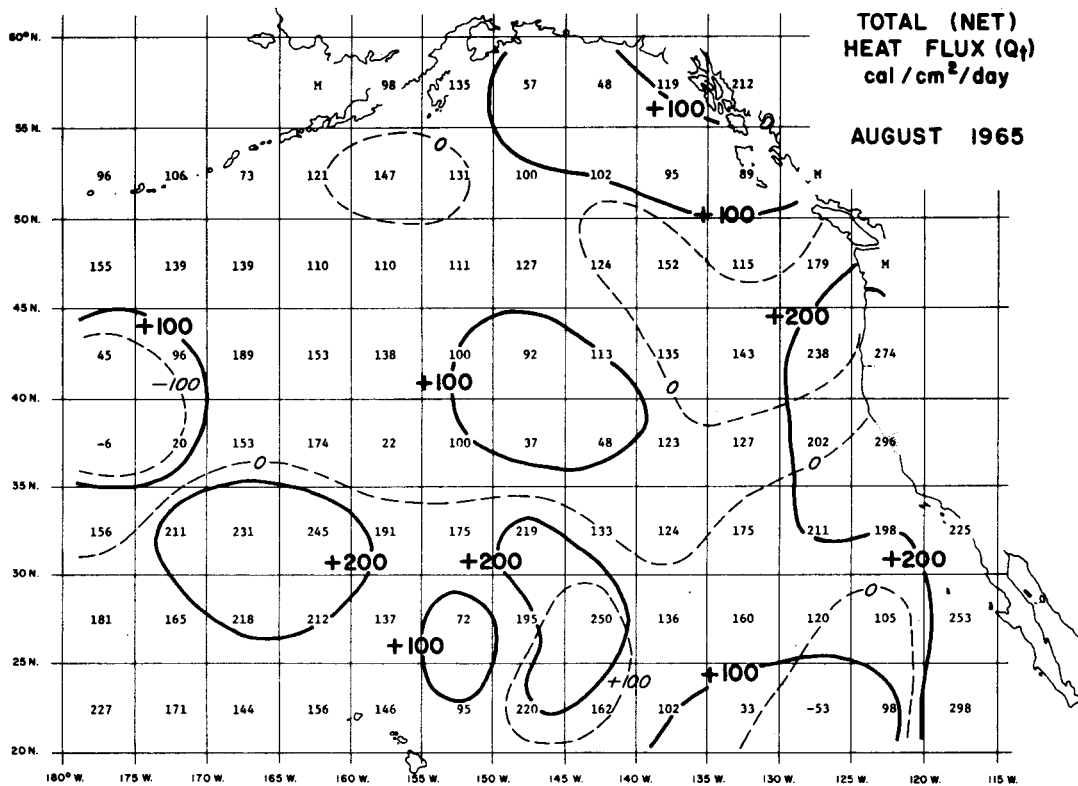
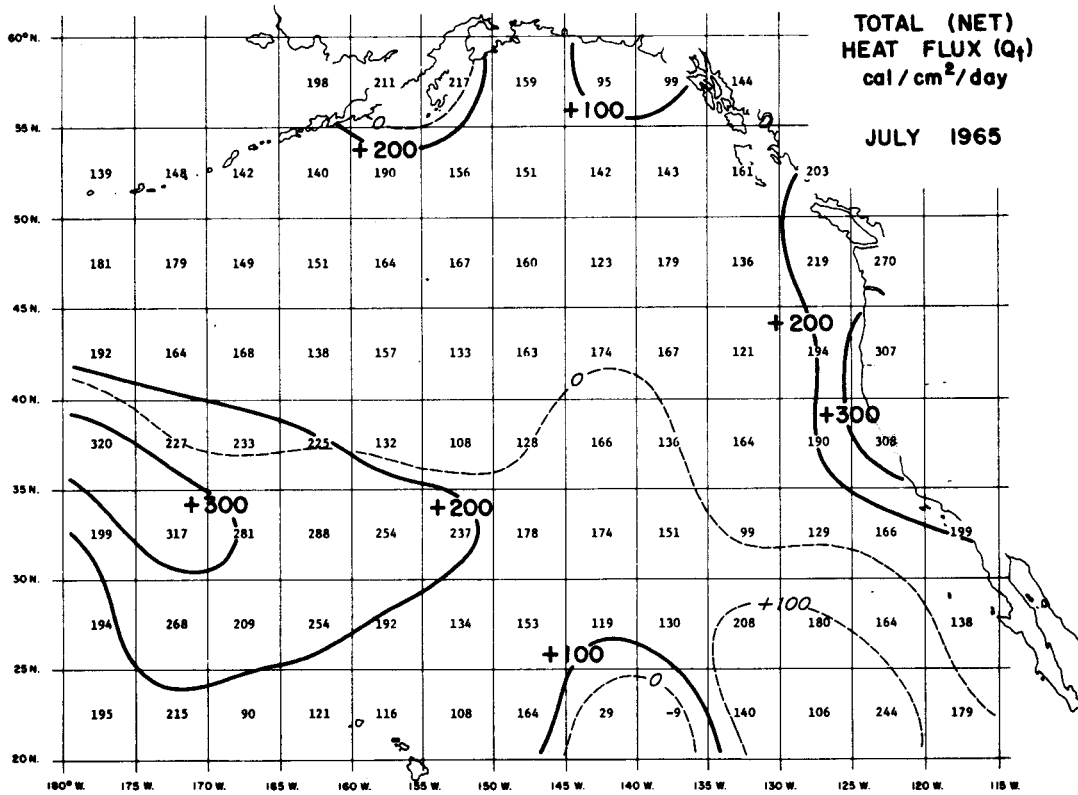


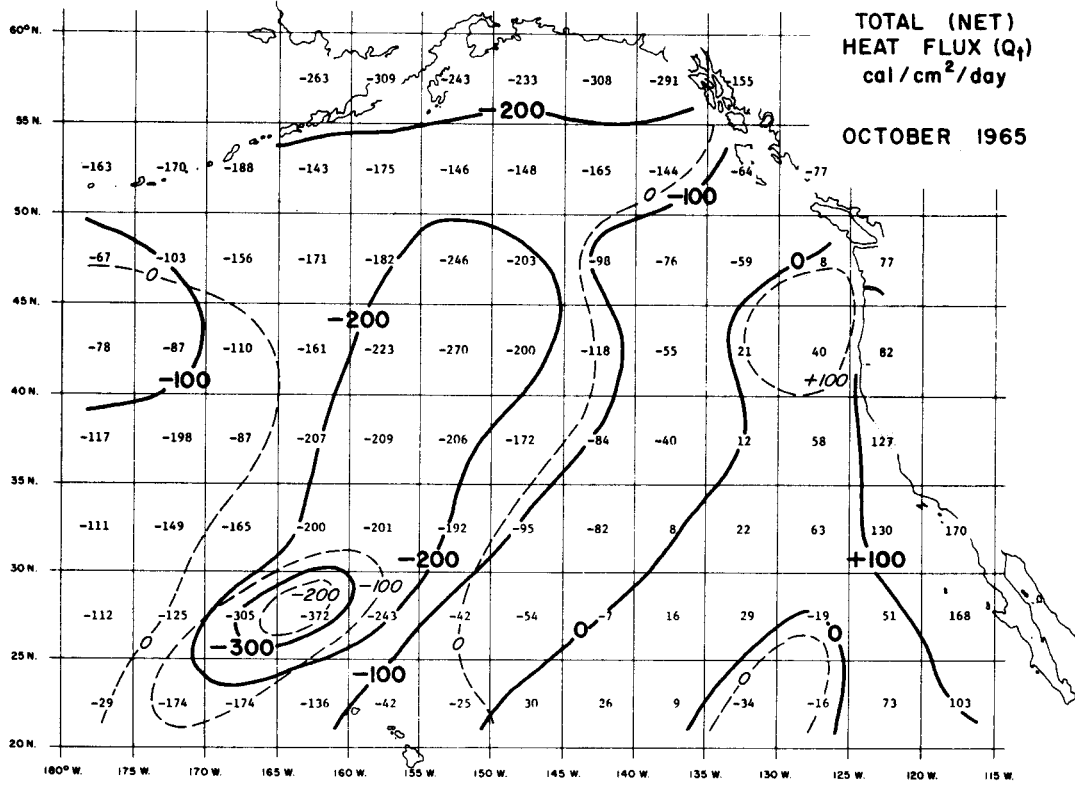
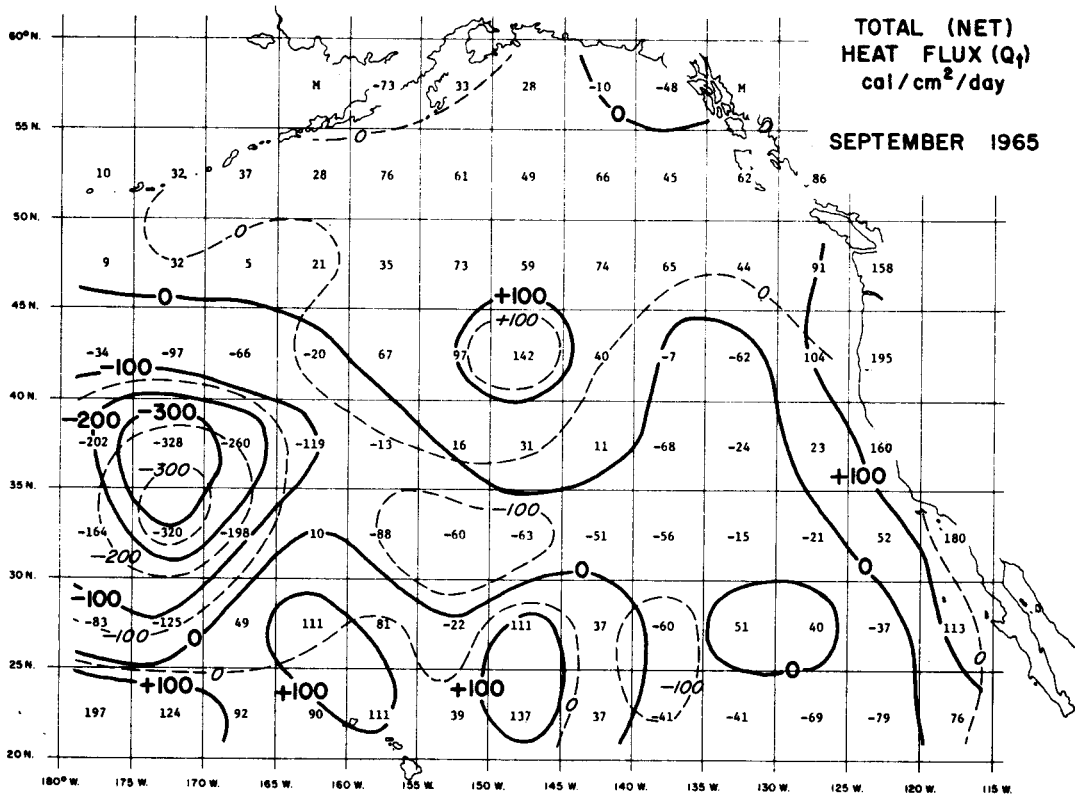


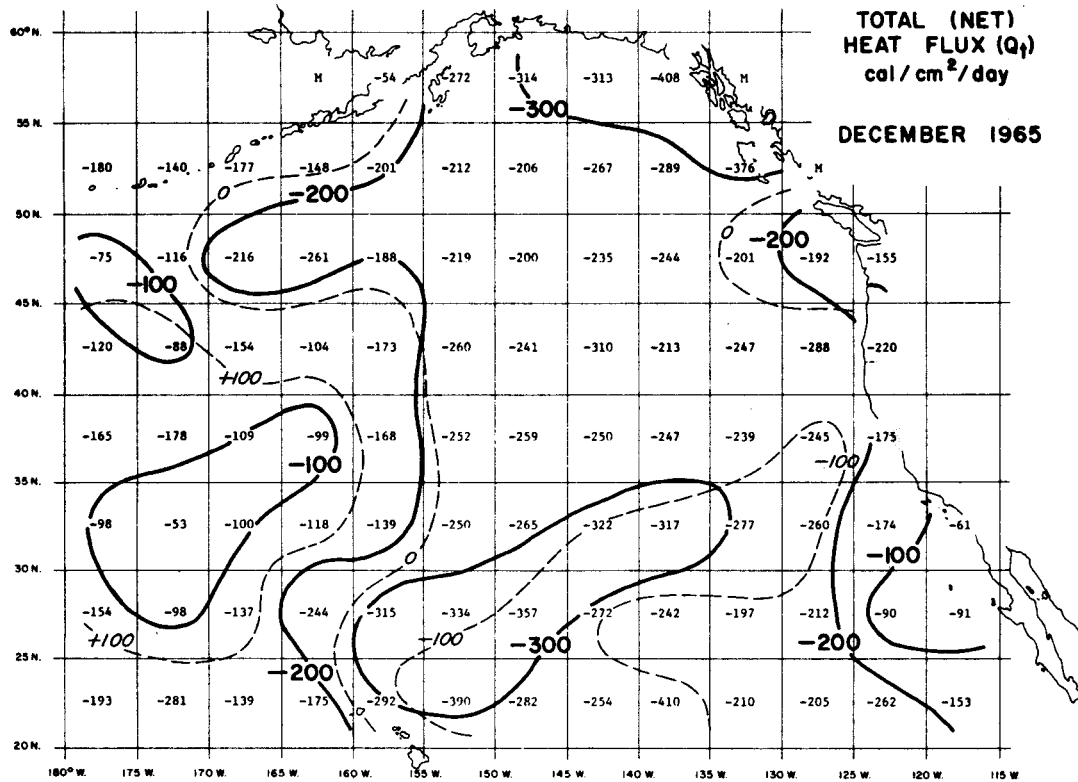
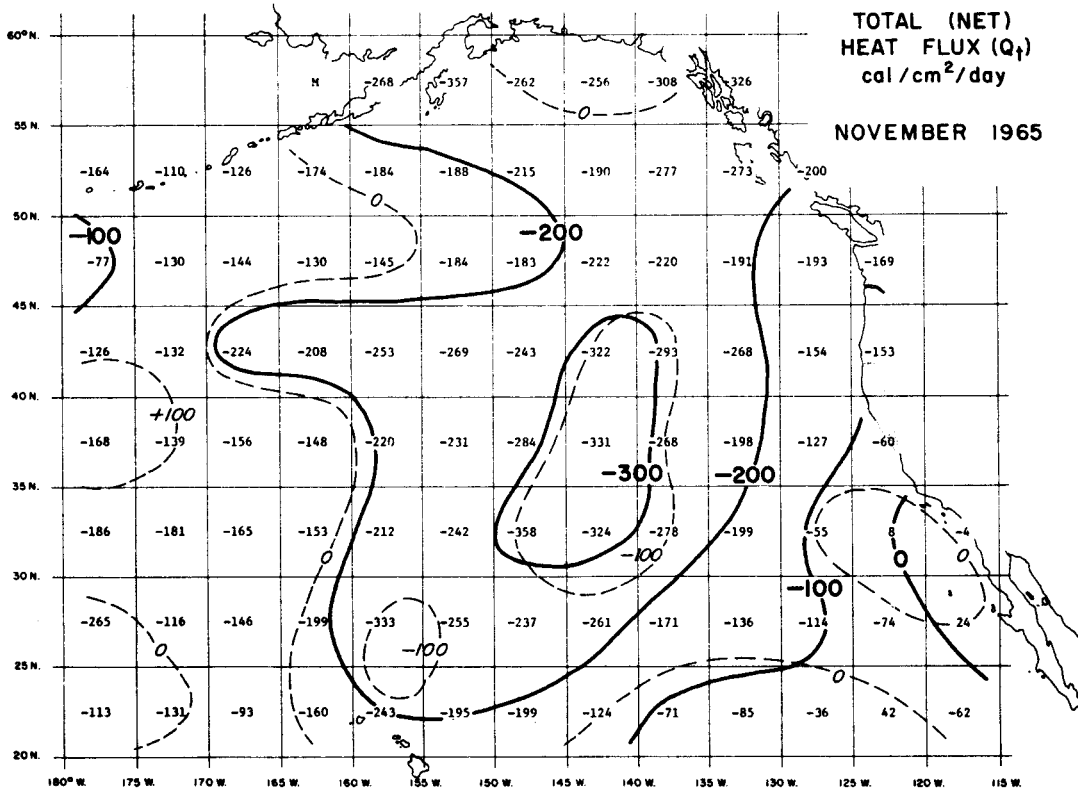


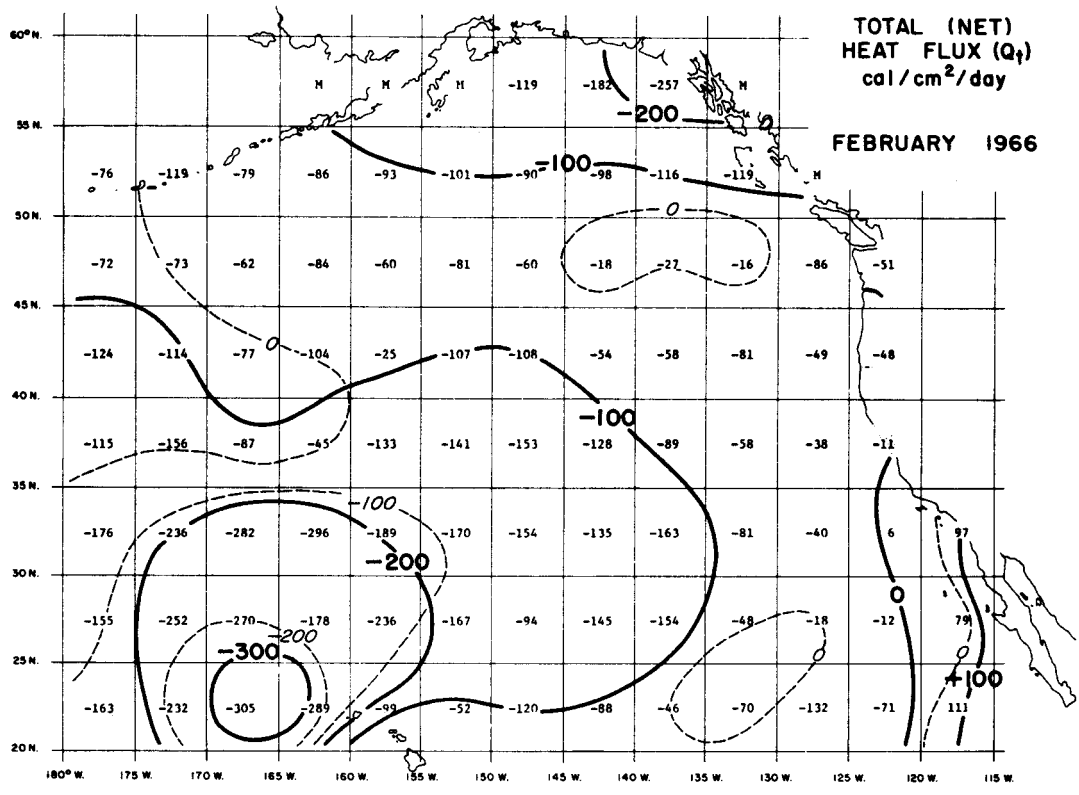
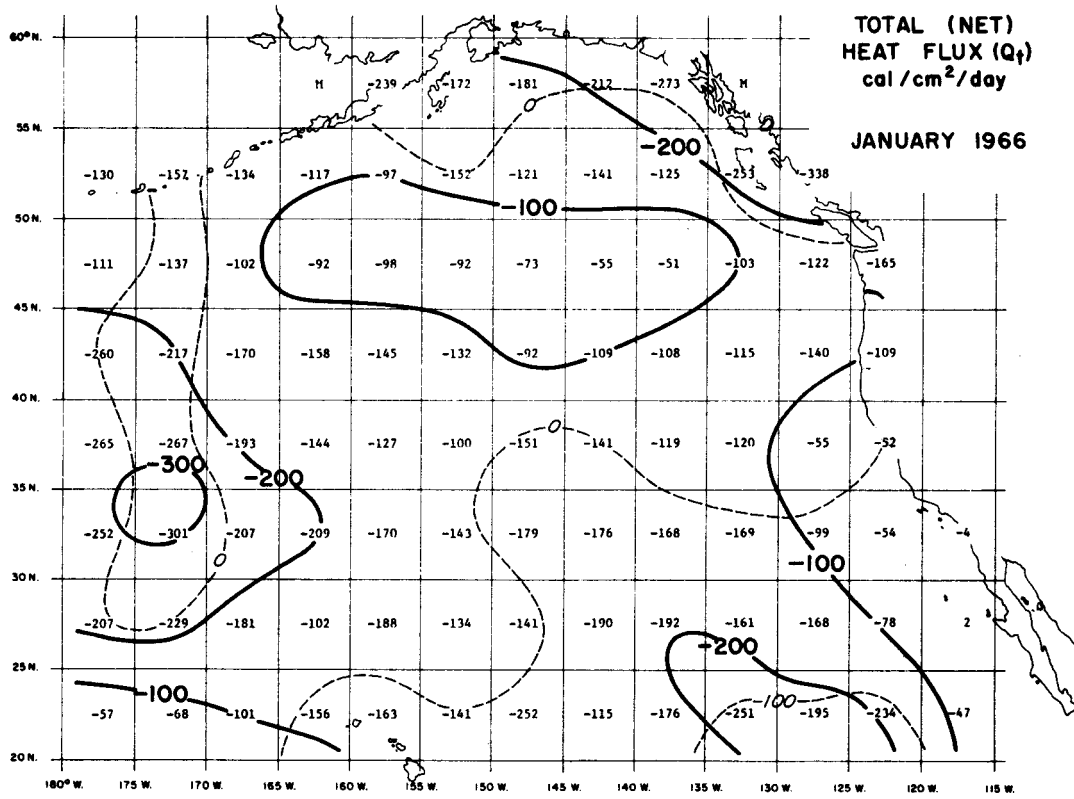


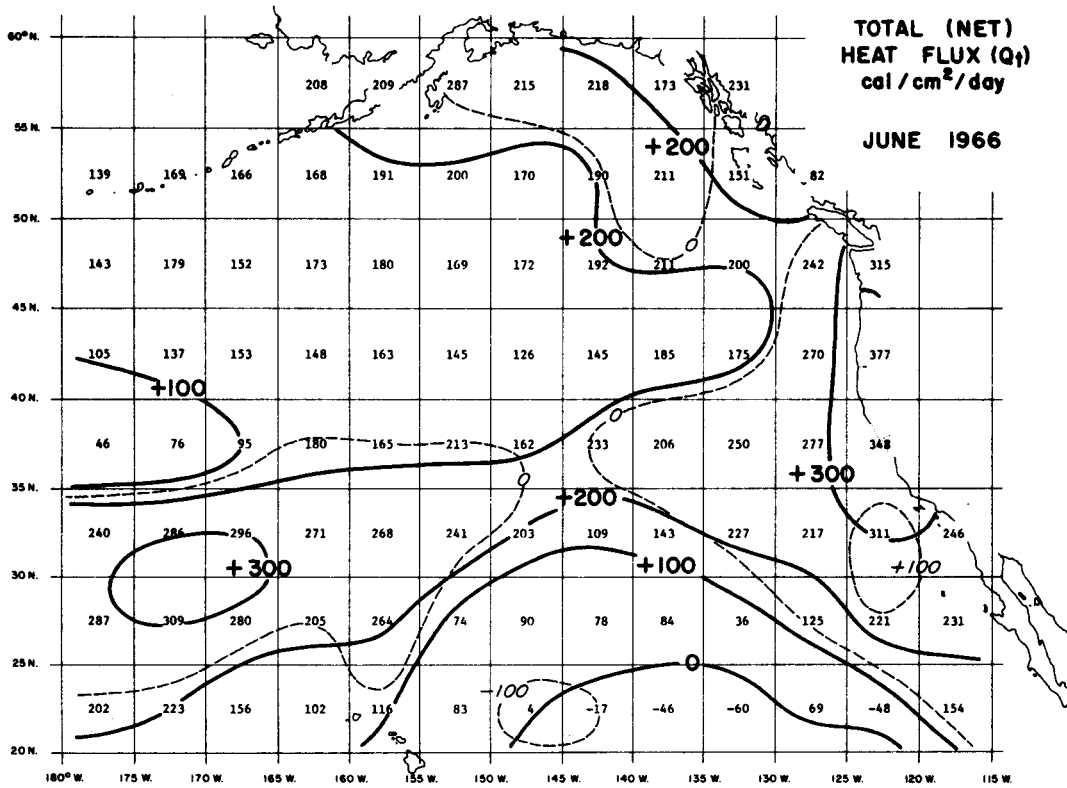
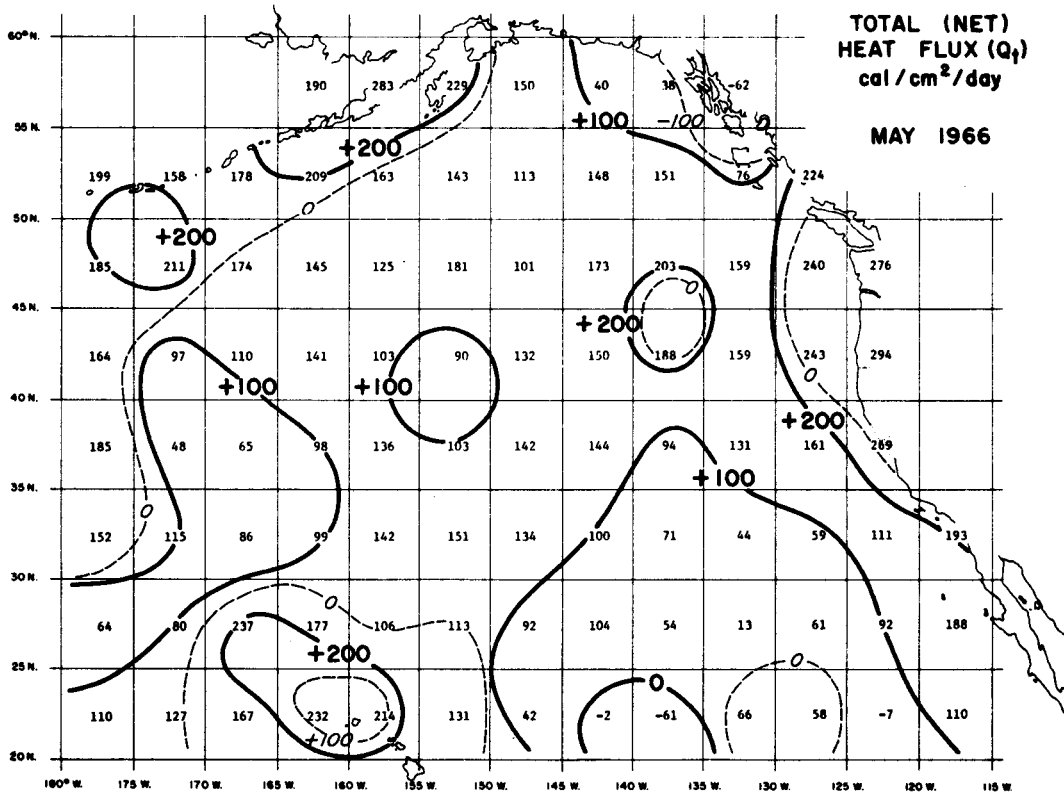


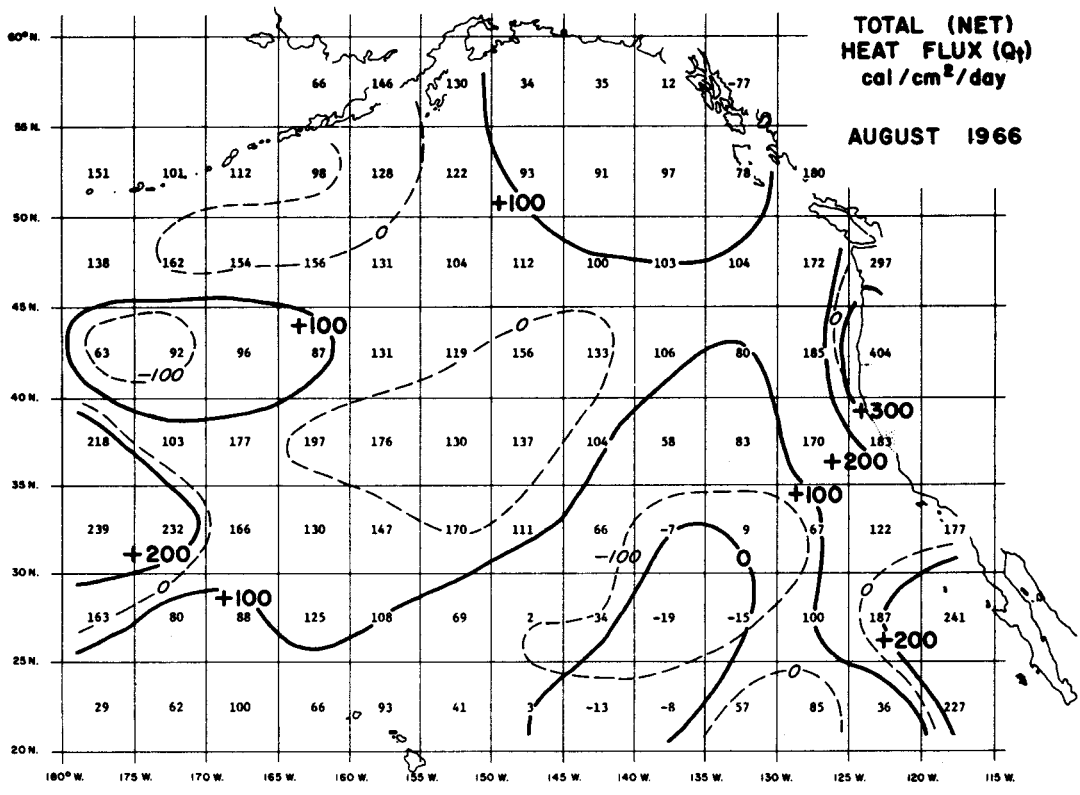
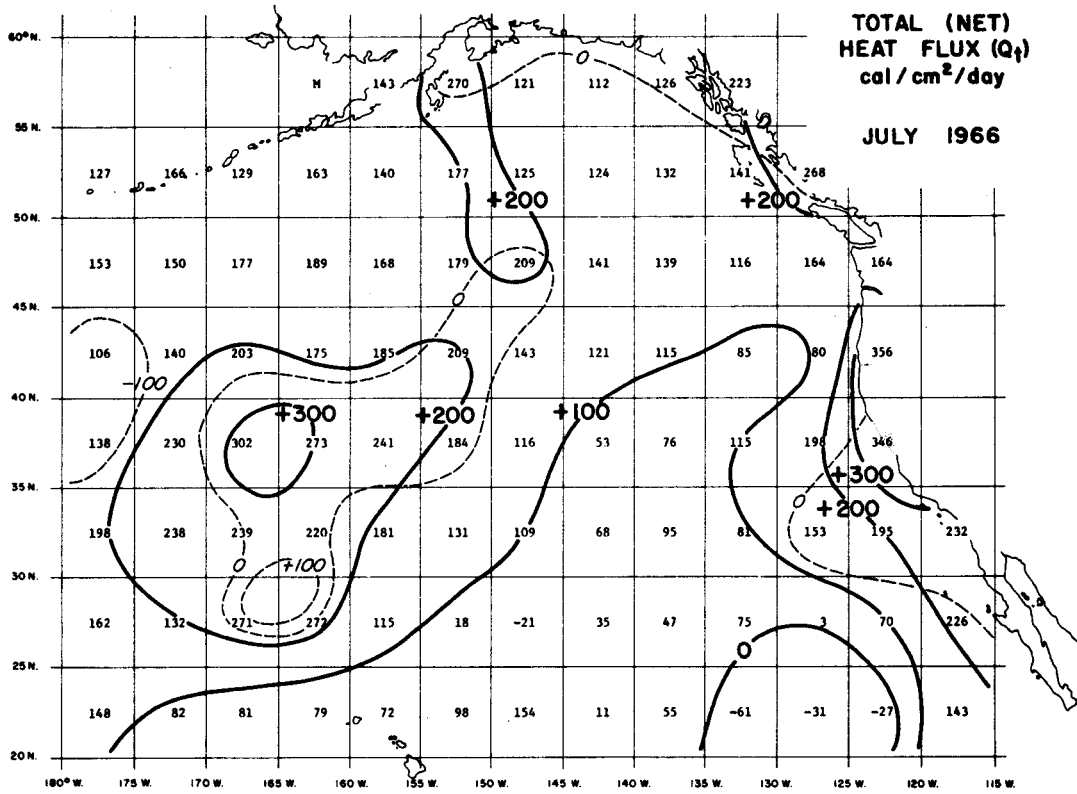


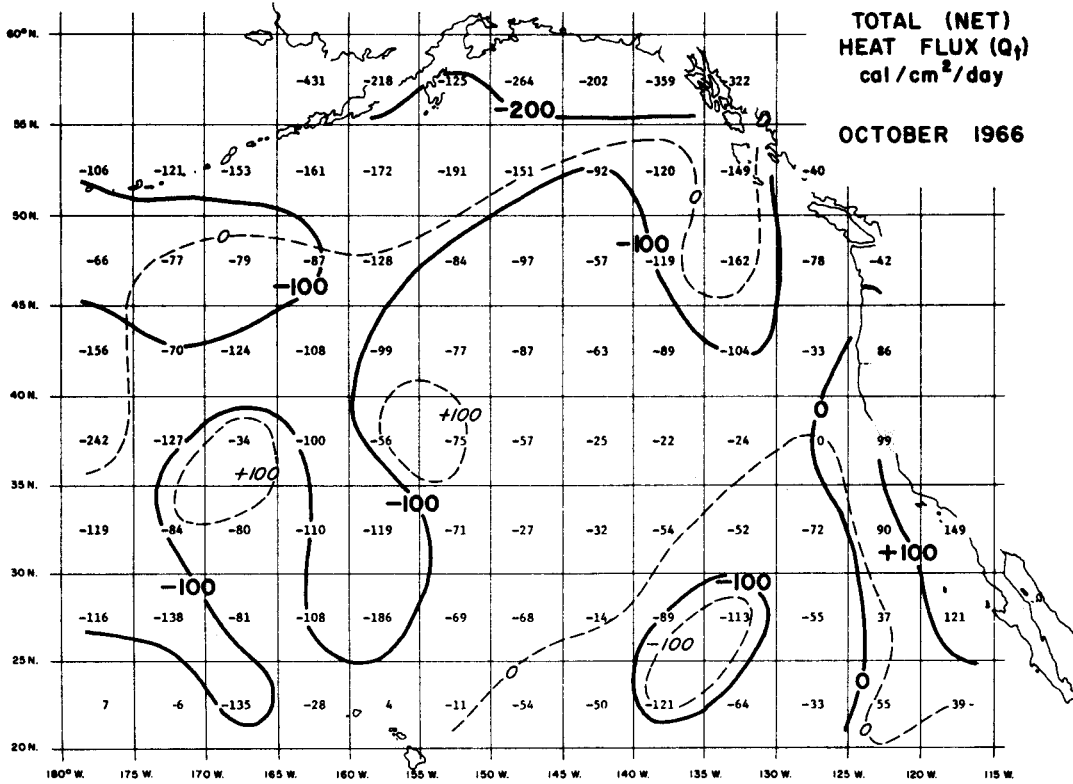
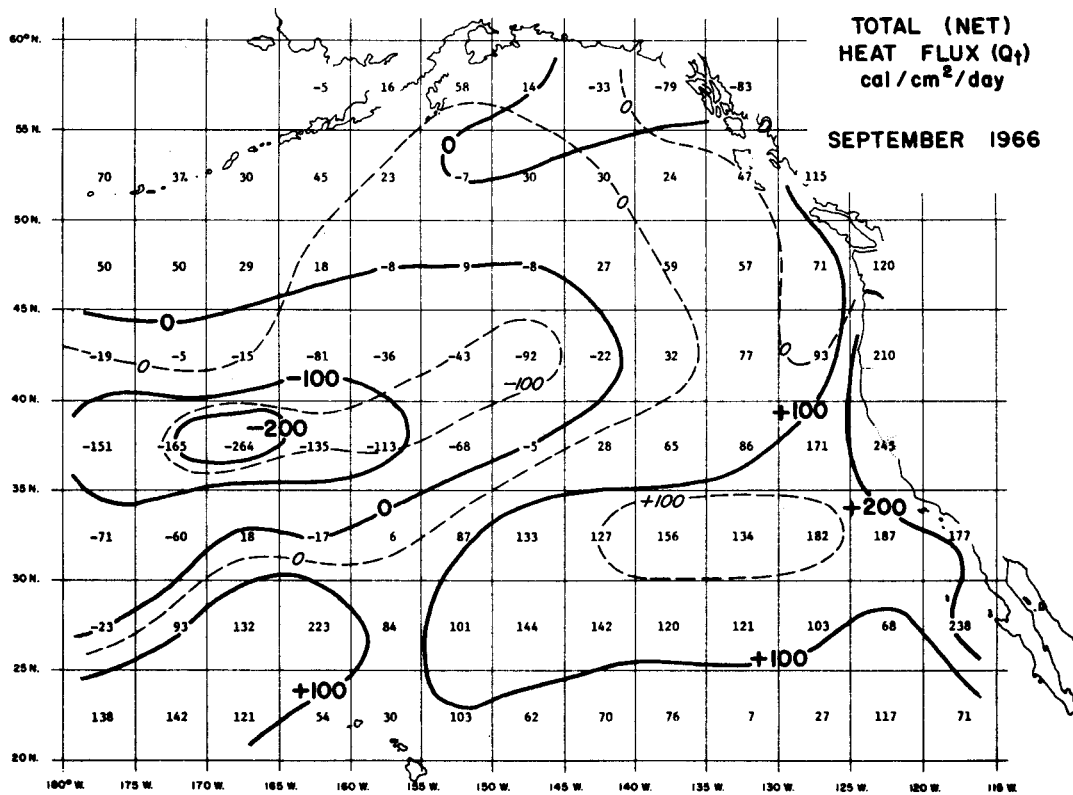


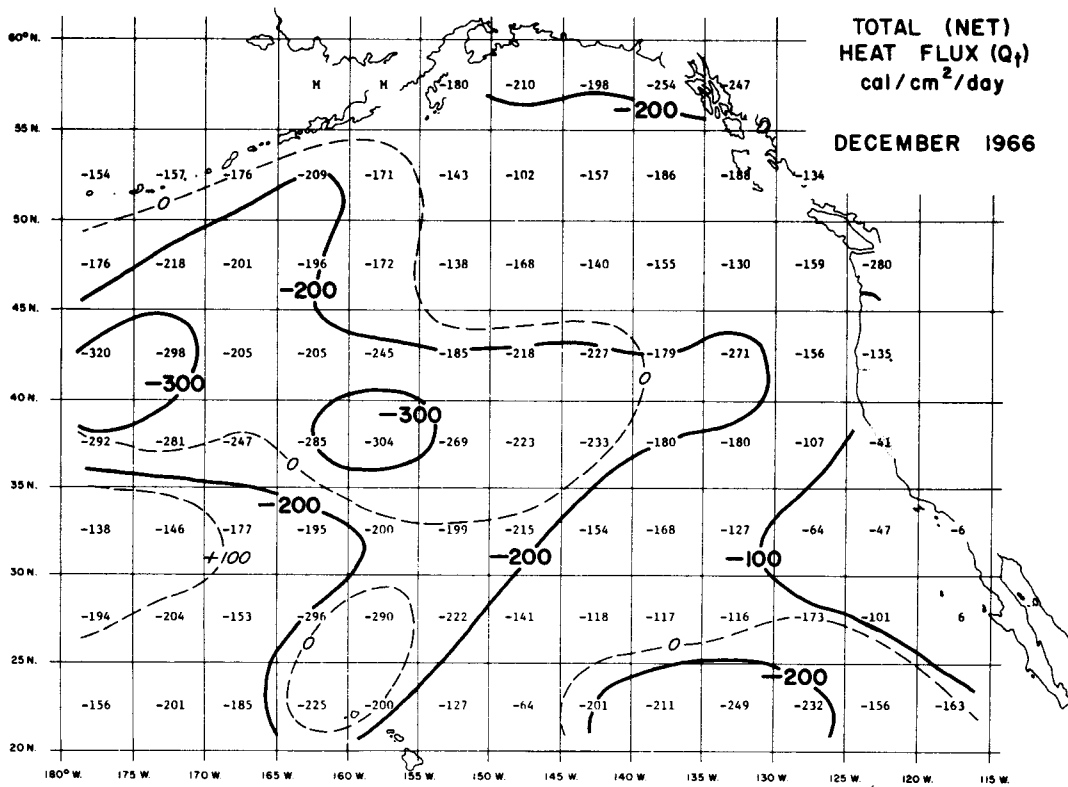
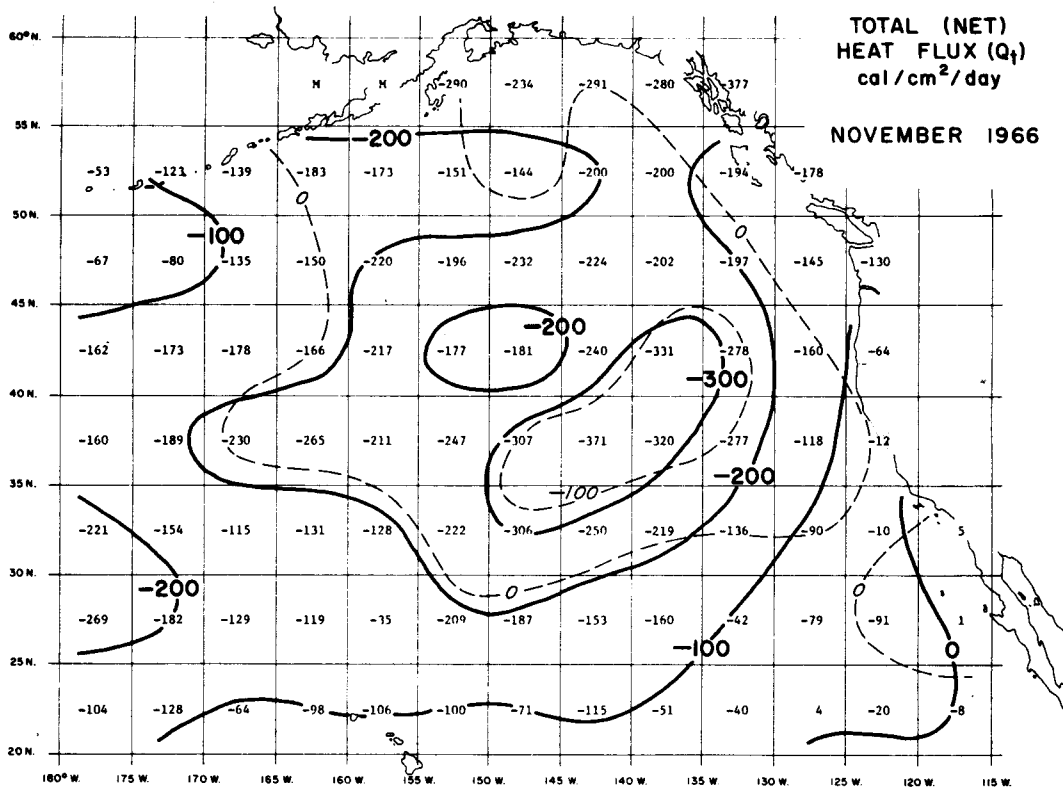


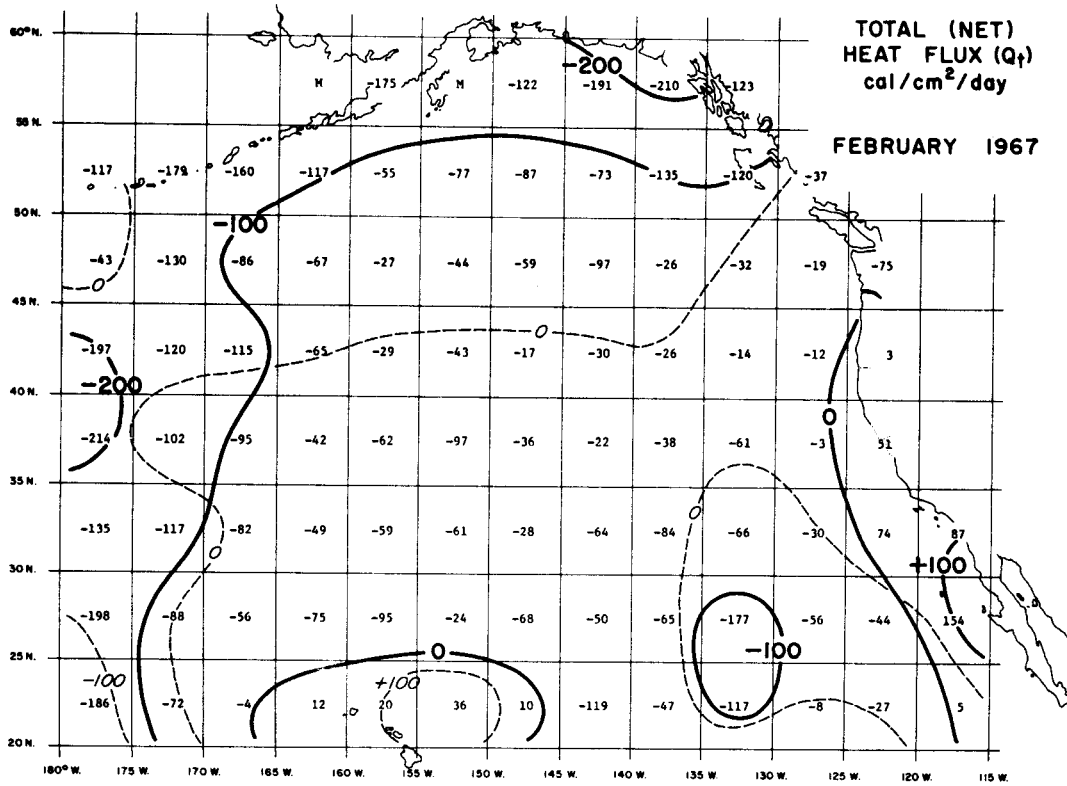
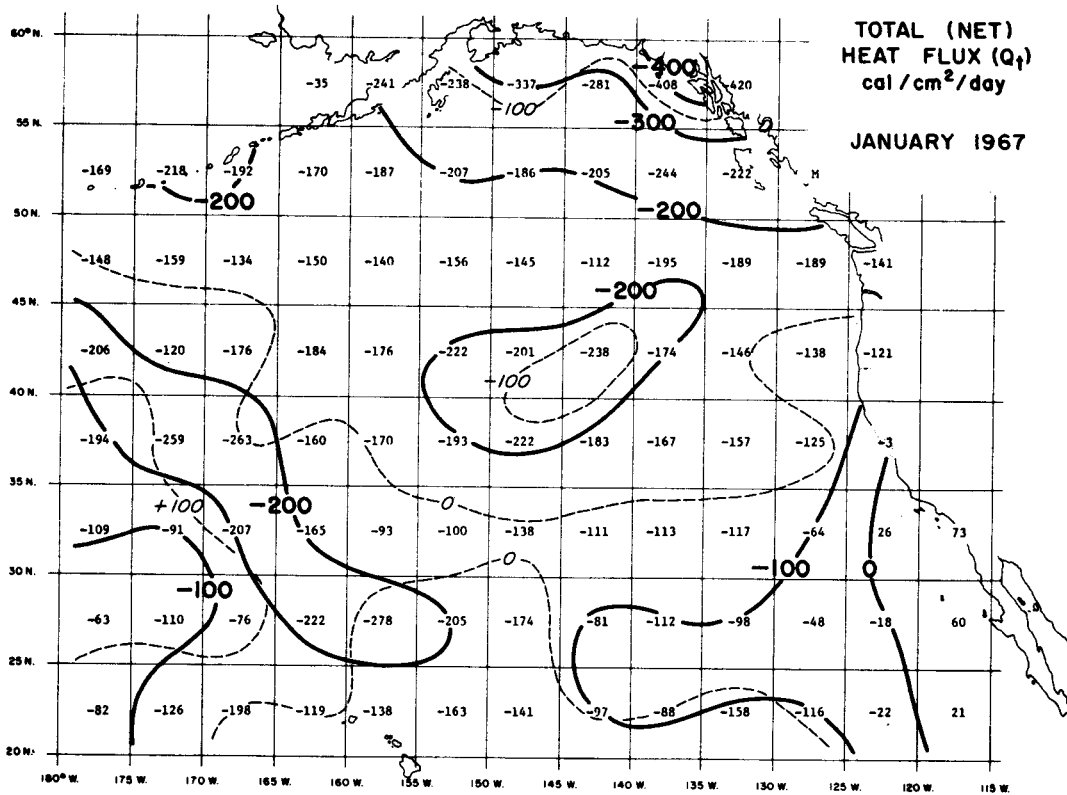


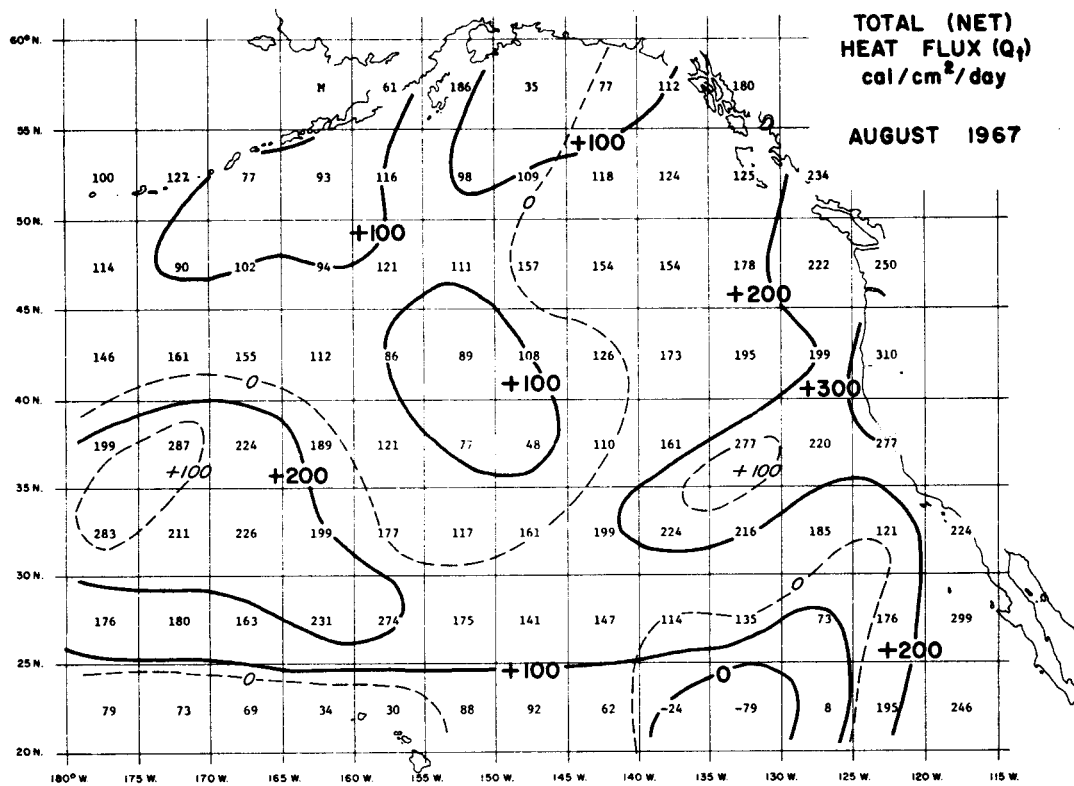
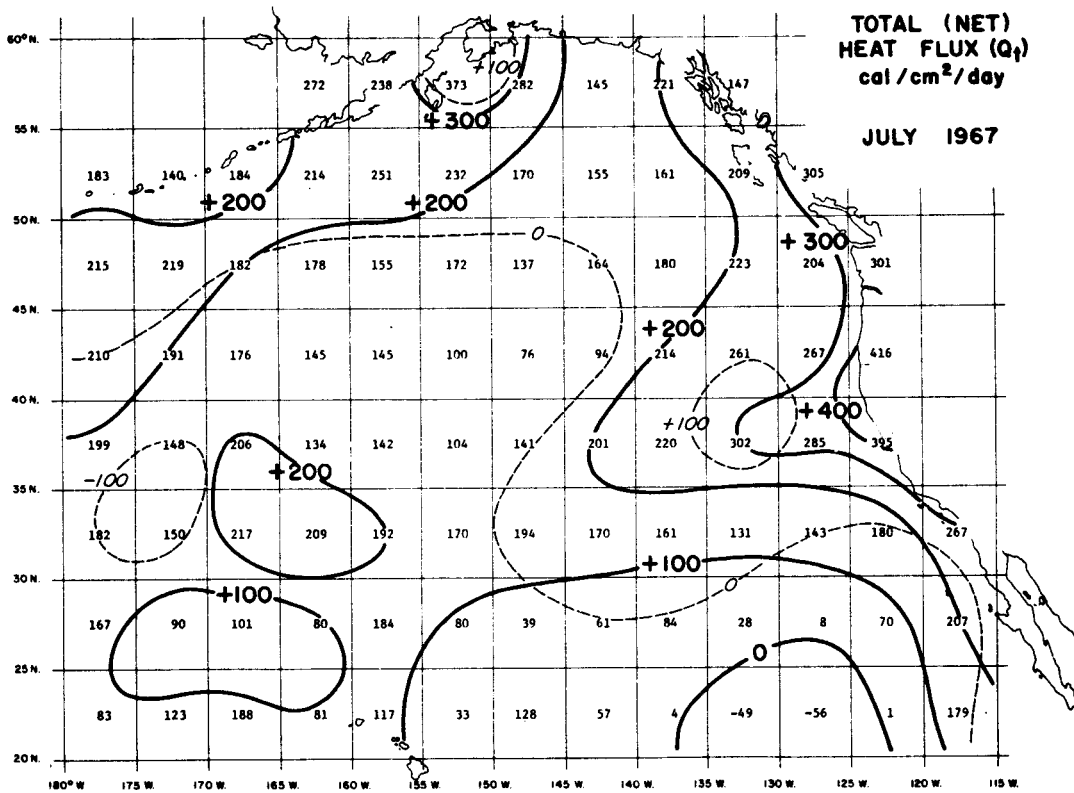


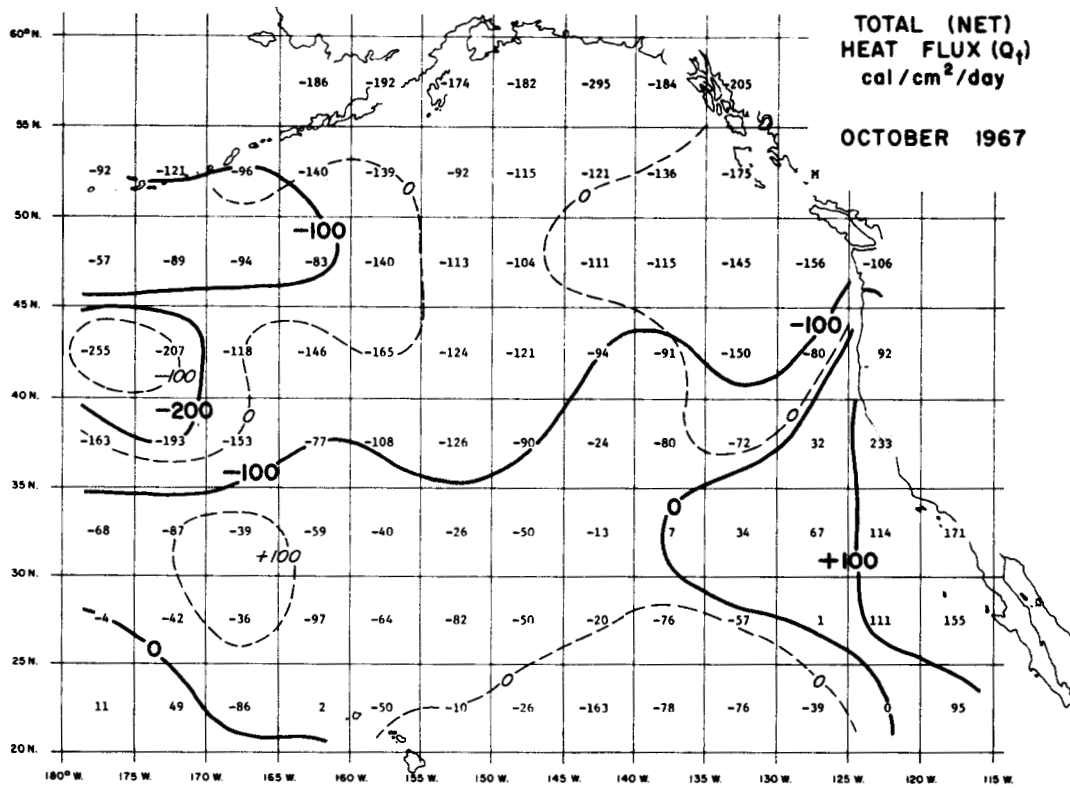
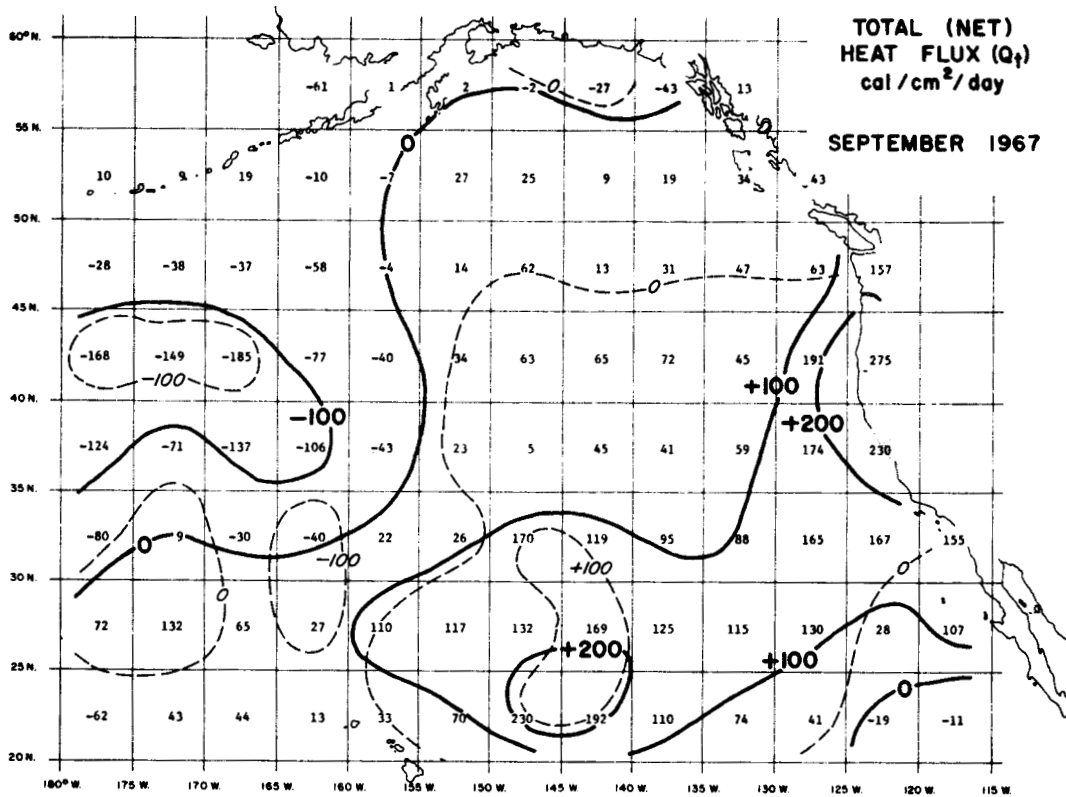


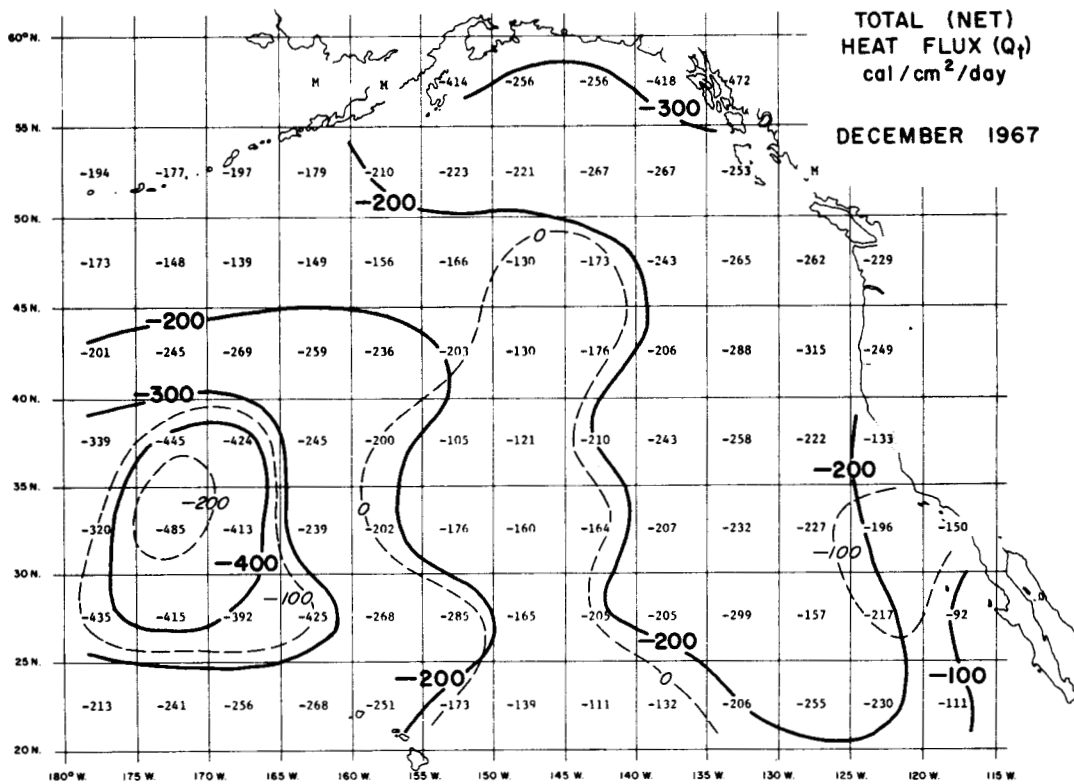
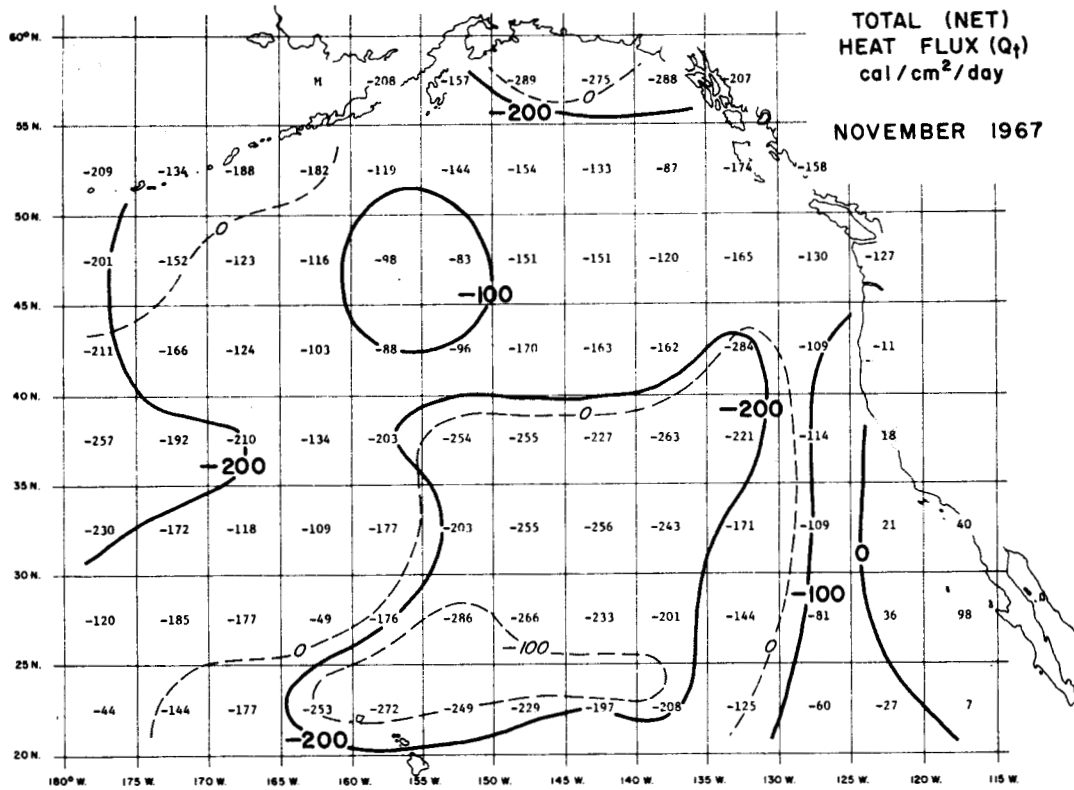


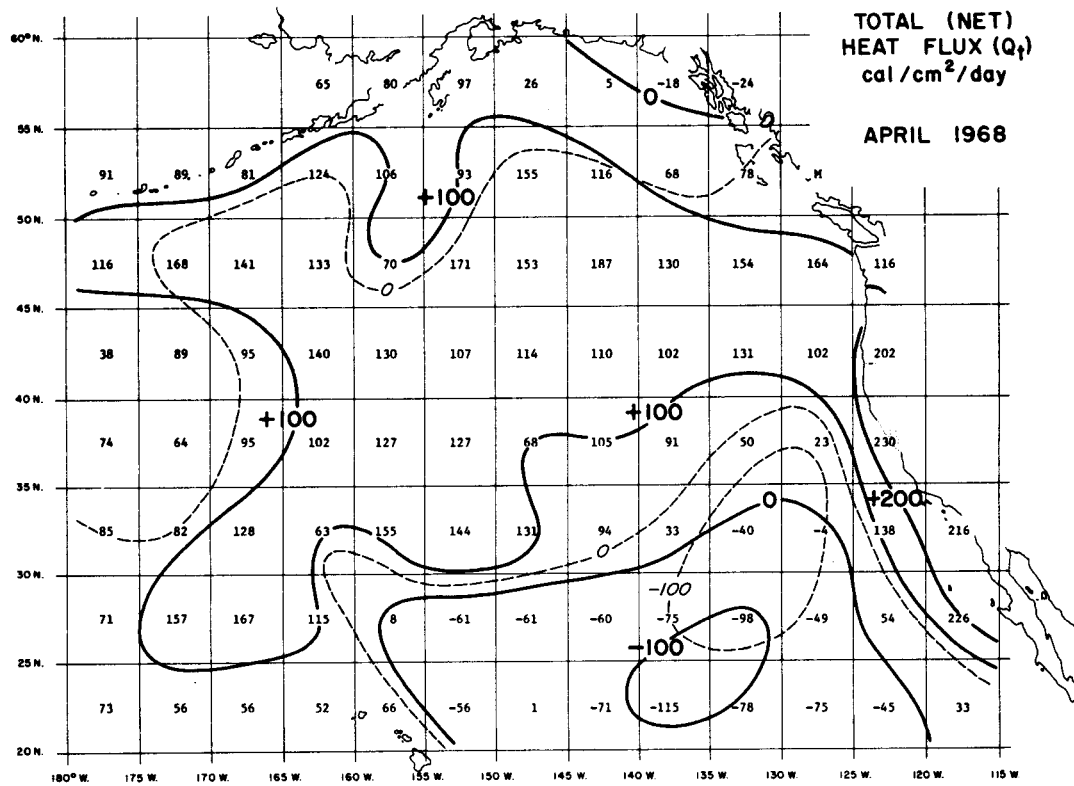
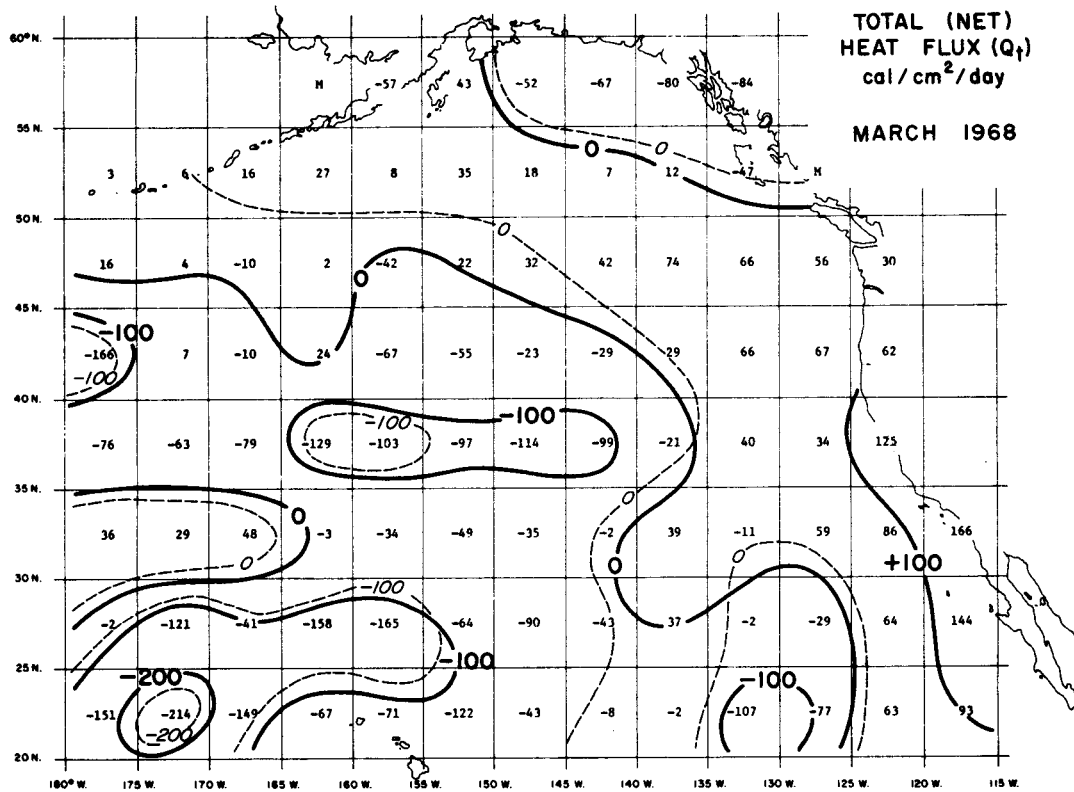


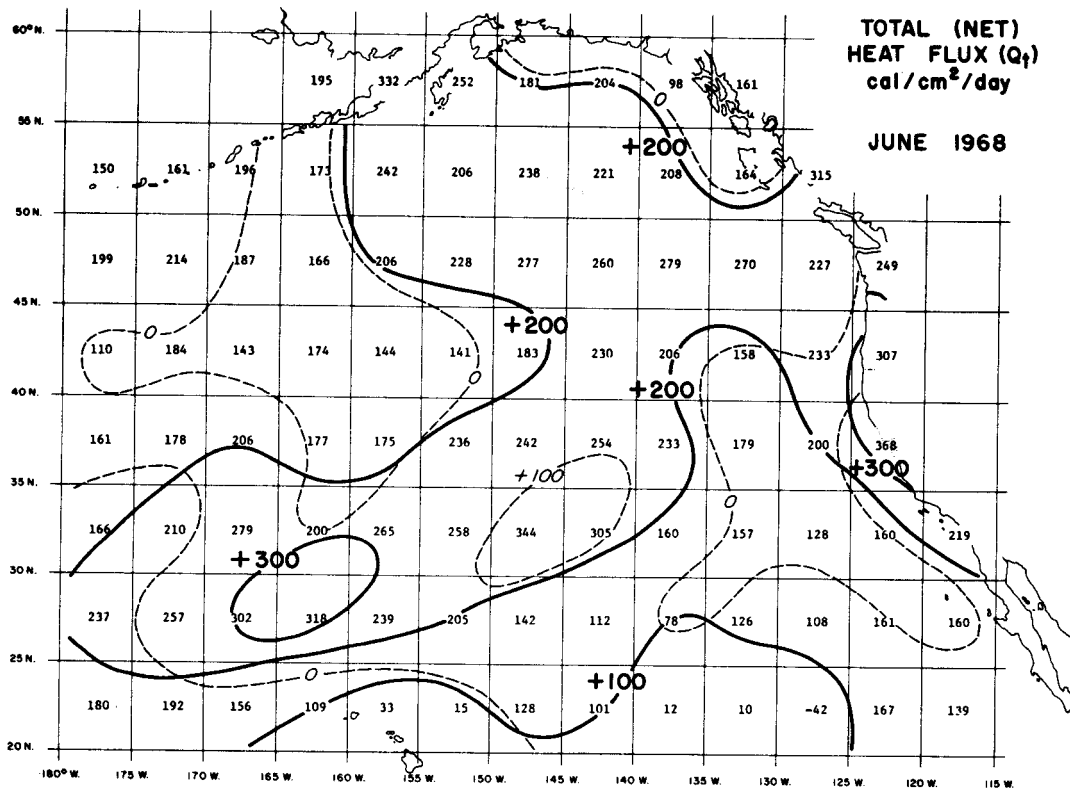
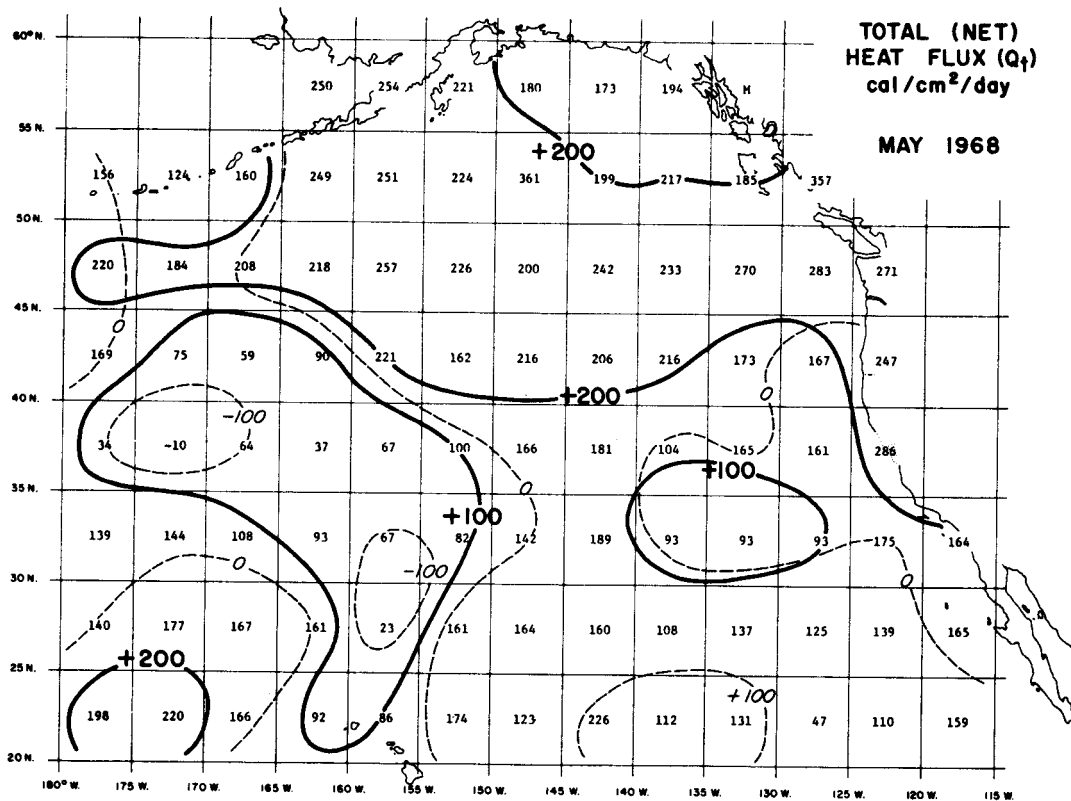


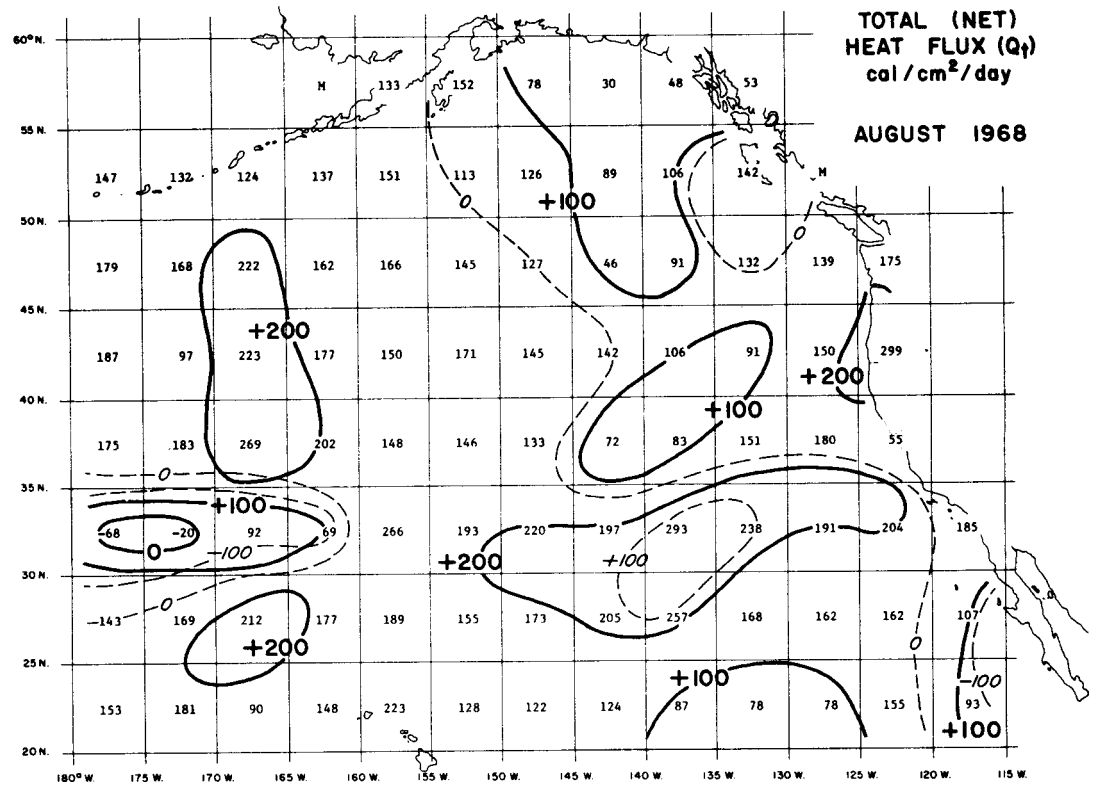
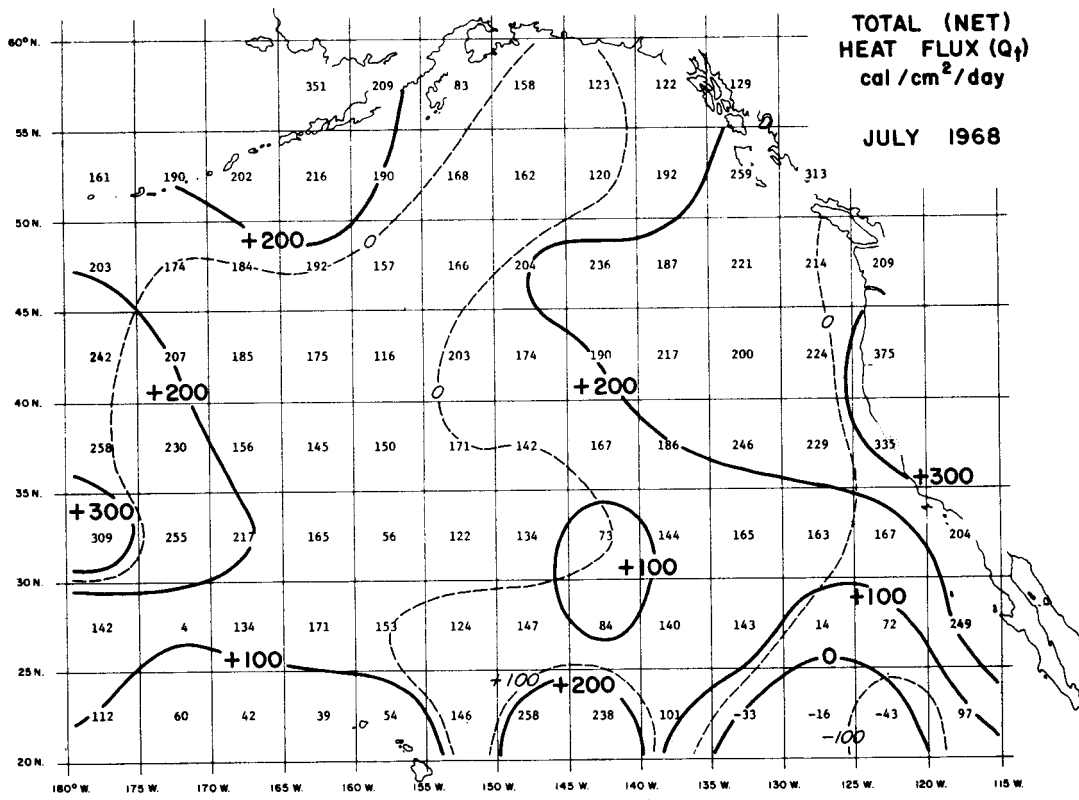


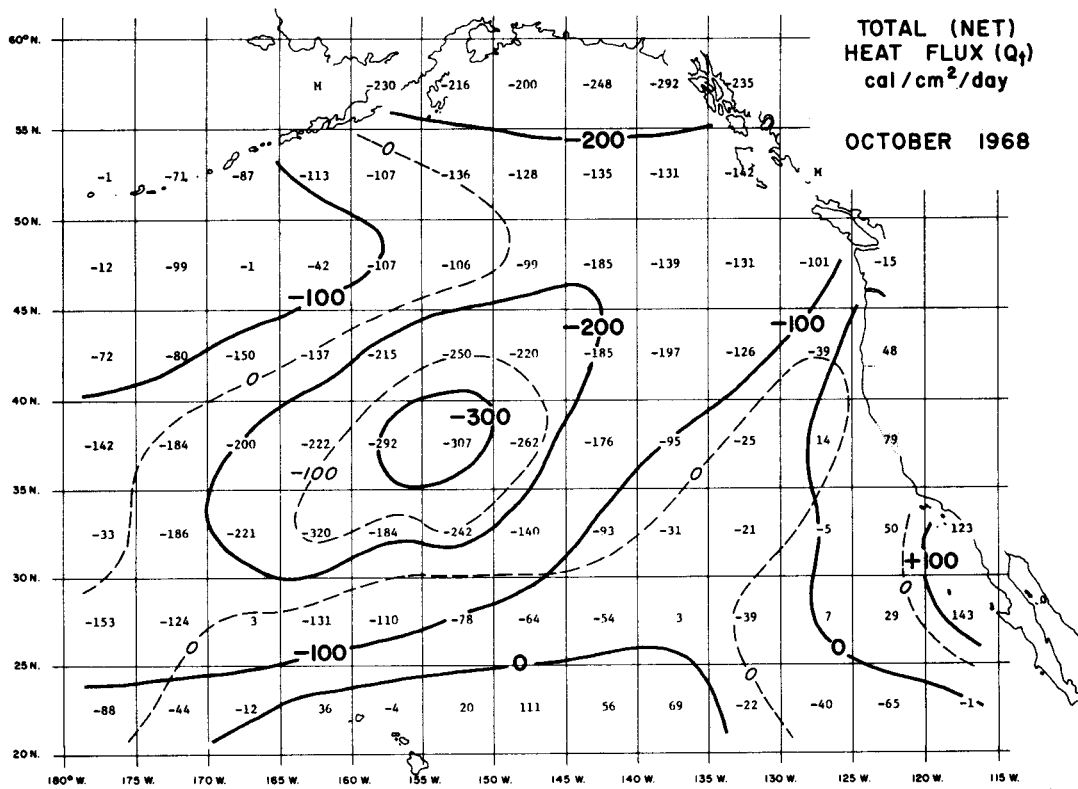
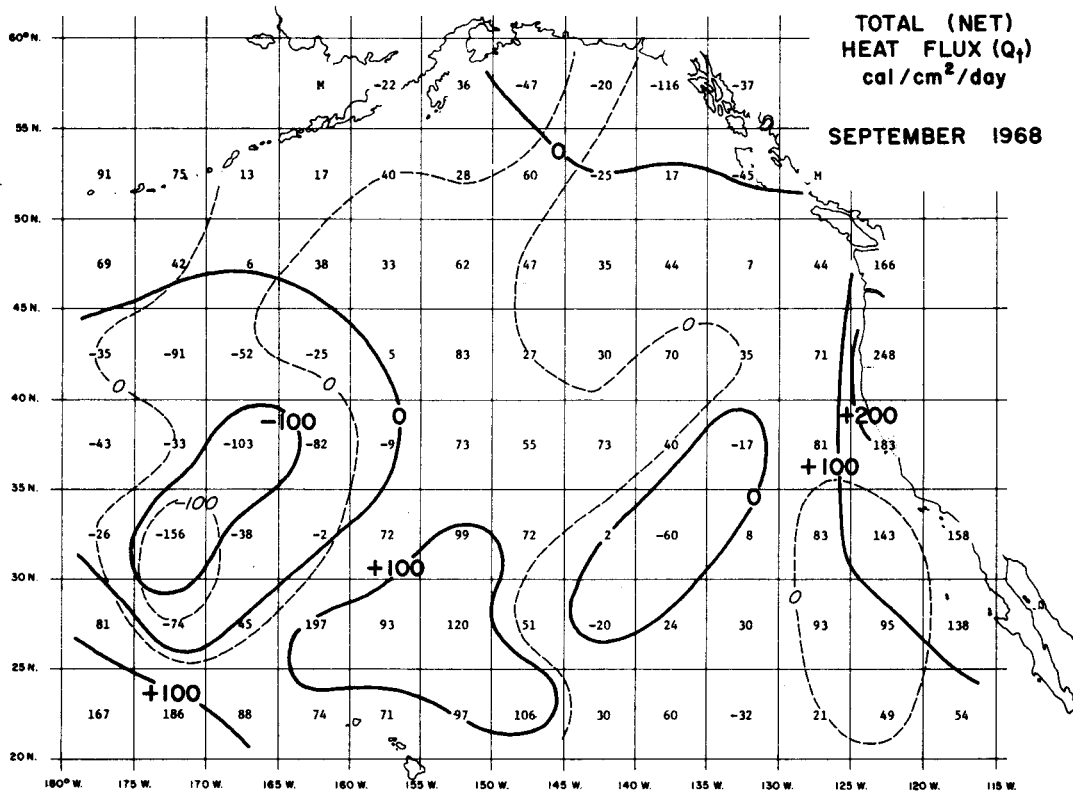


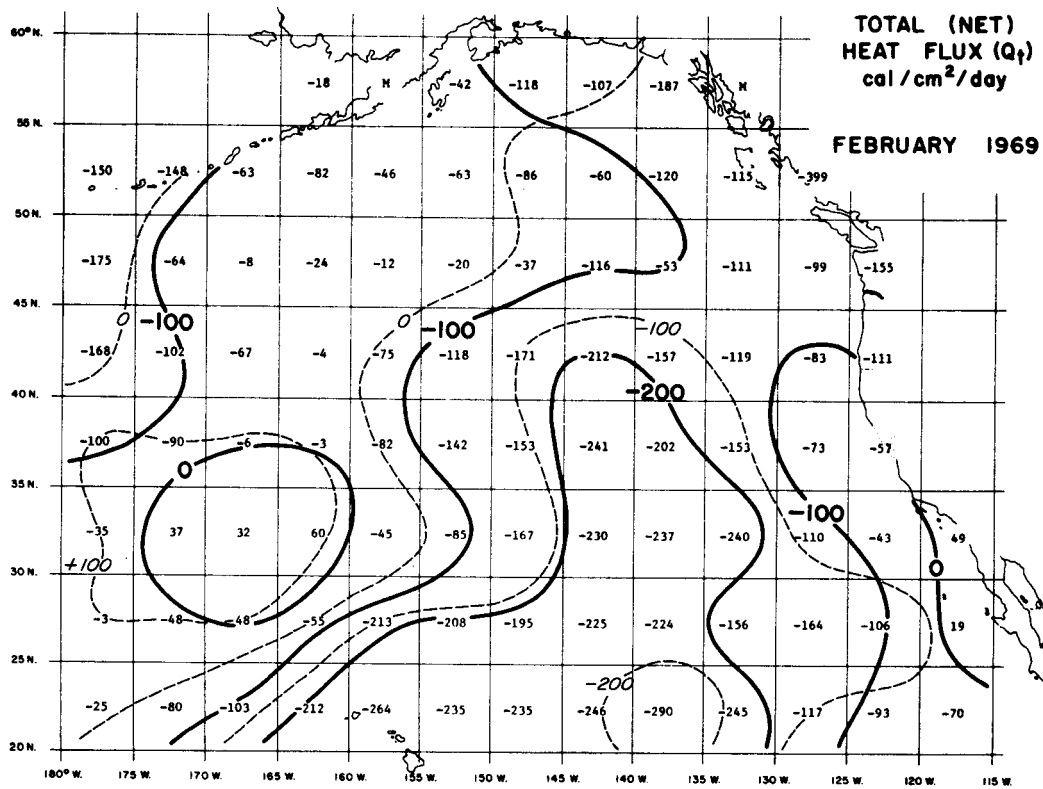
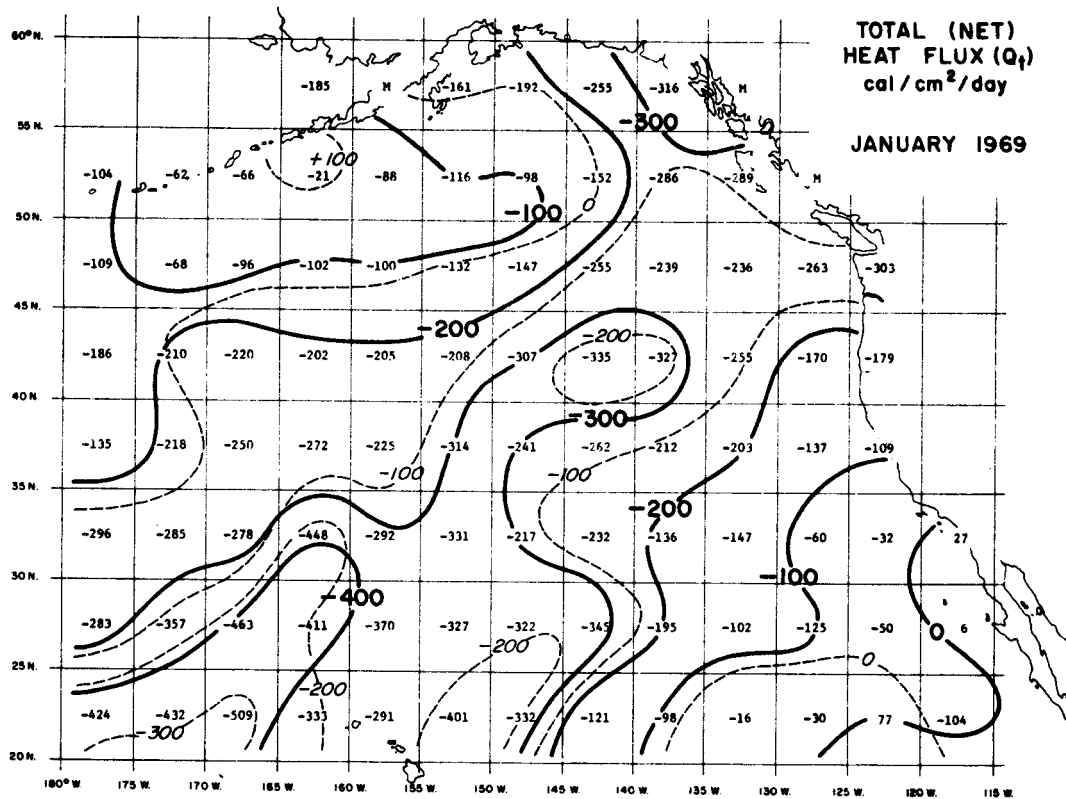


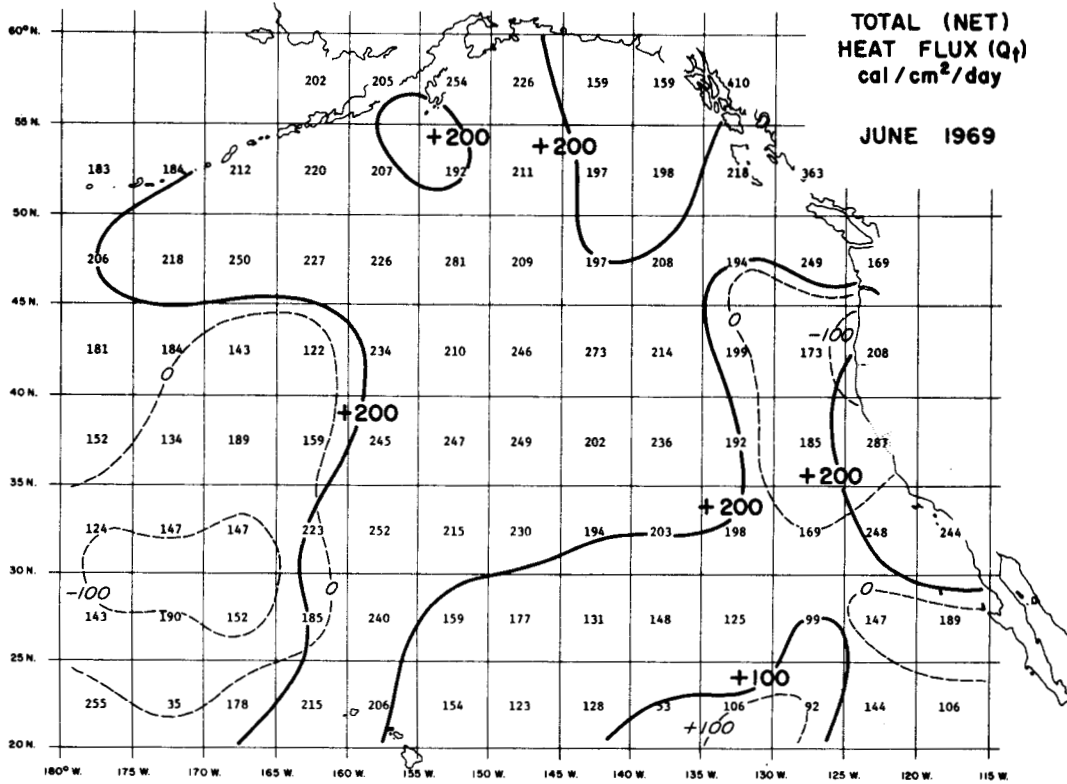
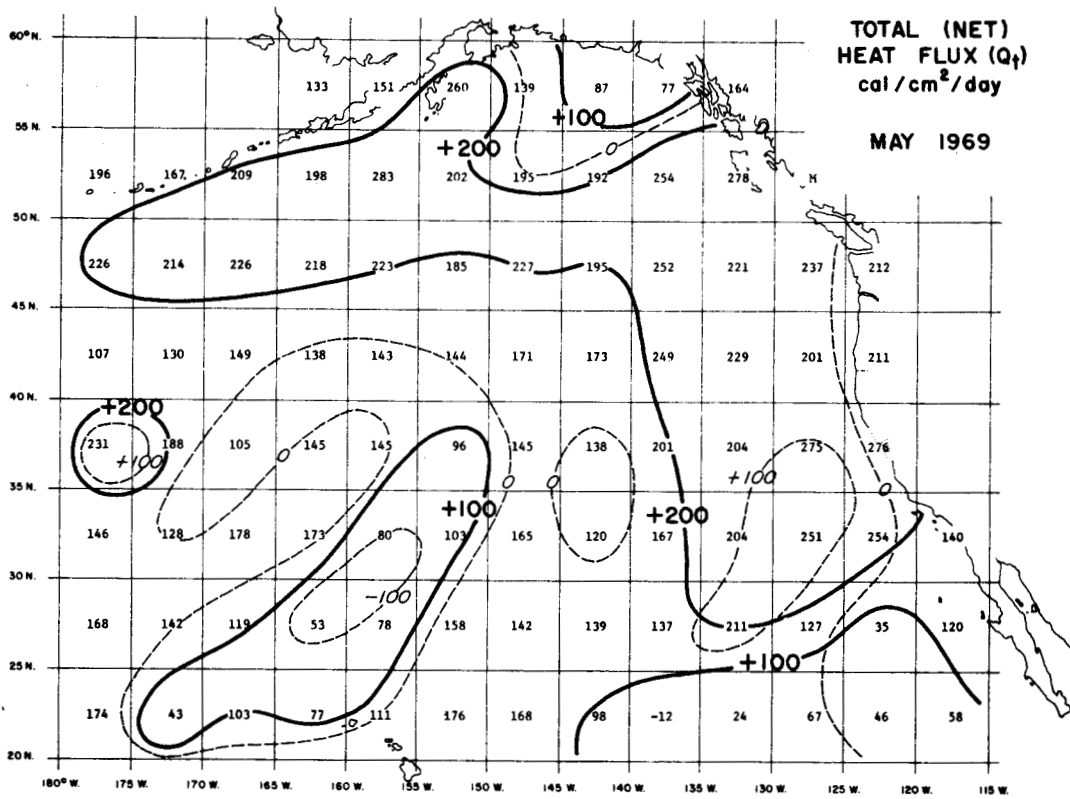


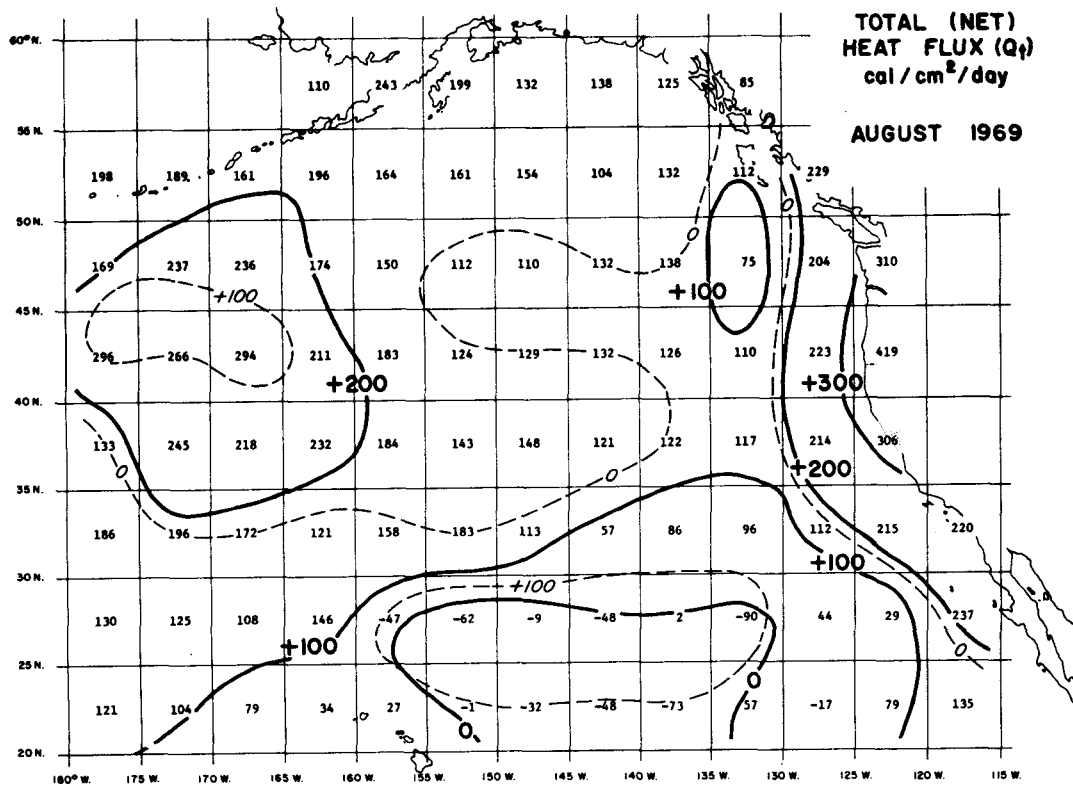
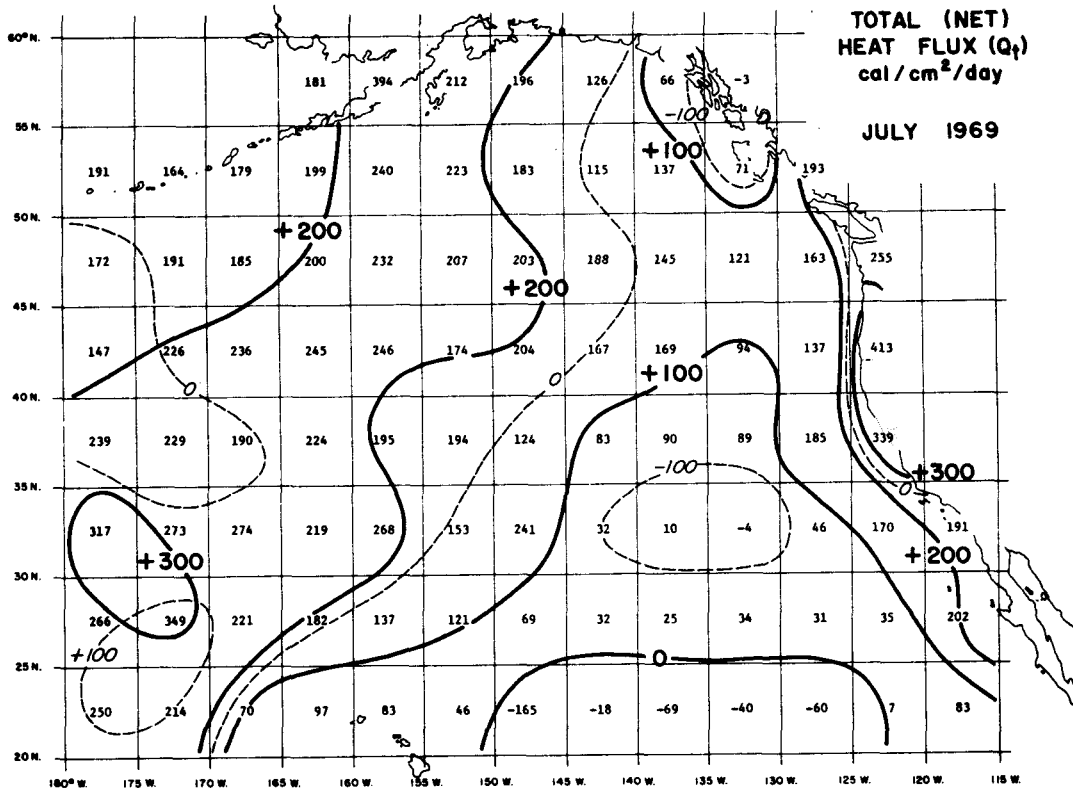


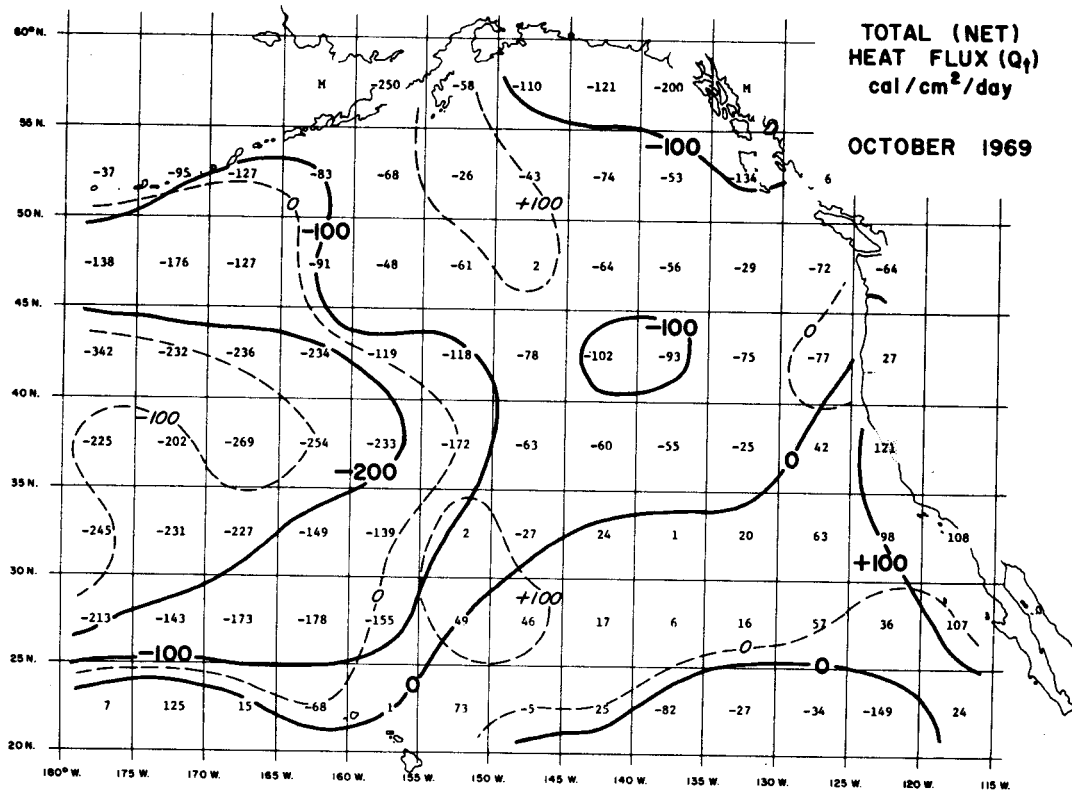
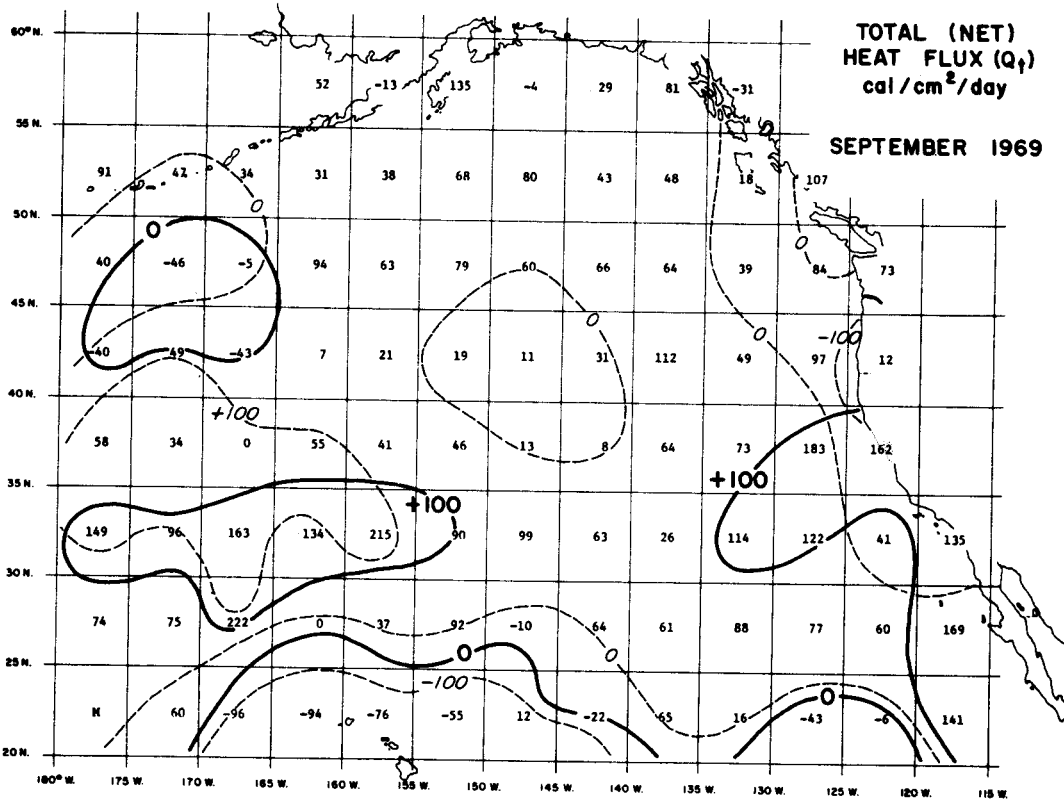


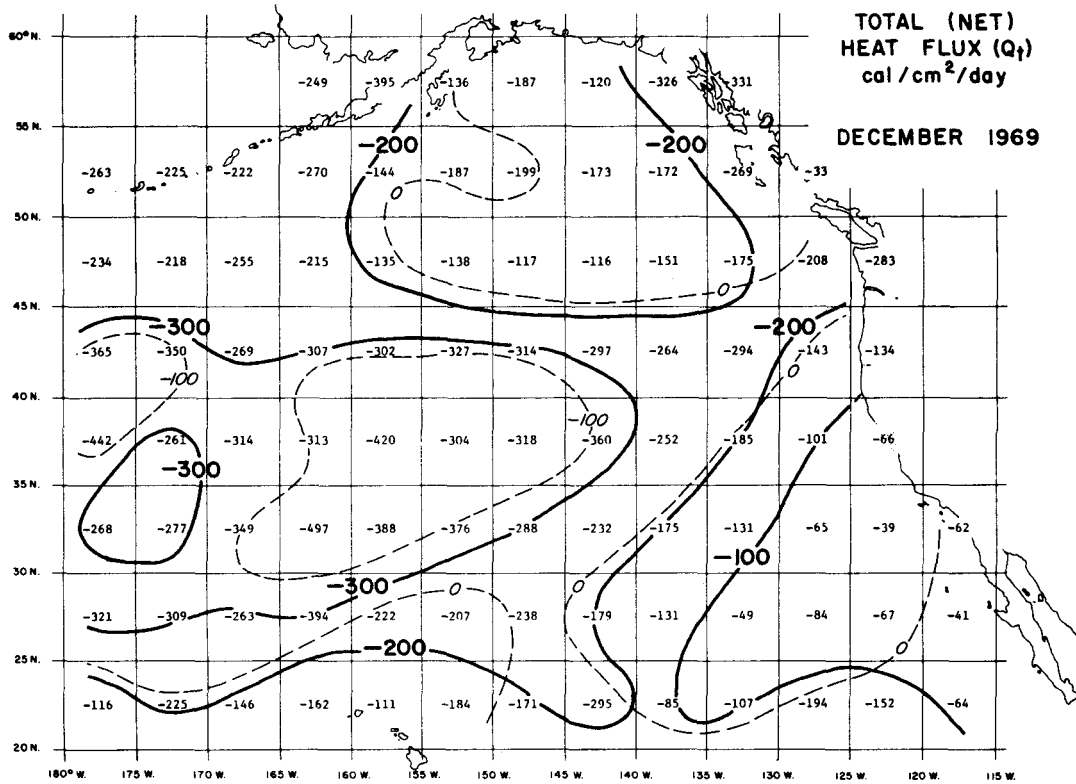
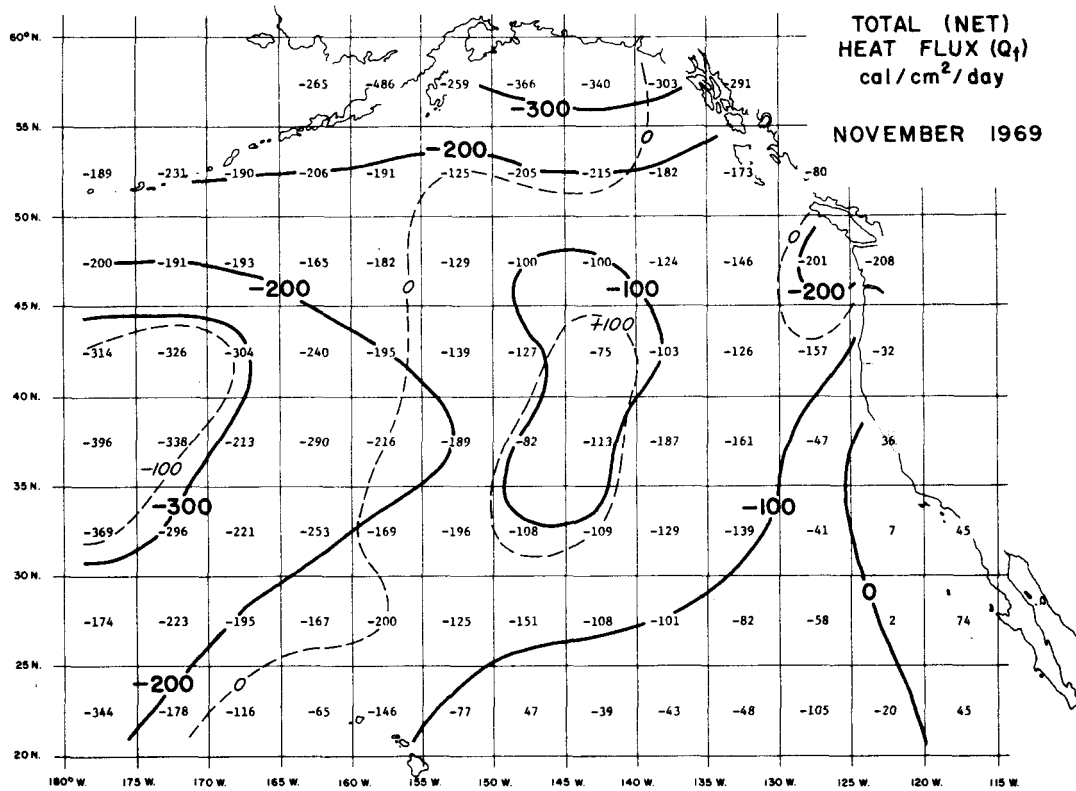


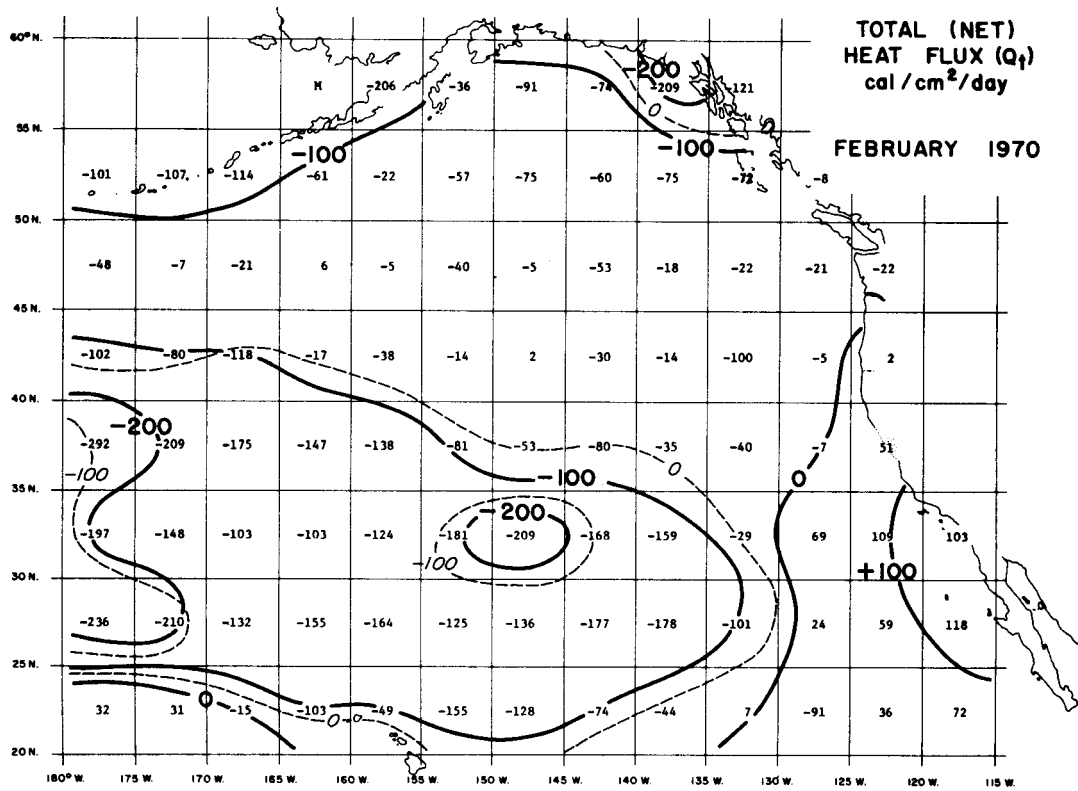
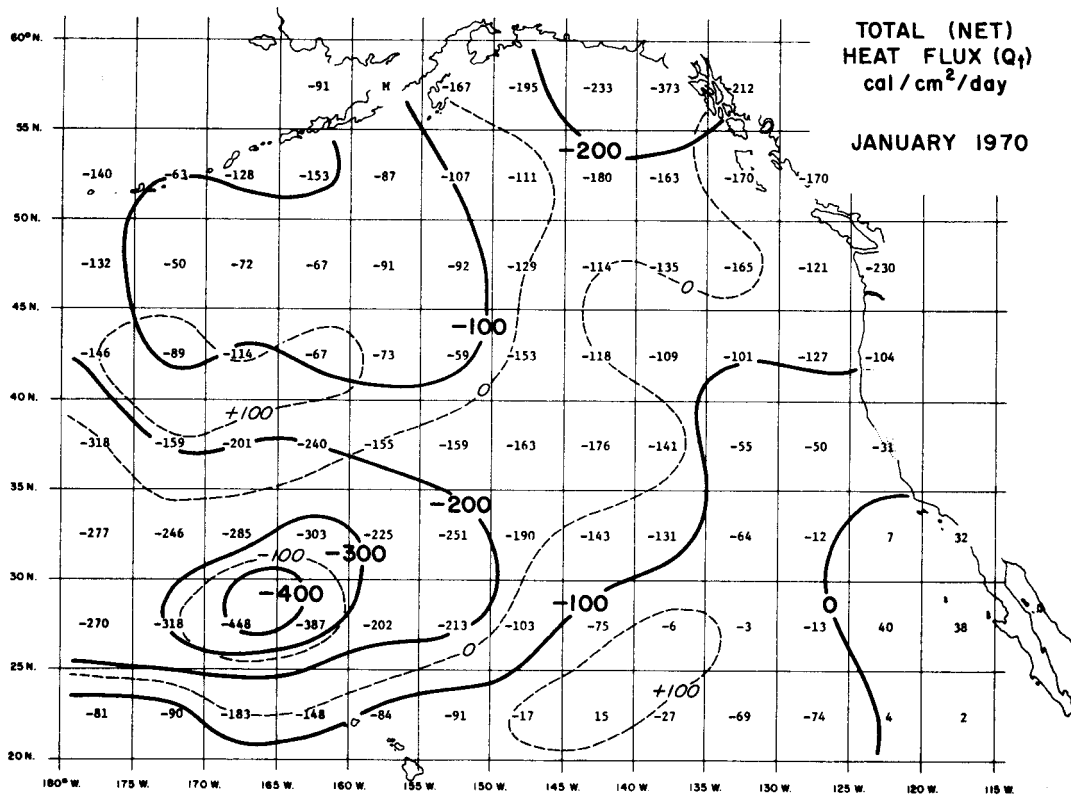


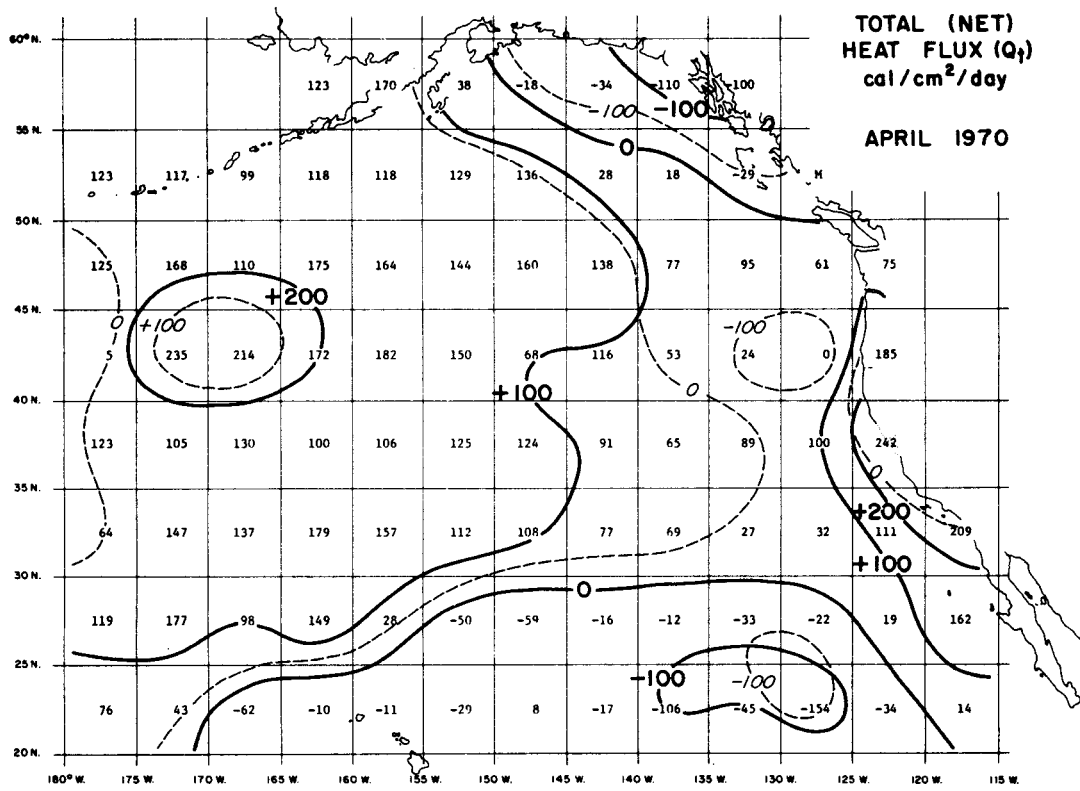
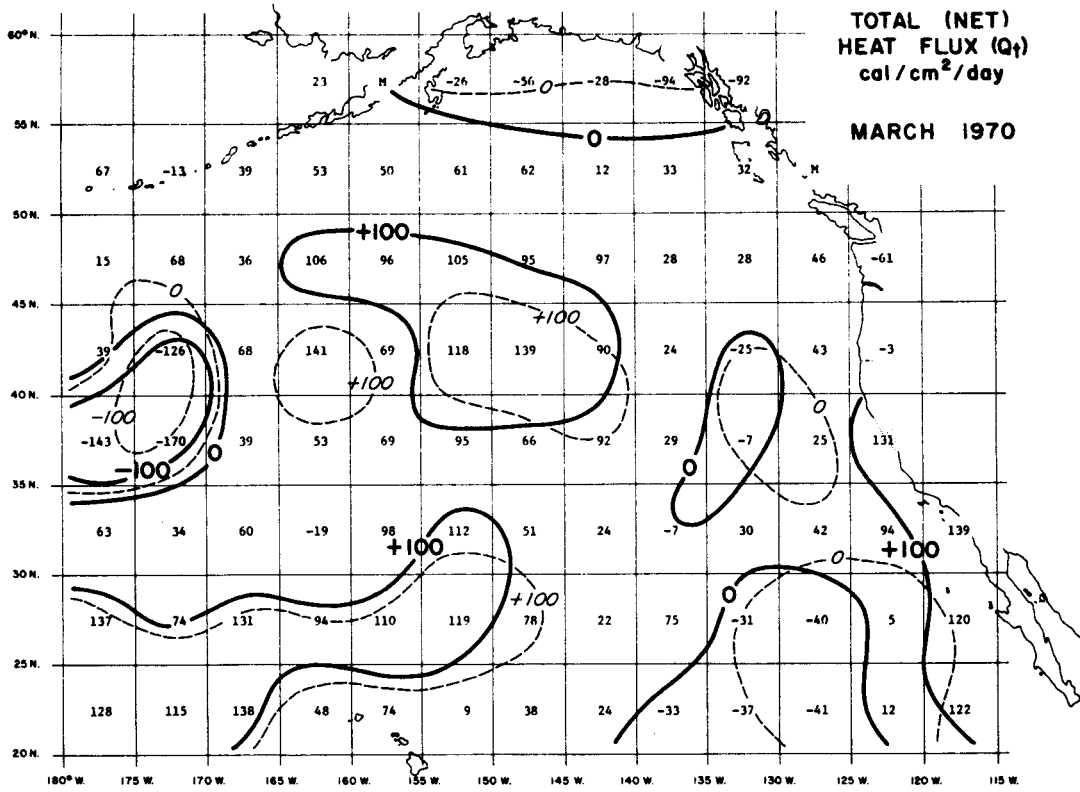


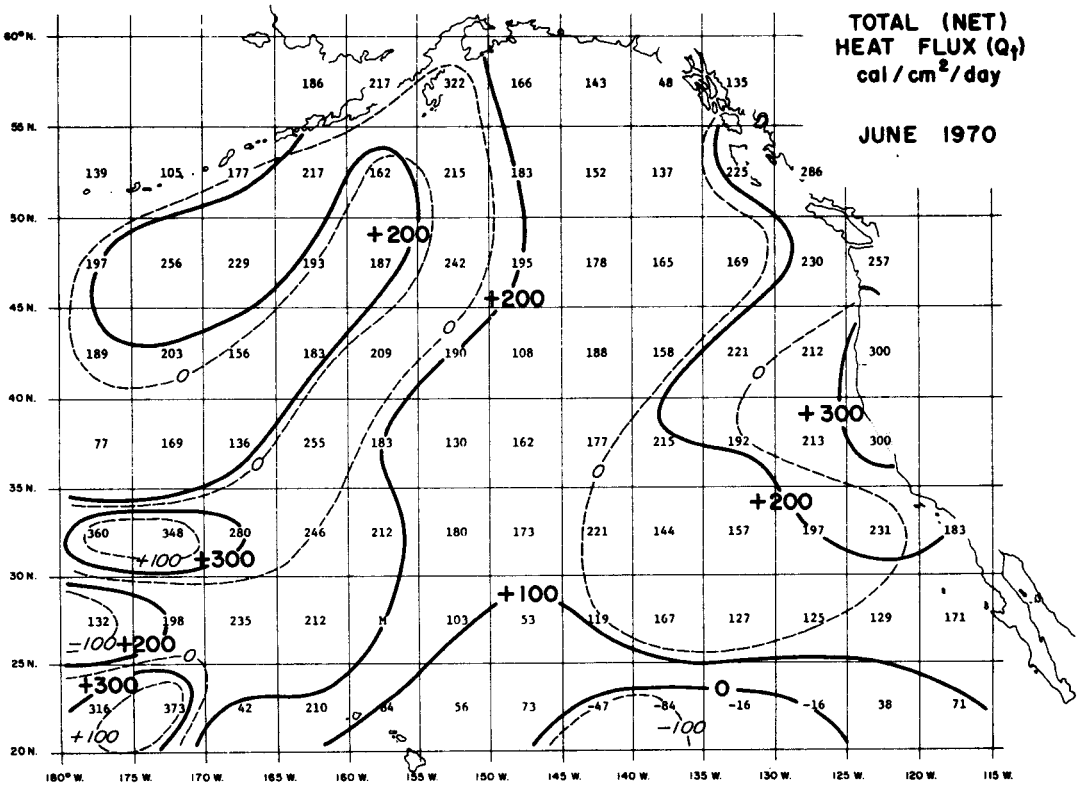
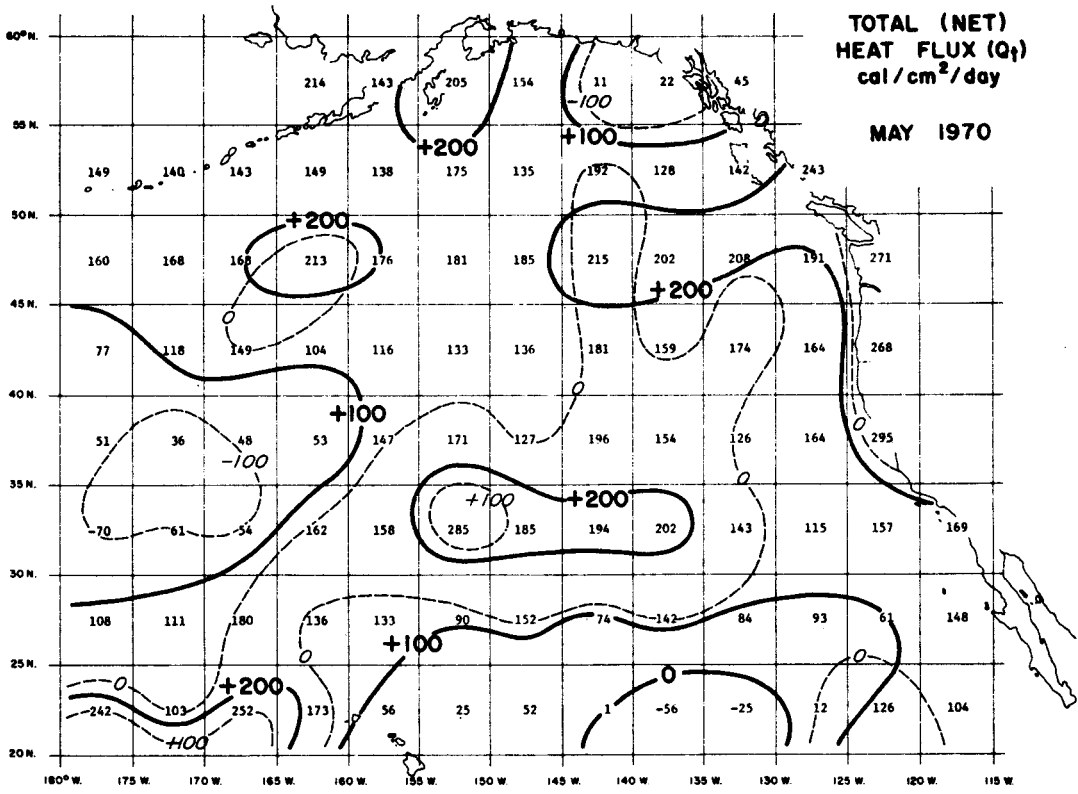


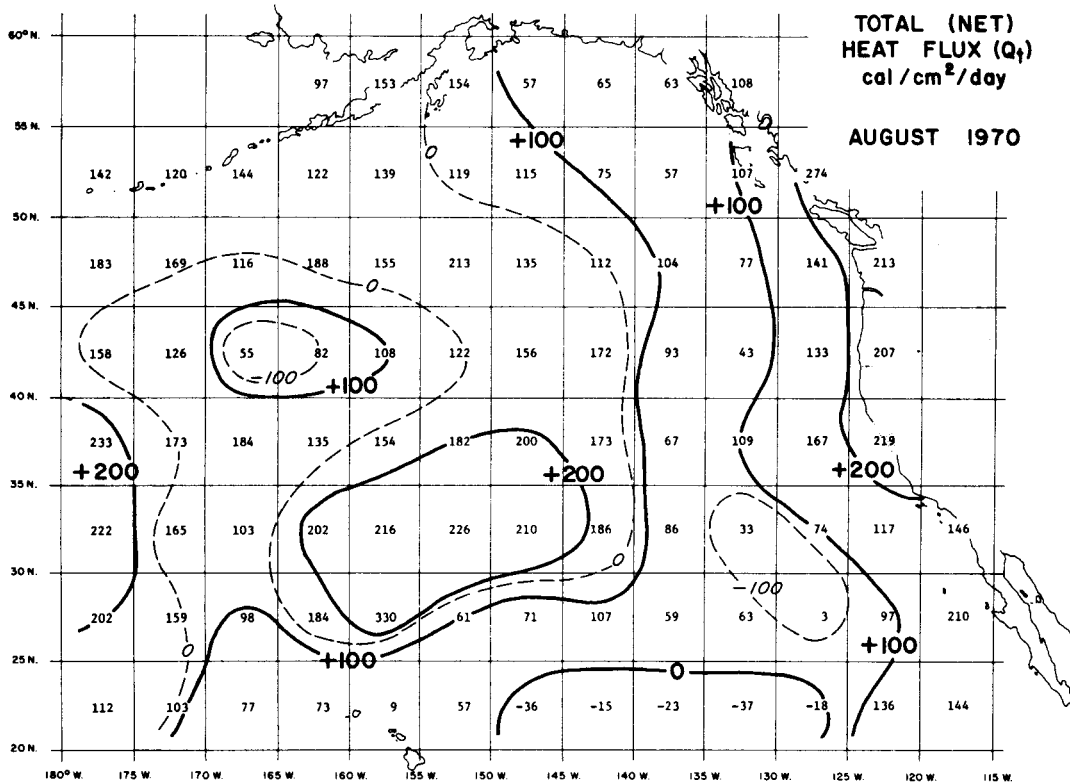
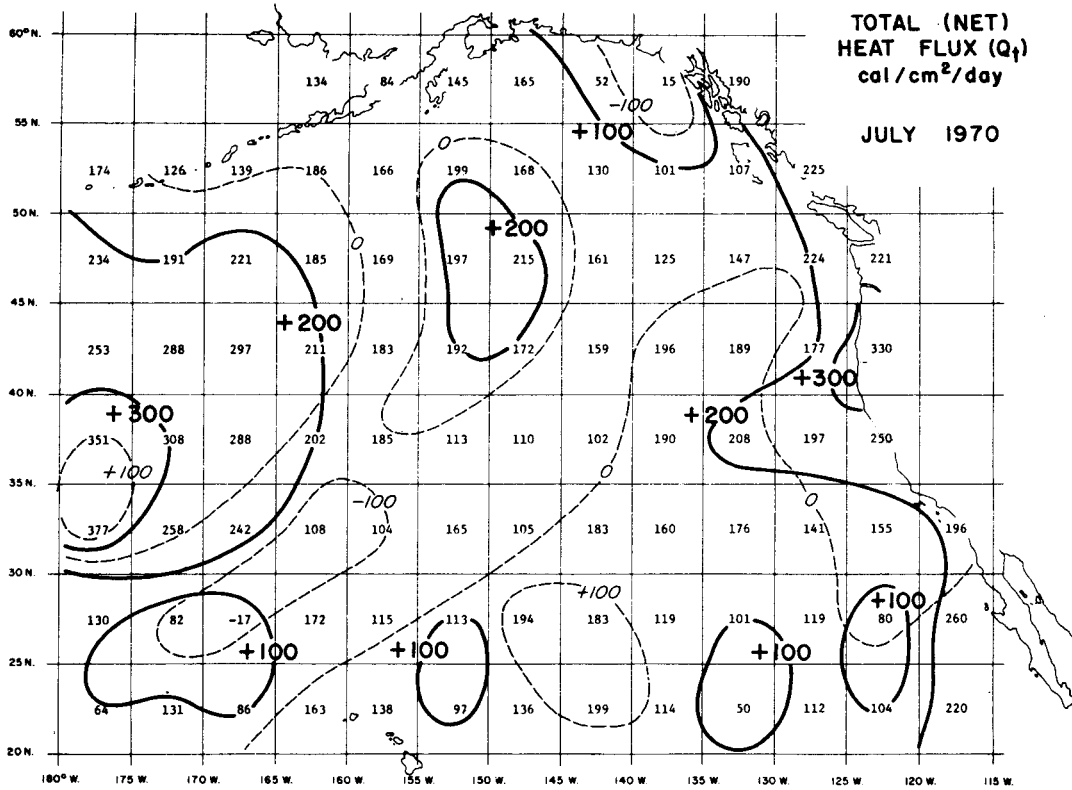


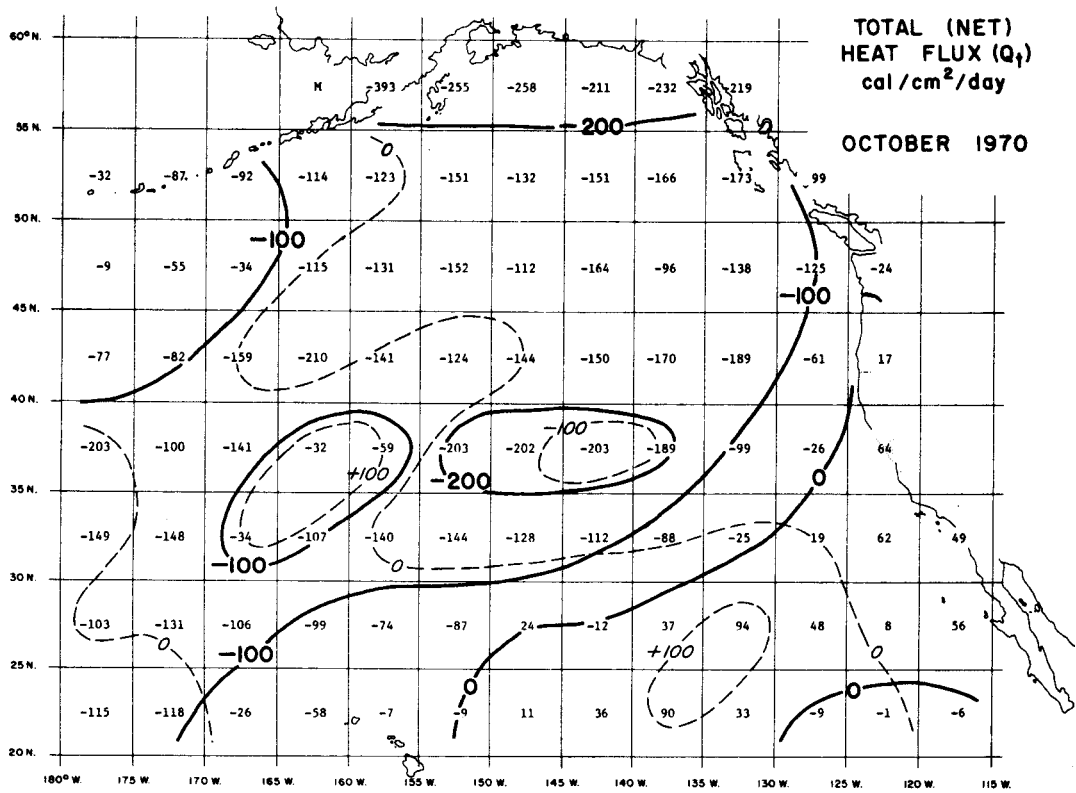
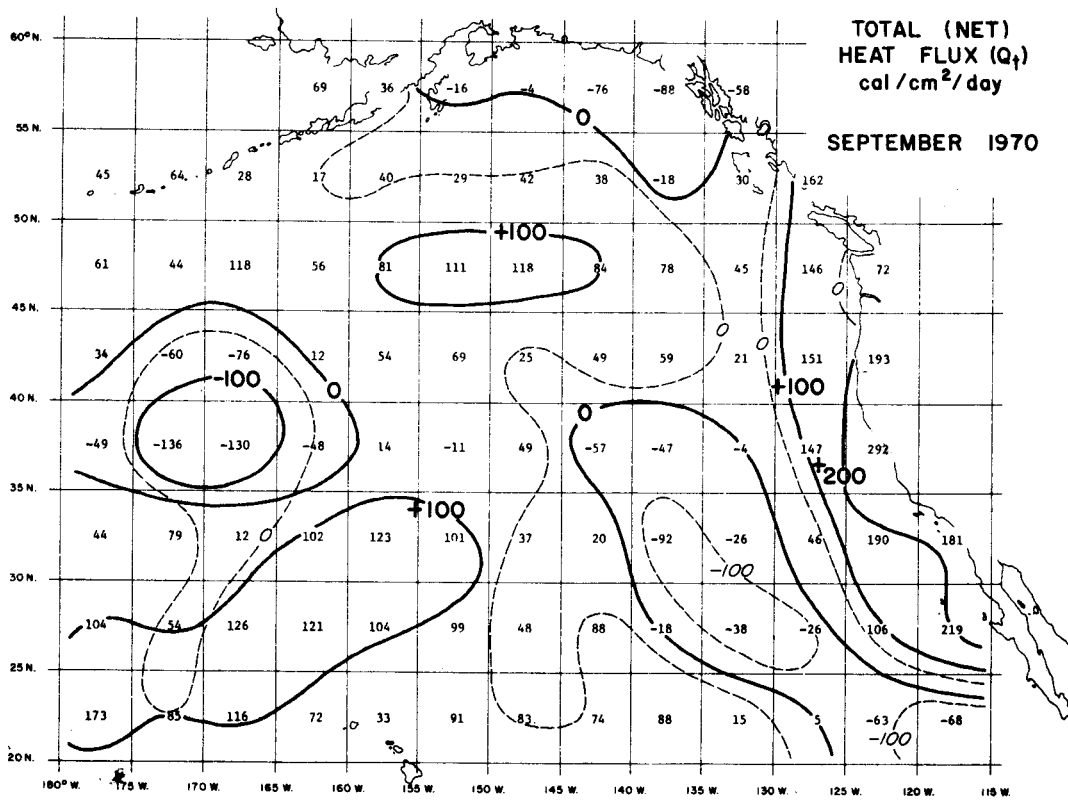


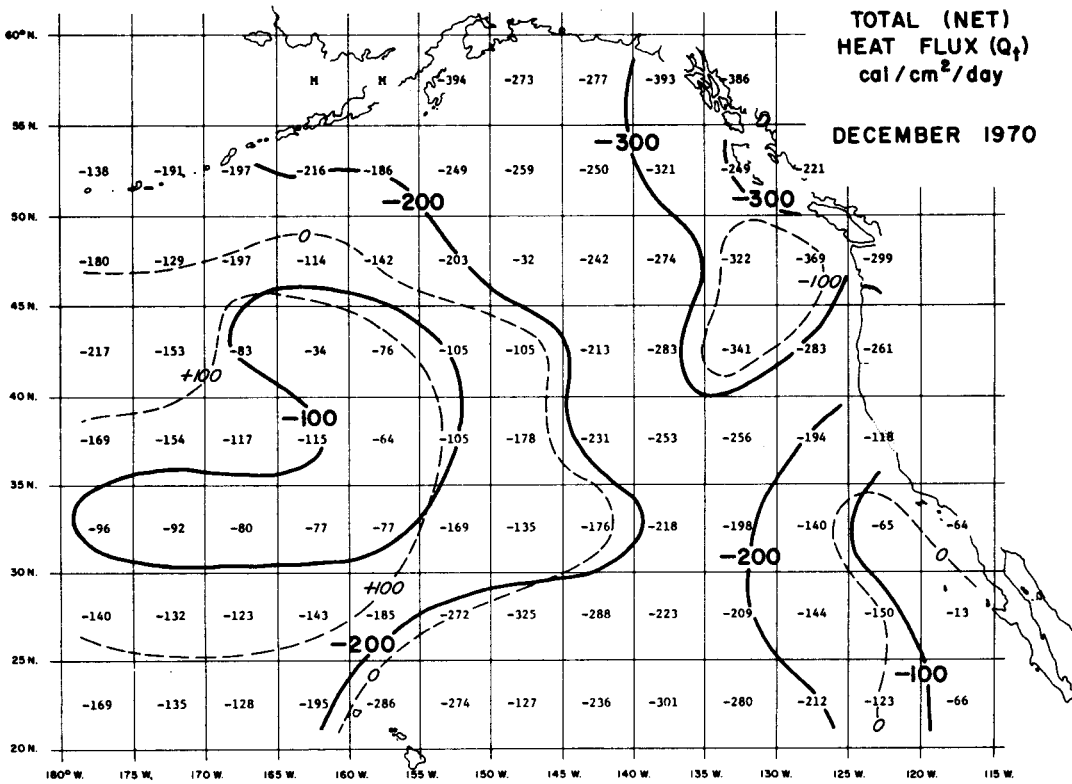
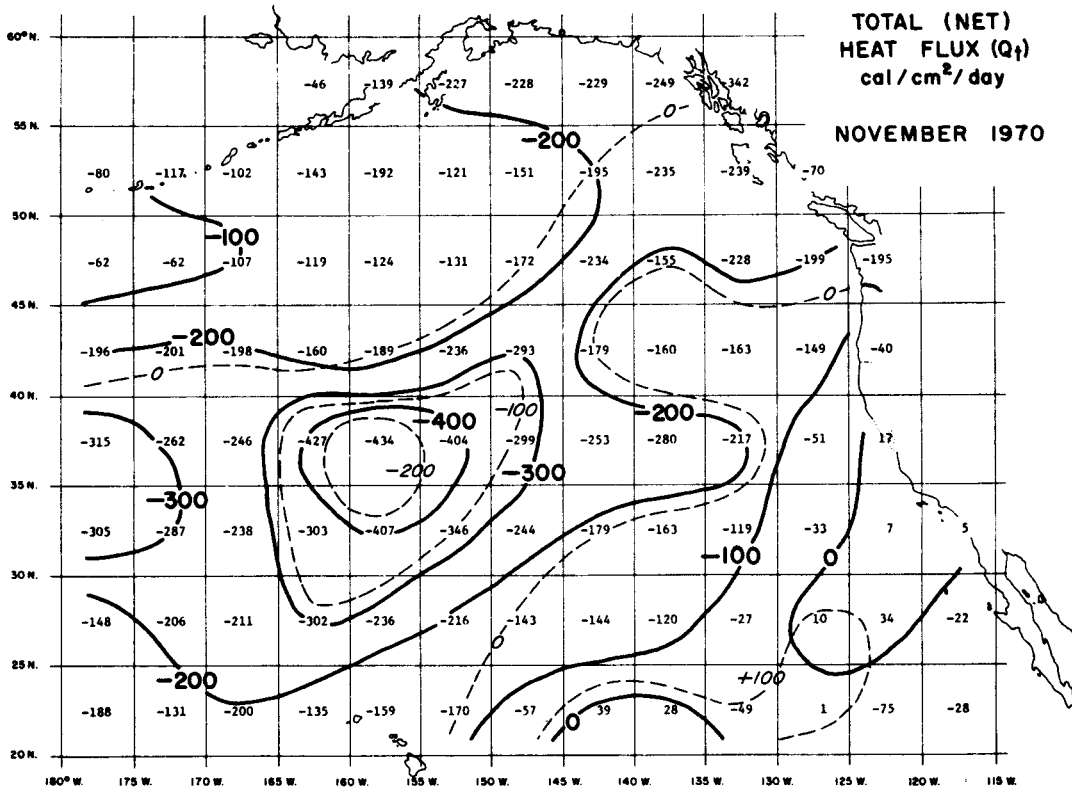


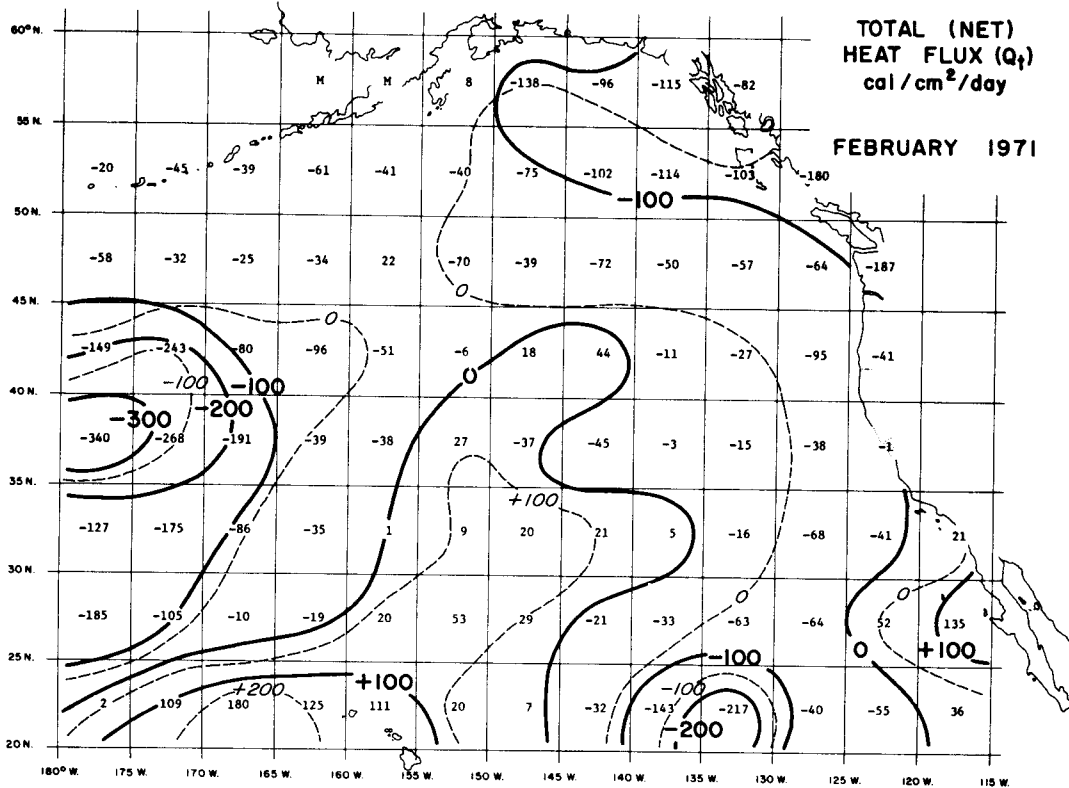
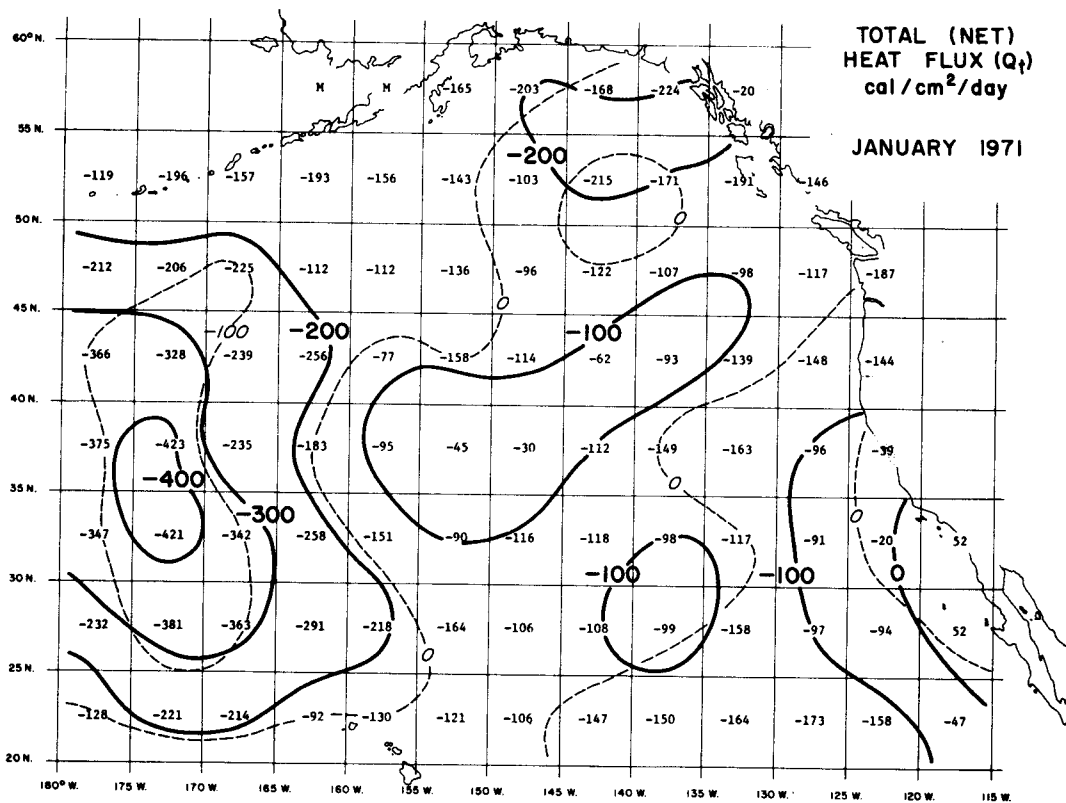


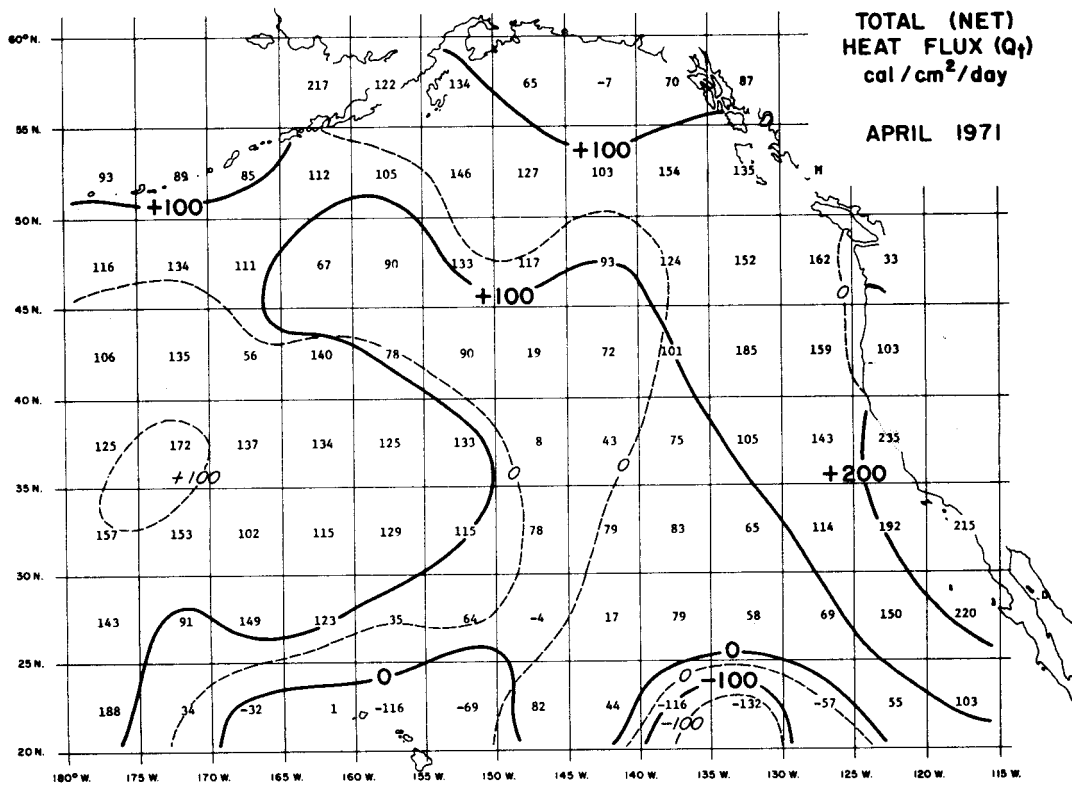
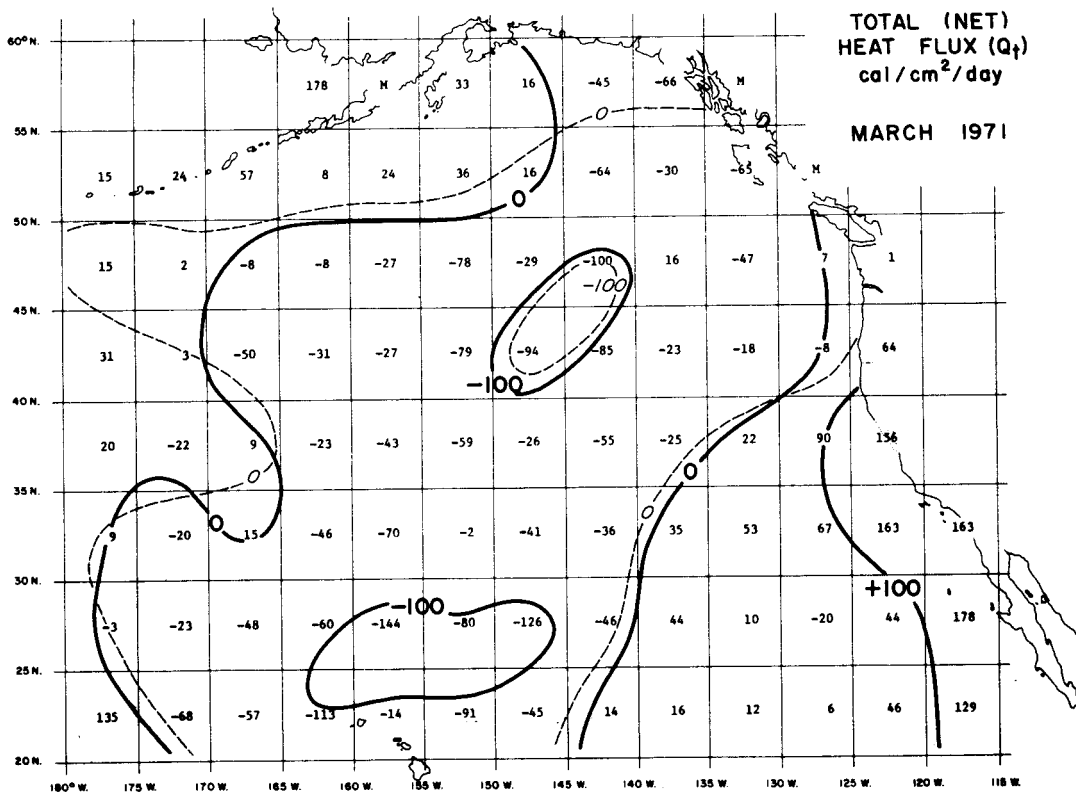


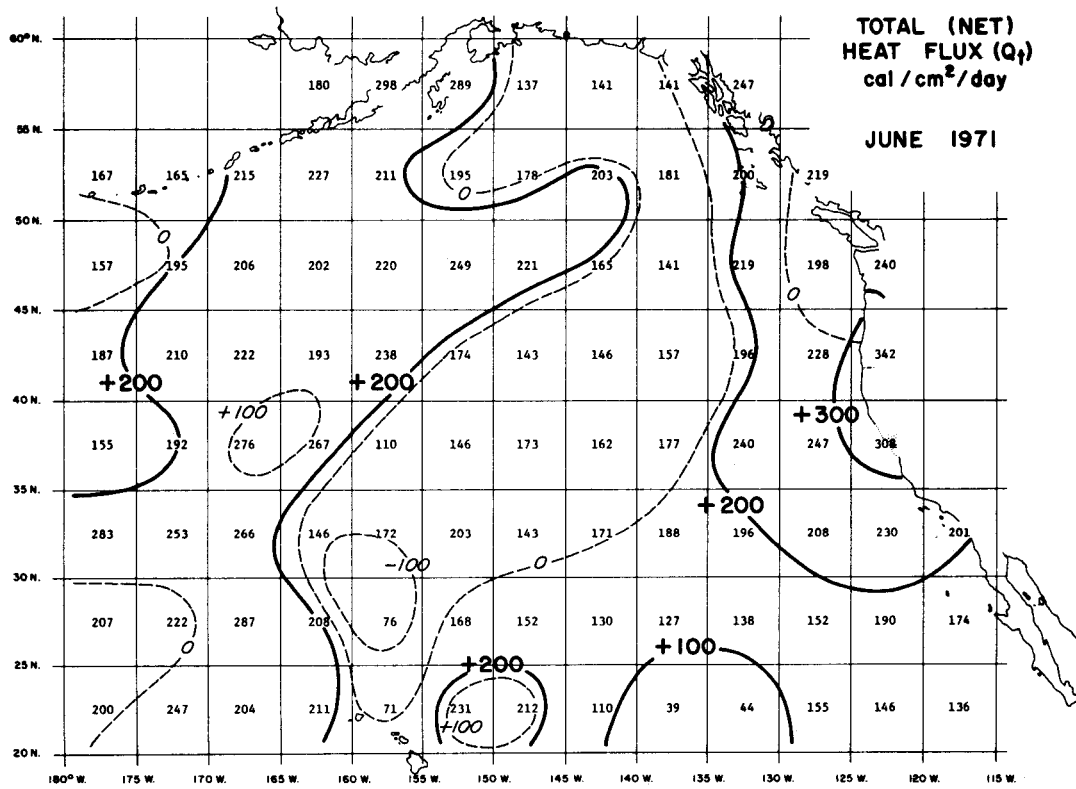
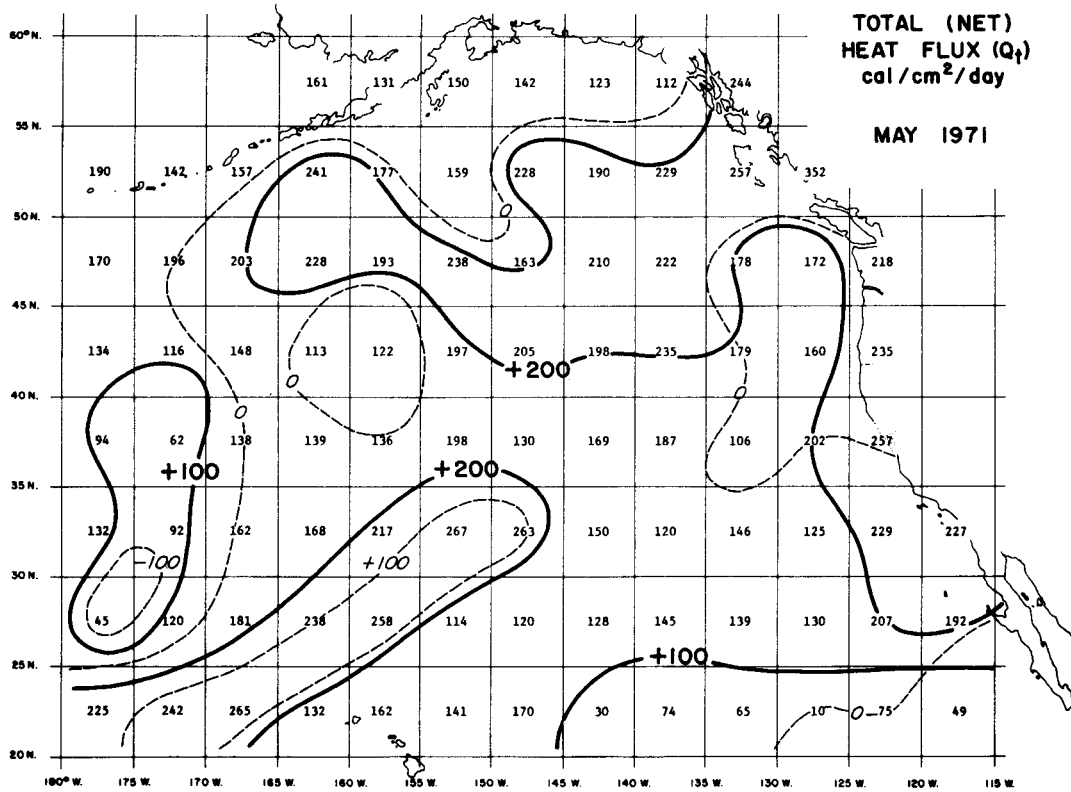


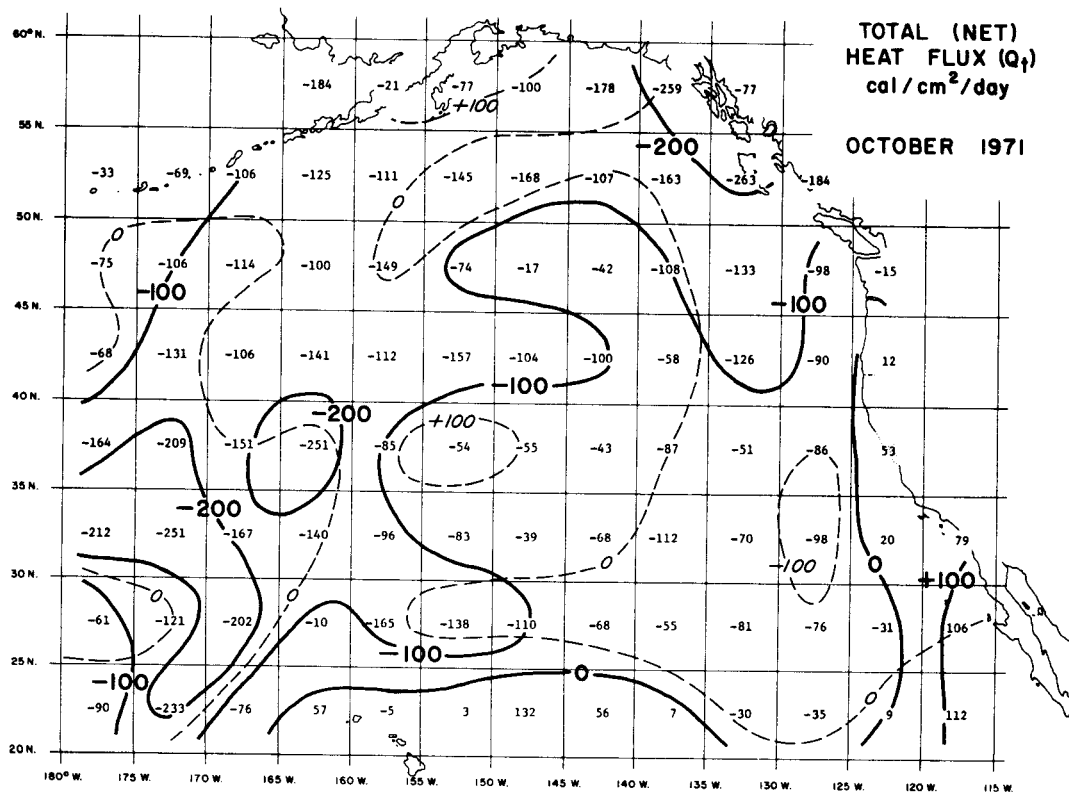
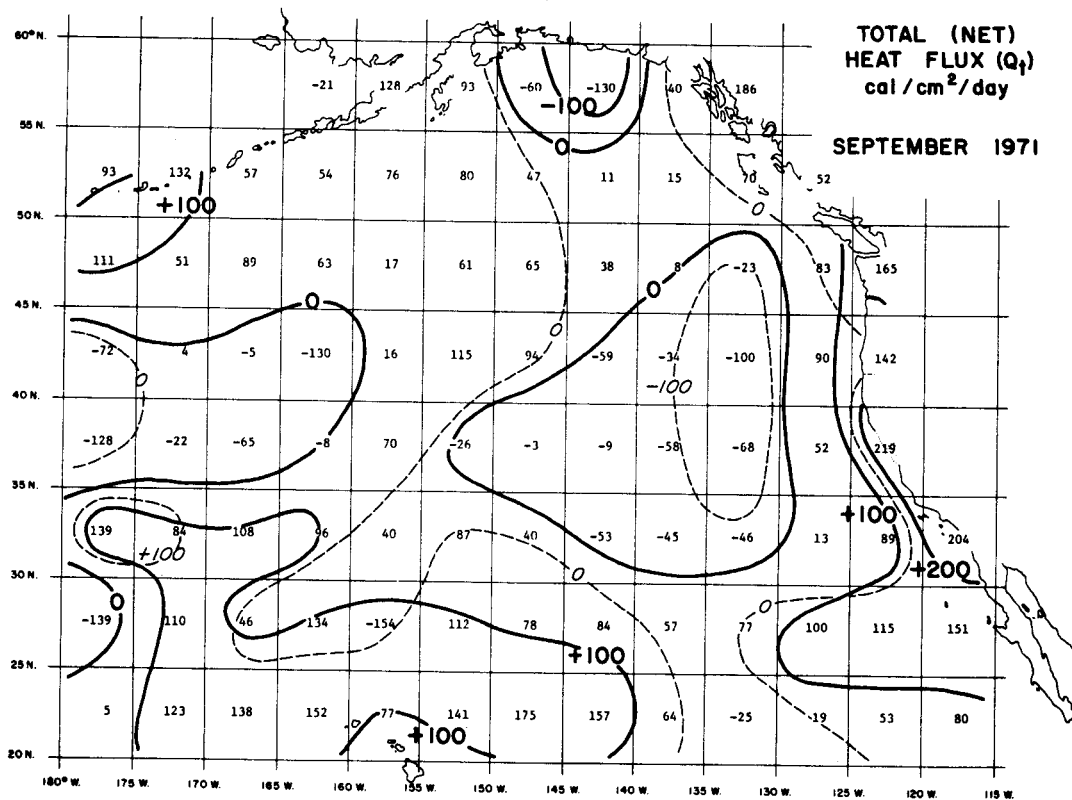


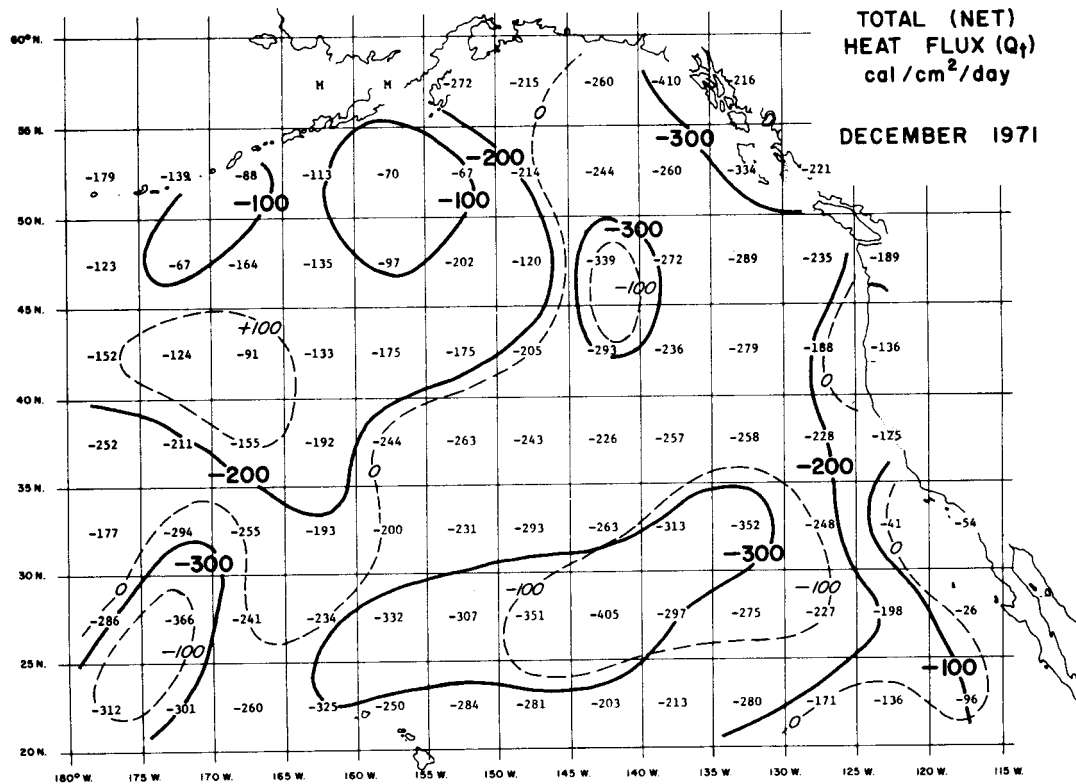
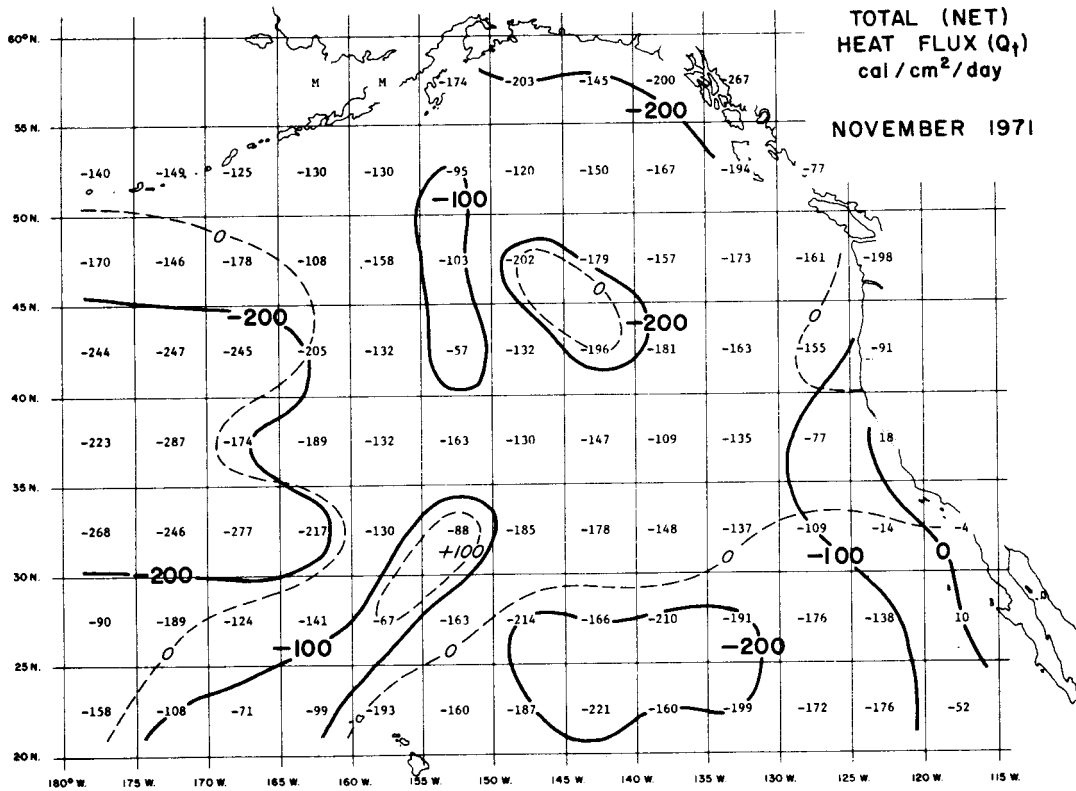




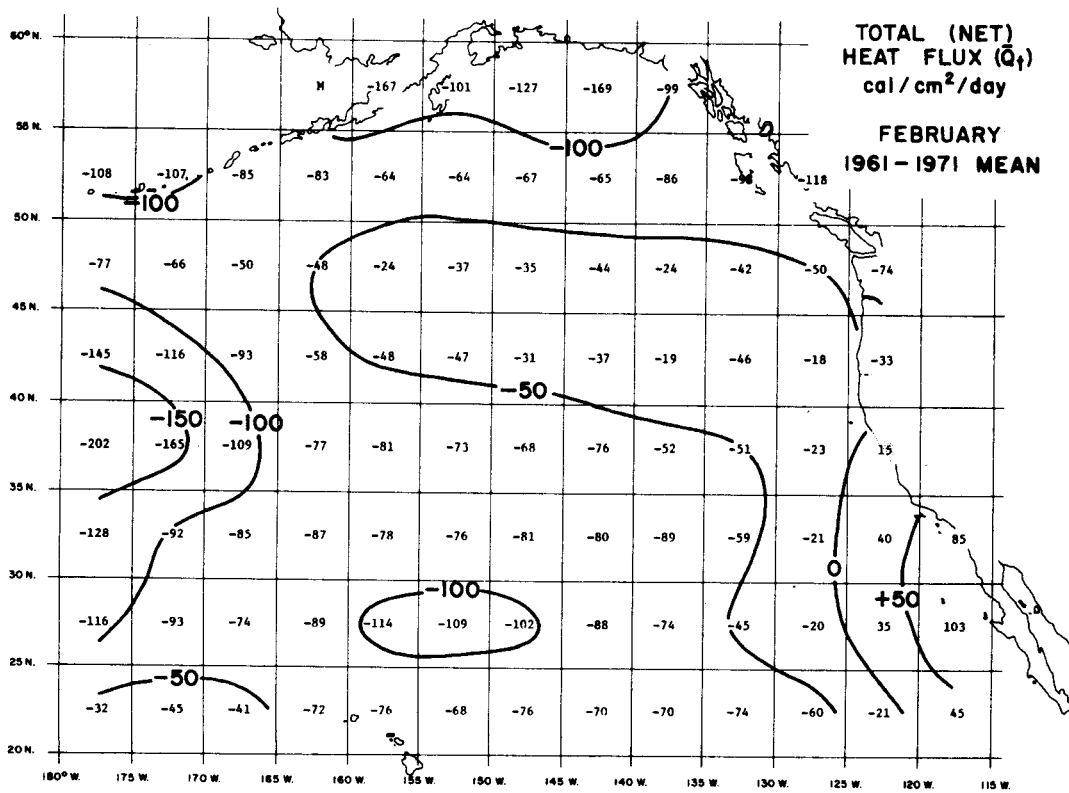
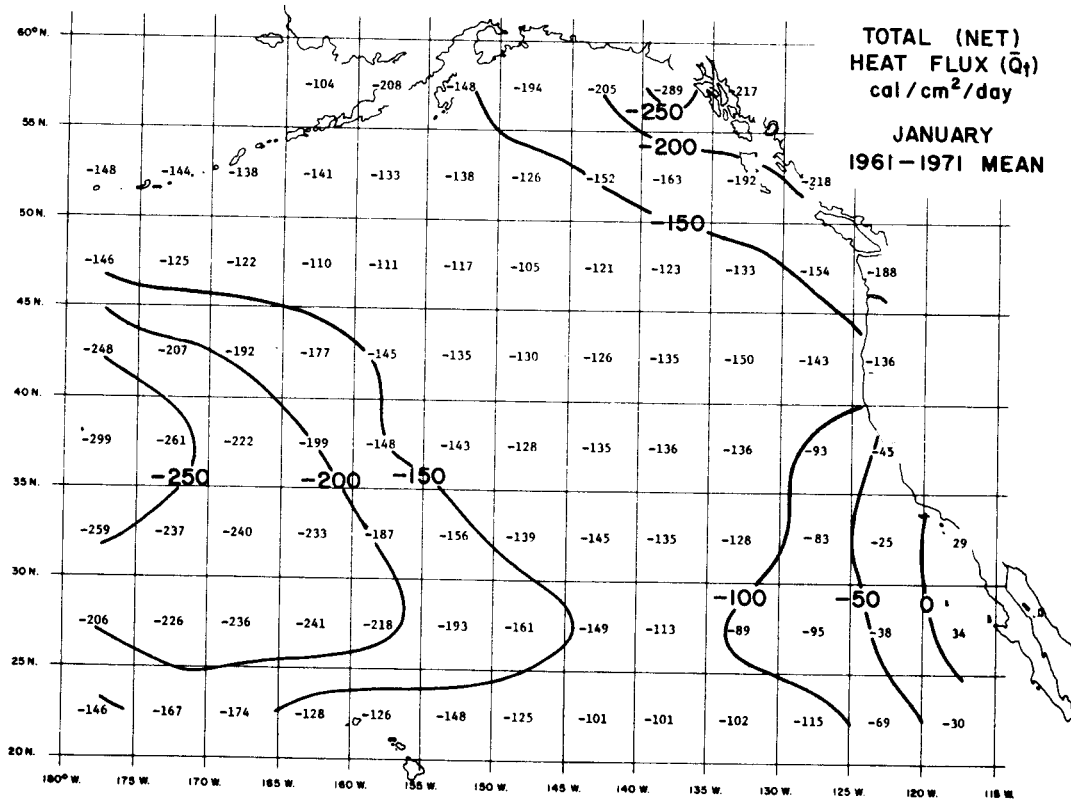


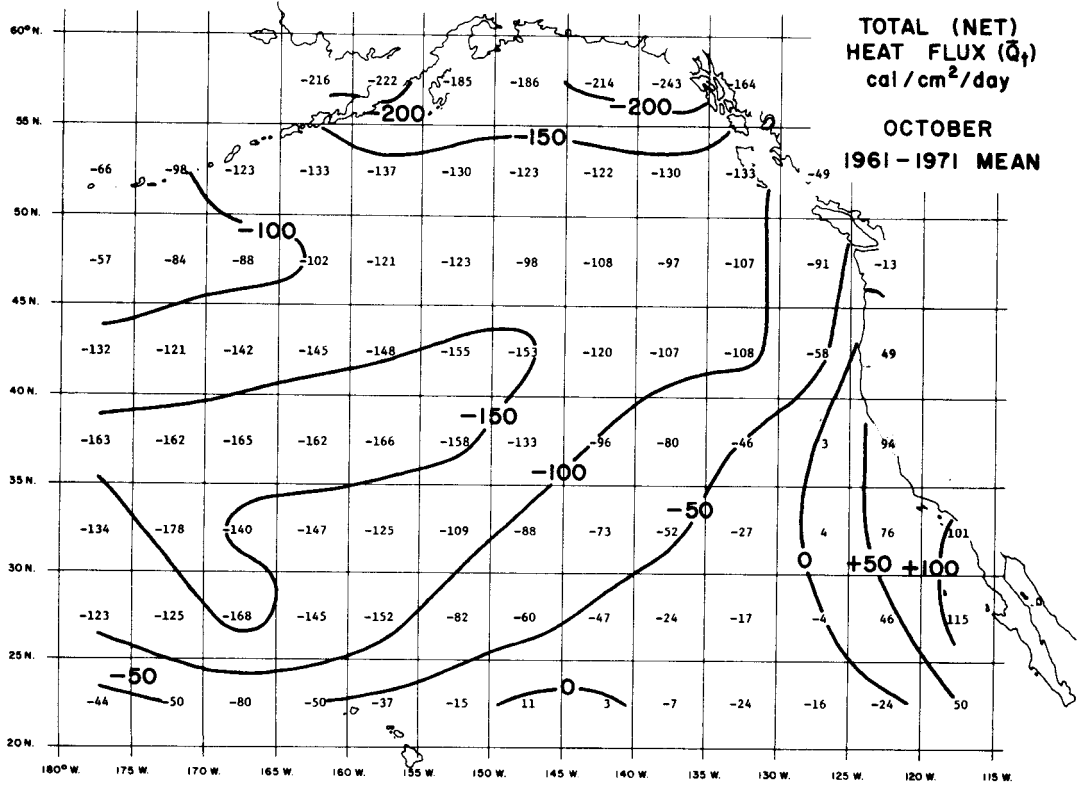
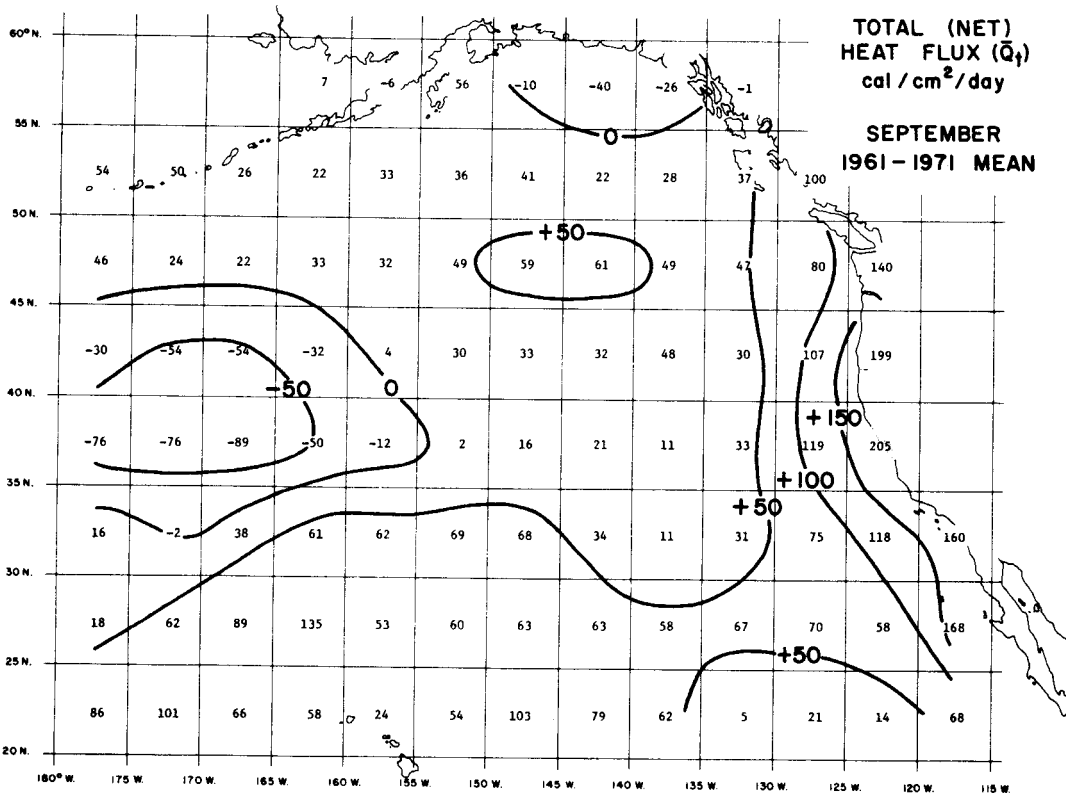




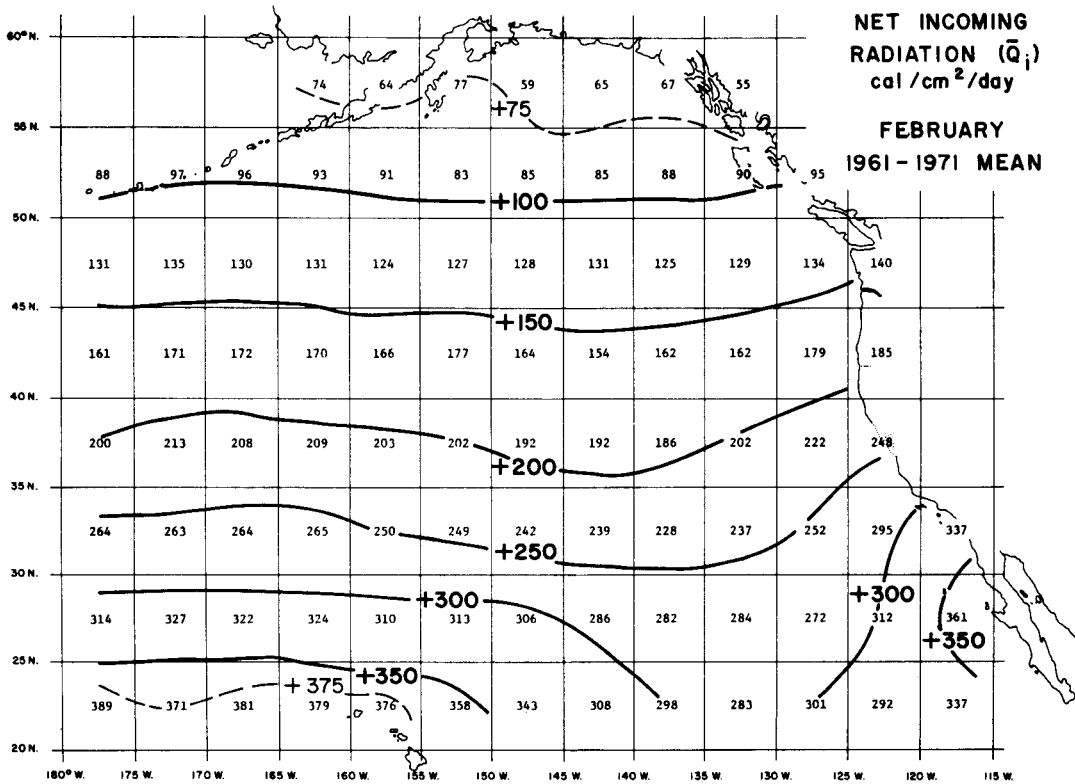
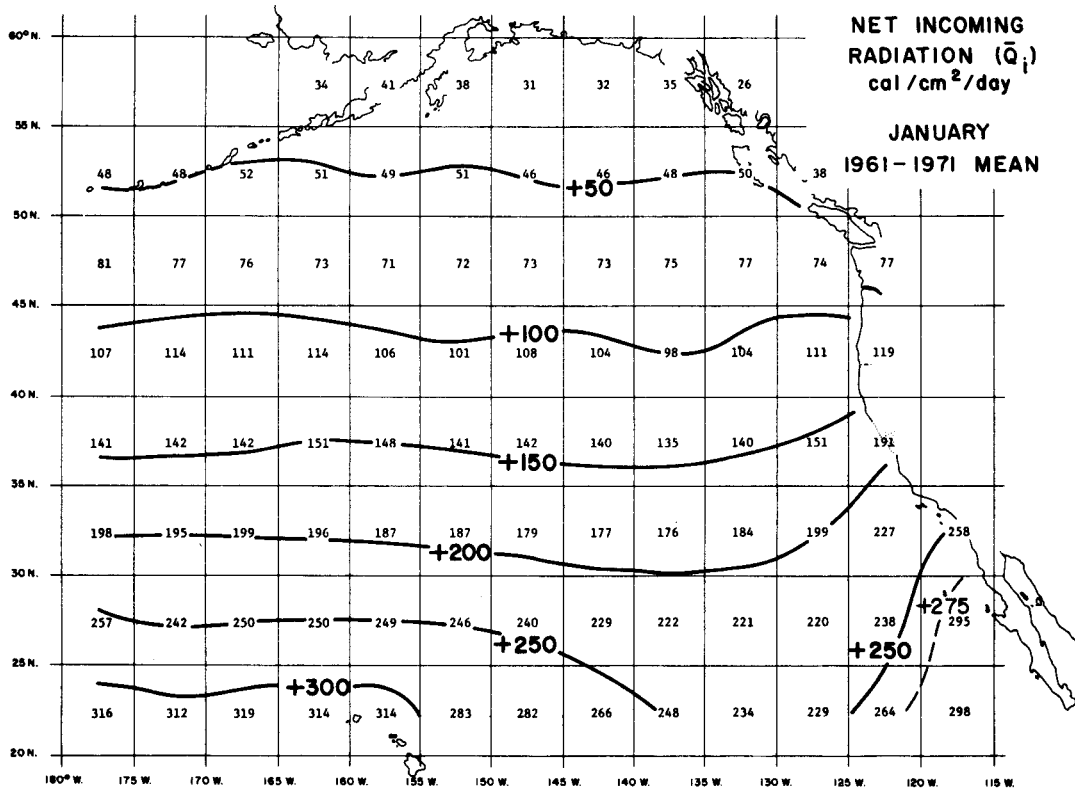


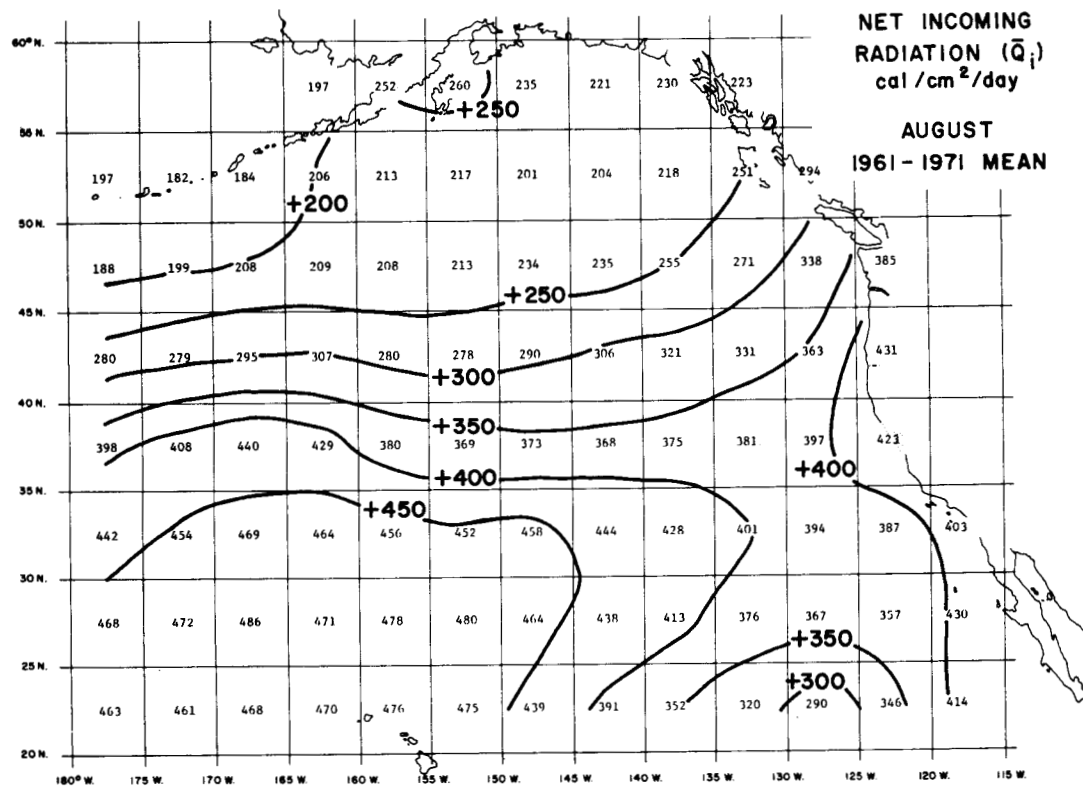
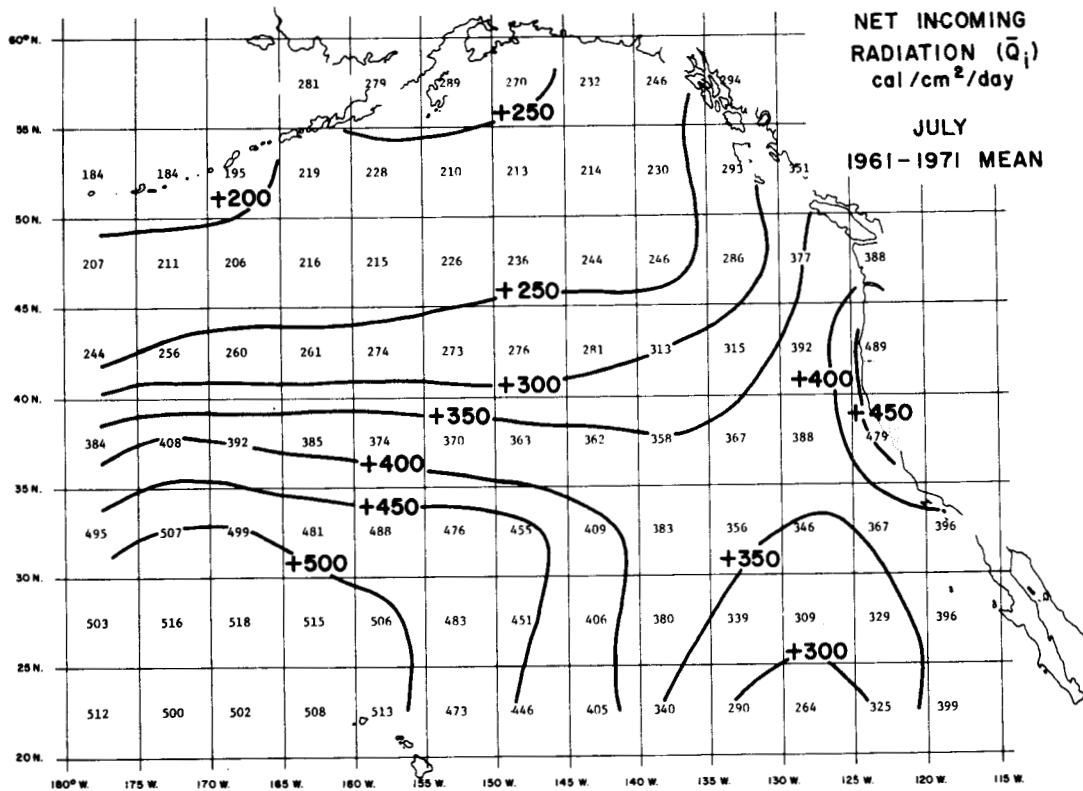
PART 2. TOTAL (NET) HEAT FLUX 1961-71 MEAN MONTHLY VALUES (NORMALS).

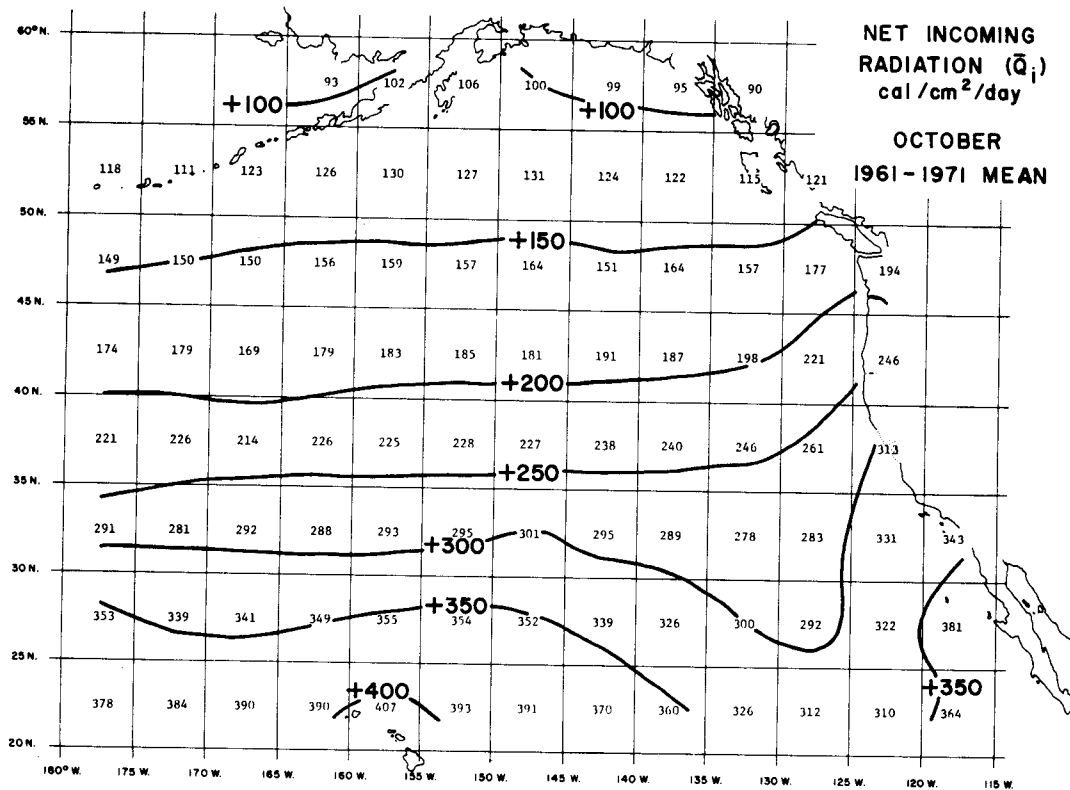
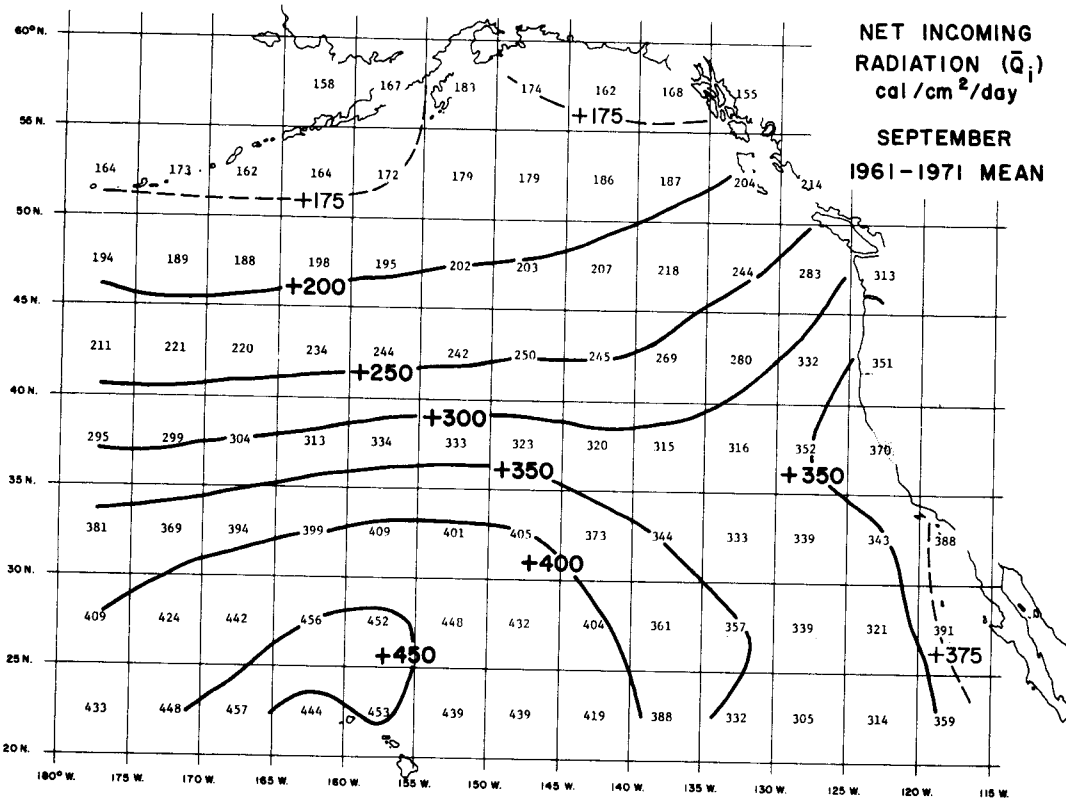


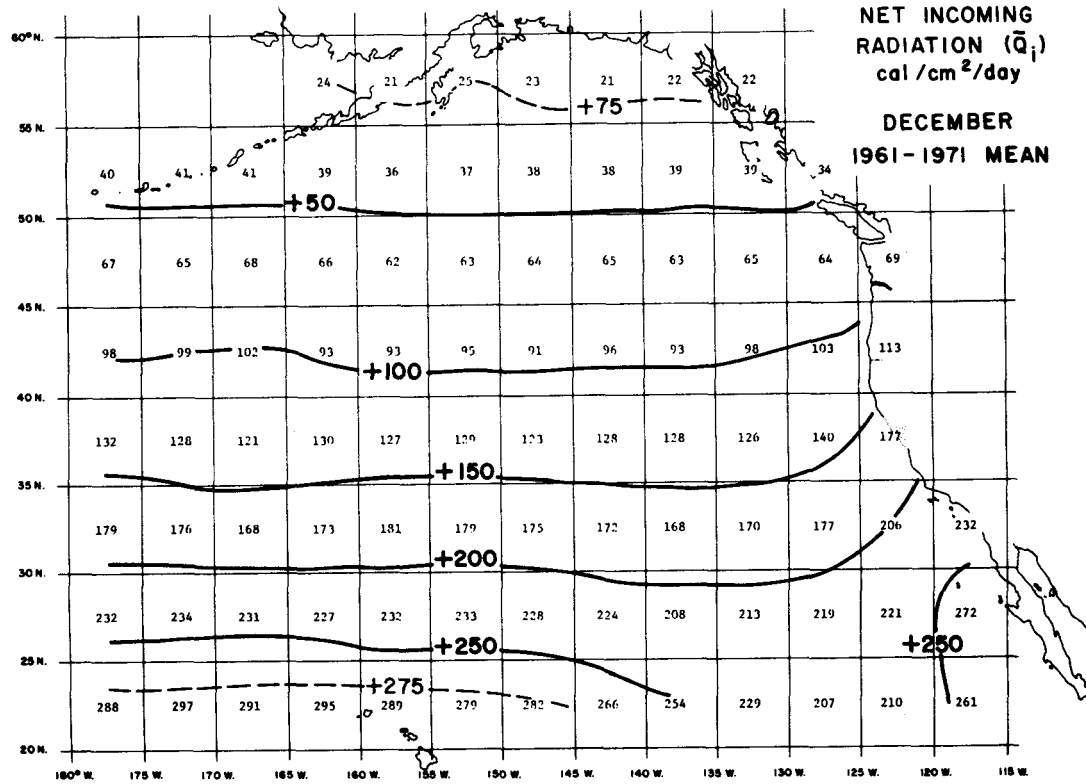
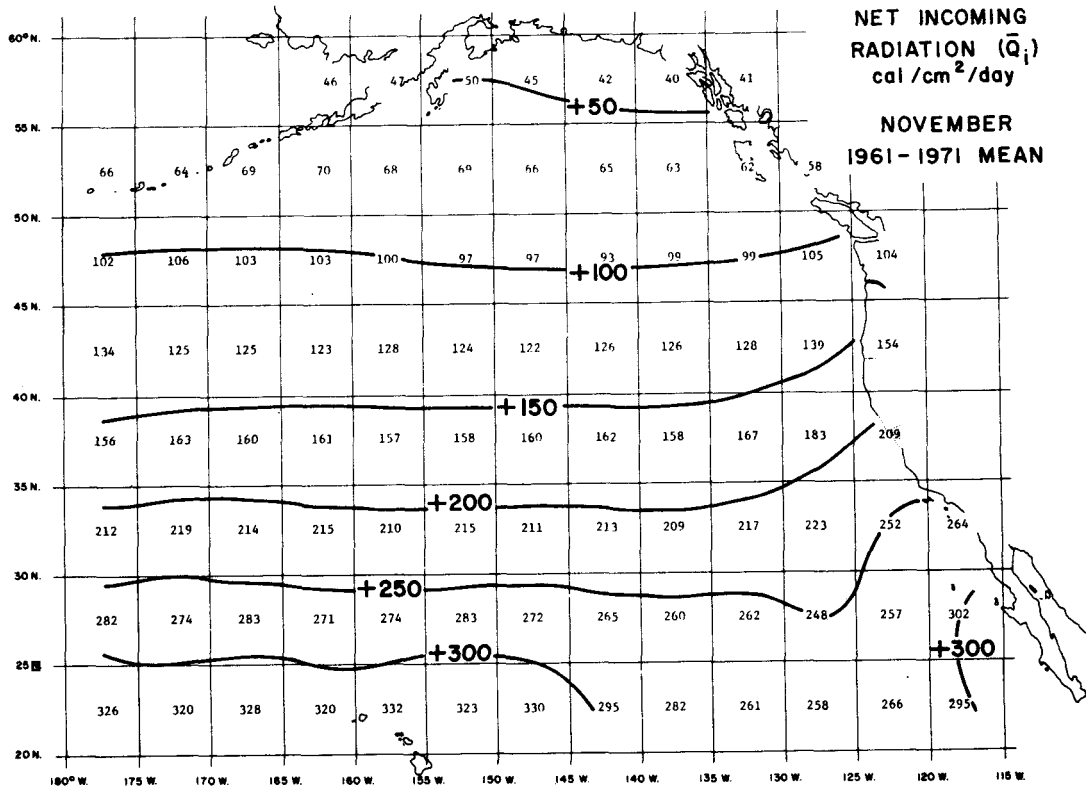


PART 3. NET INCOMING RADIATION 1961-71 MEAN MONTHLY VALUES (NORMALS).









PART 5. EVAPORATIVE HEAT FLUX 1961-71 MEAN MONTHLY VALUES (NORMALS).

